



**US Army Corps  
of Engineers®**  
Engineer Research and  
Development Center

**ERDC**  
INNOVATIVE SOLUTIONS  
for a safer, better world

## **General Model Study of Scour at Proposed Pier Extensions – Santa Ana River at BNSF Bridge, Corona, California**

Jeremy A. Sharp, Tate O. McAlpin, Gary L. Bell,  
Howard E. Park, and Ronald E. Heath

November 2017



**The U.S. Army Engineer Research and Development Center (ERDC)** solves the nation's toughest engineering and environmental challenges. ERDC develops innovative solutions in civil and military engineering, geospatial sciences, water resources, and environmental sciences for the Army, the Department of Defense, civilian agencies, and our nation's public good. Find out more at [www.erdcl.usace.army.mil](http://www.erdcl.usace.army.mil).

To search for other technical reports published by ERDC, visit the ERDC online library at <http://acwc.sdp.sirsi.net/client/default>.



# **General Model Study of Scour at Proposed Pier Extensions – Santa Ana River at BNSF Bridge, Corona, California**

Jeremy A. Sharp, Tate O. McAlpin, Gary L. Bell,  
Howard E. Park, and Ronald E. Heath

*Coastal and Hydraulics Laboratory  
U.S. Army Engineer Research and Development Center  
3909 Halls Ferry Road  
Vicksburg, MS 39180-6199*

Final report

Approved for public release; distribution is unlimited.

Prepared for U.S. Army Corps of Engineers, Los Angeles District  
915 Wilshire Blvd, Suite 1101  
Los Angeles, CA 90017

Under Project Number 104779

## Abstract

A proposed pier nose extension intended to reduce the local pier scour at the Burlington Northern Santa Fe Railway crossing on the Santa Ana River near Corona, CA, was tested in a general physical model. The applied model was a 1:30 Froude-scaled model of the bridge piers, other related structures, and the adjacent channel. Data from the model provided a qualitative and quantitative evaluation of the local scour behavior at the estimated worst-case scenarios for both the existing and proposed conditions. The existing conditions represent the current prototype configuration exposed to potentially larger future dam releases from the upstream Prado Dam. The proposed condition includes pier nose extensions, concrete caps (pile enclosures), and flow guide walls, all intended to reduce scour at the bridge. The primary location for the minimum scour elevation (maximum scour depth) occurred around pier set 5. The proposed conditions showed as high as 60% improvement in reducing the scour depth with the proposed conditions configuration.

**DISCLAIMER:** The contents of this report are not to be used for advertising, publication, or promotional purposes. Citation of trade names does not constitute an official endorsement or approval of the use of such commercial products. All product names and trademarks cited are the property of their respective owners. The findings of this report are not to be construed as an official Department of the Army position unless so designated by other authorized documents.  
**DESTROY THIS REPORT WHEN NO LONGER NEEDED. DO NOT RETURN IT TO THE ORIGINATOR.**

# Contents

<b>Abstract .....</b>	<b>ii</b>
<b>Figures and Tables.....</b>	<b>v</b>
<b>Preface.....</b>	<b>viii</b>
<b>Unit Conversion Factors .....</b>	<b>ix</b>
<b>1 Introduction.....</b>	<b>1</b>
1.1 Purpose .....	1
1.2 Background.....	2
1.3 Model history .....	7
1.4 Approach .....	8
<b>2 Process and Setup .....</b>	<b>9</b>
2.1 Model construction.....	9
2.2 Lidar .....	12
2.3 Boundary conditions .....	13
2.4 Data collection.....	15
2.5 Test Outline .....	17
<b>3 Scale Factor .....</b>	<b>18</b>
3.1 Introduction.....	18
3.2 Process and setup.....	20
3.3 Results and discussion .....	22
3.4 Application .....	24
3.5 Recommendation .....	28
<b>4 Uncertainties .....</b>	<b>29</b>
<b>5 Data and Results.....</b>	<b>32</b>
<b>6 Discussion .....</b>	<b>51</b>
6.1 Maximum scour depth .....	51
6.2 Correlation and comparison .....	54
6.3 Sensitivity testing.....	63
<b>7 Conclusion and Recommendation .....</b>	<b>67</b>
<b>References .....</b>	<b>68</b>
<b>Appendix A: Water Surface Data .....</b>	<b>70</b>
<b>Appendix B: Approach Velocity Data .....</b>	<b>79</b>
<b>Appendix C: Lidar Data .....</b>	<b>86</b>

---

<b>Appendix D: ERDC/CHL LR-15-2 .....</b>	<b>91</b>
<b>Appendix E: ERDC/CHL LR-15-1.....</b>	<b>105</b>
<b>Report Documentation Page</b>	

# Figures and Tables

## Figures

Figure 1. Location map of BNSF Railway Bridge above and domain below.....	2
Figure 2. BNSF Railway Bridge pier set 6 and west abutment. ....	4
Figure 3. BNSF Railway Bridge showing alignment of trestles to piers. ....	5
Figure 4. BNSF Railway Bridge crossing on the Santa Ana River near Corona, CA; original proposed alternative (above) and new proposed alternative (below). ....	6
Figure 5. Section model of proposed conditions (above) and original pier extension design (below). ....	8
Figure 6. View of flume prior to model construction.....	10
Figure 7. Flume and general model extents overlaid on Google Earth image. ....	10
Figure 8. Construction of existing pier structures during model construction.....	11
Figure 9. Vertical alignment of fixed plywood template that defines upstream extents. ....	12
Figure 10. Lidar measurement of the bed post-test. ....	13
Figure 11. Head differential for BIF 12 × 7.25 venturi meter.....	14
Figure 12. Location of stilling well gages shown with proposed conditions and pre-test bathymetry contours. ....	16
Figure 13. Typical configuration of pier sets at the BNSF railroad bridge, plan view above and 3D rendering below.....	19
Figure 14. Test configuration of round piers and pier sets for test 5.....	21
Figure 15. Test and prototype material gradations. ....	22
Figure 16. Maximum scour depth for round pier test. ....	24
Figure 17. Literature data as compared to scale factor test data. ....	26
Figure 18. Scaled and un-scaled BNSF bridge pier set scour depths as compared to round piers. ....	28
Figure 19. Santa Ana River directly downstream of the BNSF Railway Bridge, looking upstream. ....	30
Figure 20. Apparent emergent rock downstream of the BNSF Railway Bridge, looking downstream. ....	31
Figure 21. Location for maximum scour for both new and original proposed and existing conditions. ....	34
Figure 22. Typical scour at pier set 5 for 30,000 cfs flow test, existing conditions. ....	35
Figure 23. Typical scour at pier set 5 for 30,000 cfs flow test, original proposed conditions. ....	35
Figure 24. Typical scour at pier set 5 for 30,000 cfs flow test, original proposed conditions. ....	36
Figure 25. Typical scour at pier set 5 for 30,000 cfs flow test, new proposed conditions. ....	36
Figure 26. Test 3 (15,000 cfs existing conditions) pre-test lidar scan (typical). ....	37
Figure 27. Test 8 (30,000 cfs original proposed conditions) pre-test lidar scan (typical). ....	37
Figure 28. Test 13 (30,000 cfs new proposed conditions) pre-test lidar scan (typical). ....	38
Figure 29. Test 3 (15,000 cfs existing conditions) post-test lidar scan.....	38



Figure 30. Test 1 (30,000 cfs existing conditions) post-test lidar scan.....	39
Figure 31. Test 7 (15,000 cfs original proposed conditions) post-test lidar scan.....	39
Figure 32. Test 8 (30,000 cfs original proposed conditions) post-test lidar scan. ....	40
Figure 33. Test 13 (30,000 cfs new proposed conditions) post-test lidar scan.....	40
Figure 34. Test 14 (30,000 cfs new proposed conditions) post-test lidar scan.....	41
Figure 35. Test 15 (30,000 cfs new proposed conditions) post-test lidar scan.....	41
Figure 36. Test 16 (30,000 cfs new proposed conditions) post-test lidar scan.....	42
Figure 37. Test 4 (15,000 cfs existing conditions) pre- minus post-test lidar survey.....	42
Figure 38. Test 1 (30,000 cfs existing conditions) pre- minus post-test lidar survey. ....	43
Figure 39. Test 7 (15,000 cfs original proposed conditions) pre- minus post-test lidar survey.....	43
Figure 40. Test 8 (30,000 cfs original proposed conditions) pre- minus post-test lidar survey.....	44
Figure 41. Test 13 (30,000 cfs new proposed conditions) pre- minus post-test lidar survey. ....	44
Figure 42. Test 14 (30,000 cfs new proposed conditions) pre- minus post-test lidar survey.....	45
Figure 43. Test 15 (30,000 cfs new proposed conditions) pre- minus post-test lidar survey.....	45
Figure 44. Test 16 (30,000 cfs new proposed conditions) pre- minus post-test lidar survey.....	46
Figure 45. Time series of unscaled scour hole minimum elevation (scour depth) comparison between existing and proposed conditions at 15,000 cfs flow case as measured on left side of 1938 Pier 5 (see Figure 4 for a layout schematic). ....	46
Figure 46. Time series of unscaled scour hole minimum elevation (scour depth) comparison between existing and original and new proposed conditions at 30,000 cfs flow Test 5, 8 and 14. ....	47
Figure 47. Verification of measuring technique with single beam fathometer array for Test 9 (unscaled results). ....	47
Figure 48. Existing conditions minimum scour elevations (scour depth) at Pier 5 for both measured and scaled at 15,000 and 30,000 cfs flow conditions. ....	48
Figure 49. Variations in scour depth with changes in tailwater control at Pier 5 for 30,000 cfs flow case.....	48
Figure 50. Original proposed conditions (overlaid on existing conditions) minimum scour elevations for both measured and scaled for Pier 5 at 15,000 and 30,000 cfs flow conditions. ....	49
Figure 51. Original and new proposed conditions (overlaid on existing conditions) minimum scour elevations for both measured and scaled for Pier 5 at 30,000 cfs flow conditions. ....	49
Figure 52. Location and elevation of unscaled scour depths. ....	53
Figure 53. Correlation of scour depth vs. WSE for existing condition tests. ....	56
Figure 54. Correlation of scour depth vs. velocity for existing condition tests.....	56
Figure 55. Correlation of scour depth vs. WSE for original proposed condition tests. ....	57
Figure 56. Correlation of scour depth vs. velocity for original proposed condition tests. ....	57
Figure 57. Comparison of total head loss through the bridge and scour elevation for 15,000 cfs flow case.....	58

Figure 58. Comparison of total head loss through the bridge and scour elevation for 30,000 cfs flow case. ....	59
Figure 59. Cross section at bridge through scour holes for existing and original proposed minimum elevation for all tests at 30,000 cfs (un-scaled values and no channel degradation, circle represents location of maximum scour).....	61
Figure 60. Cross section at bridge through scour holes for existing, original and new proposed minimum elevation for all tests at 30,000 cfs (un-scaled values and no channel degradation, circles represent the maximum scour). ....	62
Figure 61. Test 11 (30,000 cfs original proposed conditions) pre-test lidar scan. ....	63
Figure 62. Test 12 (30,000 cfs original proposed conditions) pre-test lidar scan.....	64
Figure 63. Test 11 (30,000 cfs original proposed conditions) post-test lidar scan. ....	64
Figure 64. Test 12 (30,000 cfs original proposed conditions) post-test lidar scan. ....	65
Figure 65. Test 11 (30,000 cfs original proposed conditions) pre- minus post-test lidar survey (blues indicate deposition and yellows/reds indicate scour). ....	65
Figure 66. Test 12 (30,000 cfs original proposed conditions) pre- minus post-test lidar survey (blues indicate deposition and yellows/reds indicate scour). ....	66

## Tables

Table 1. Collected data for round pier tests.....	23
Table 2. Scale factors from literature data and corresponding exponents. ....	26
Table 3. Scaled and un-scaled BNSF bridge pier set scour depths. ....	27
Table 4. Test conditions for each test, discharge and approach depth. ....	32
Table 5. Scour data collected from all tests. ....	50
Table 6. Percentage Improvement from original proposed to existing conditions test.....	52
Table 7. Percentage Improvement from new and original proposed to existing conditions test for 30,000 cfs flows only. ....	54
Table 8. Correlation of various variables.....	55
Table 9. Percentage increase above existing conditions in velocity between the piers. ....	58

## Preface

This study was conducted for the U.S. Army Engineer District, Los Angeles (SPL), under project identification “Local Scour Study at the BNSF Railway Bridge.” The technical monitors for SPL were Dr. Shih “James” Chieh, Project Engineer; Mr. Robert H. Kwan, Design Section Chief; and Mr. Rene A. Vermeeren, Hydrology and Hydraulics Branch Chief.

The work was performed by the U.S. Army Engineer Research and Development Center (ERDC), Coastal and Hydraulics Laboratory (CHL), River Engineering Branch (CEERD-HFR) of the Flood and Storm Protection Division (CEERD-HF). At the time of publication, Mr. Keith W. Flowers was Chief, CEERD-HFR; Dr. Cary A. Talbot was Chief, CEERD-HF. The Deputy Director of ERDC-CHL was Mr. Jeffrey R. Eckstein, and the Director was Mr. José E. Sánchez.

COL Bryan S. Green was the Commander of ERDC, and Dr. David W. Pittman was the Director.

## Unit Conversion Factors

Multiply	By	To Obtain
acres	4,046.873	square meters
acre-feet	1,233.5	cubic meters
cubic feet	0.02831685	cubic meters
cubic yards	0.7645549	cubic meters
degrees (angle)	0.01745329	radians
degrees Fahrenheit	(F-32)/1.8	degrees Celsius
feet	0.3048	meters
gallons (U.S. liquid)	3.785412 E-03	cubic meters
inches	0.0254	meters
microns	1.0 E-06	meters
miles (U.S. statute)	1,609.347	meters
pounds (force) per square foot	47.88026	pascals
square feet	0.09290304	square meters
tons (2,000 pounds, mass)	907.1847	kilograms
yards	0.9144	meters

# **1 Introduction**

## **1.1 Purpose**

This U.S. Army Engineer and Development Center (ERDC), Coastal and Hydraulics Laboratory (CHL), effort contains a description of the process to construct, apply, and evaluate a general physical model of the bridge piers and abutments of the Burlington Northern Santa Fe (BNSF) Railway crossing on the Santa Ana River near Corona, CA (Figure 1). Data from the general physical model provide a qualitative and quantitative evaluation of the scour behavior at the estimated worst-case scenario flow conditions for the current bridge configuration, original and new proposed alternative. The proposed alternatives include using a concrete cap (pile enclosure), pier nose extensions, and flow guide walls to protect the existing bridge piers.

Extensive research has gone into the evaluation of the feasibility of using pier nose extension for local scour reduction at the BNSF Railway Bridge. The 1:30 scale movable bed physical model is the culmination of this multi-year study. Documentation for the study has been a priority. In all, there are five letter reports, one technical note, and one technical report (the main text of this report). The two letter reports are included as Appendices D and E. Additionally, the technical note Sharp et al. (2016) is Chapter 4 of the main text of this document.



Figure 1. Location map of BNSF Railway Bridge above and domain below.



## 1.2 Background

The BNSF railroad bridge carries three rail lines across the Santa Ana River near Corona, CA (Figures 2 and 3). The first trestle for the bridge was built in 1938 with two more added in 1995. The bridge has seven spans and is supported in six locations, each of which consists of a set of three piers. Each set of piers includes three individual piers, two that are round (1995) and one that is parallelogram shaped (1938) (Figure 3). The piers are supported by a steel pile foundation. The bridge is at a skewed angle across the Santa Ana River. The U.S. Army Corps of Engineers

(USACE), Los Angeles District (SPL), is investigating the effect of proposed changes in the maximum controlled release discharge from Prado Dam (located upstream of the study site) on downstream channel degradation and pier scour at the BNSF railway bridge. The Santa Ana River has a history of medium- to large-scale flooding. One of the largest recorded floods occurred in March 1938—the peak volumetric flow rate reached approximately 100,000 cubic feet per second (cfs) at Riverside Narrows (Los Angeles River). In response to the damages caused by this flood, the USACE constructed Prado Dam. Following completion of construction in 1941, Prado Dam has maintained releases of 10,000 cfs or less as limited by its outlet works capacity. Improvements along the Lower Santa Ana River provide 190-year level (0.0053 annual exceedance probability) of protection under future watershed conditions with the influence of Seven Oaks Dam, which became operational in 1998, and the newly completed Prado Dam outlet works in 2008 with a release capacity of 30,000 cfs. The increase of Prado Dam release will cause serious scouring of the BNSF Railway Bridge piers immediately downstream of Prado Dam. The SPL aims to identify an effective and cost-efficient approach that will protect the BNSF railway bridge from scour caused by increased discharge from Prado Dam. To achieve this, the SPL has proposed flow guide walls protecting the outer piers and abutments and a concrete cap protecting the pier footings (Figure 4). Additionally, pier nose extensions are proposed for the four inner sets of piers supporting the BNSF Railway Bridge (Figure 4) with the intent of moving local scour away from the bridge piers. The original proposed alternative was tested, but due to construction challenges, a new proposed alternative (wider and longer) was required (Figure 4).



Figure 2. BNSF Railway Bridge pier set 6 and west abutment.

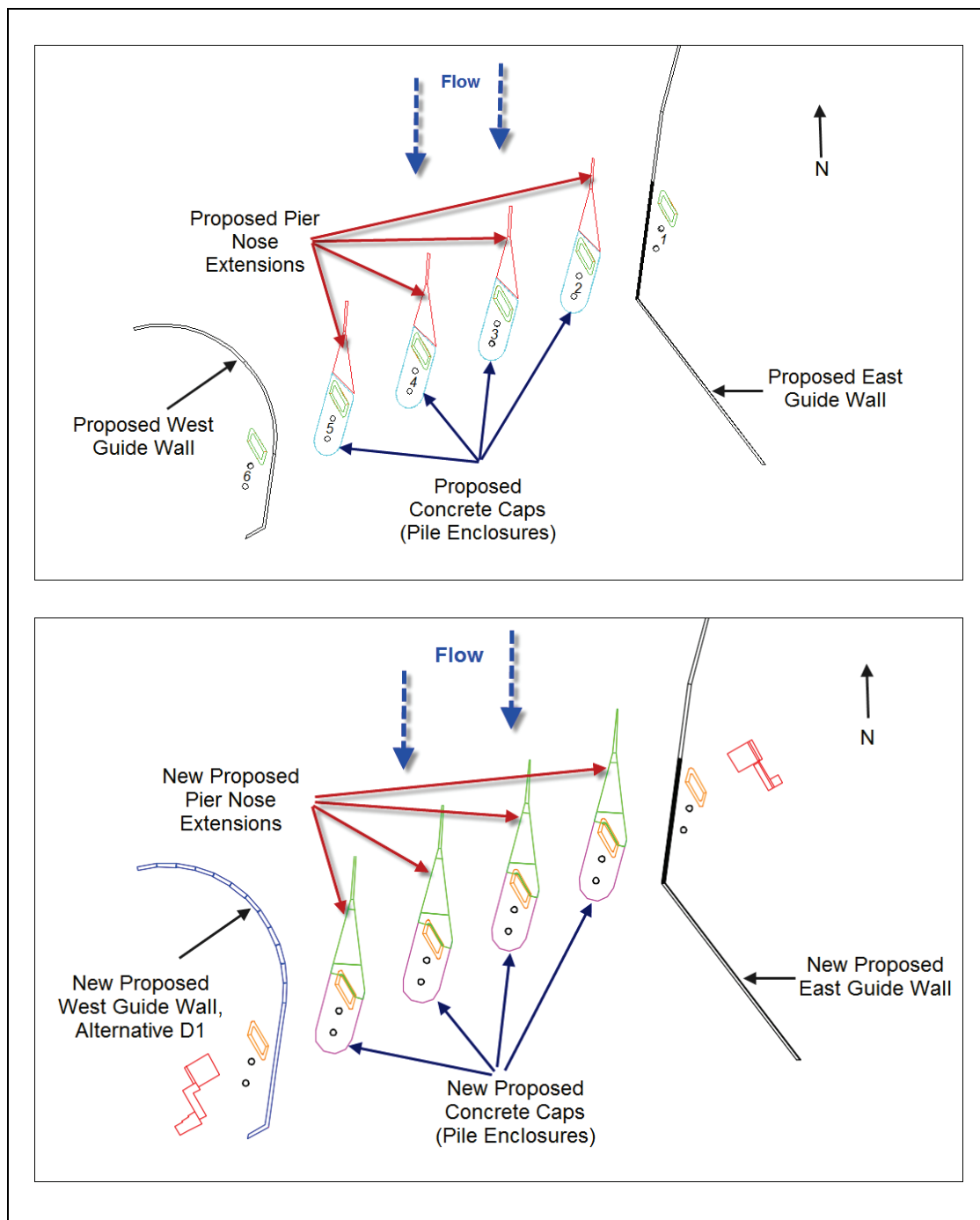


Figure 3. BNSF Railway Bridge showing alignment of trestles to piers.





Figure 4. BNSF Railway Bridge crossing on the Santa Ana River near Corona, CA; original proposed alternative (above) and new proposed alternative (below).





### 1.3 Model history

Multiple levels of evaluation have been conducted to test the proposed alternative. A one-dimensional (1D) numerical model was constructed by the SPL to calculate the velocities at the bridge. However, there was no available dataset to evaluate the performance of the 1D model. The ERDC CHL constructed a two-dimensional (2D) depth-averaged, finite element hydraulic model to compare with the 1D model. The 1D and 2D models were shown to be within a reasonable level of agreement in terms of maximum velocity. Additional details of the 1D and 2D numerical model comparison are found in Appendix D.

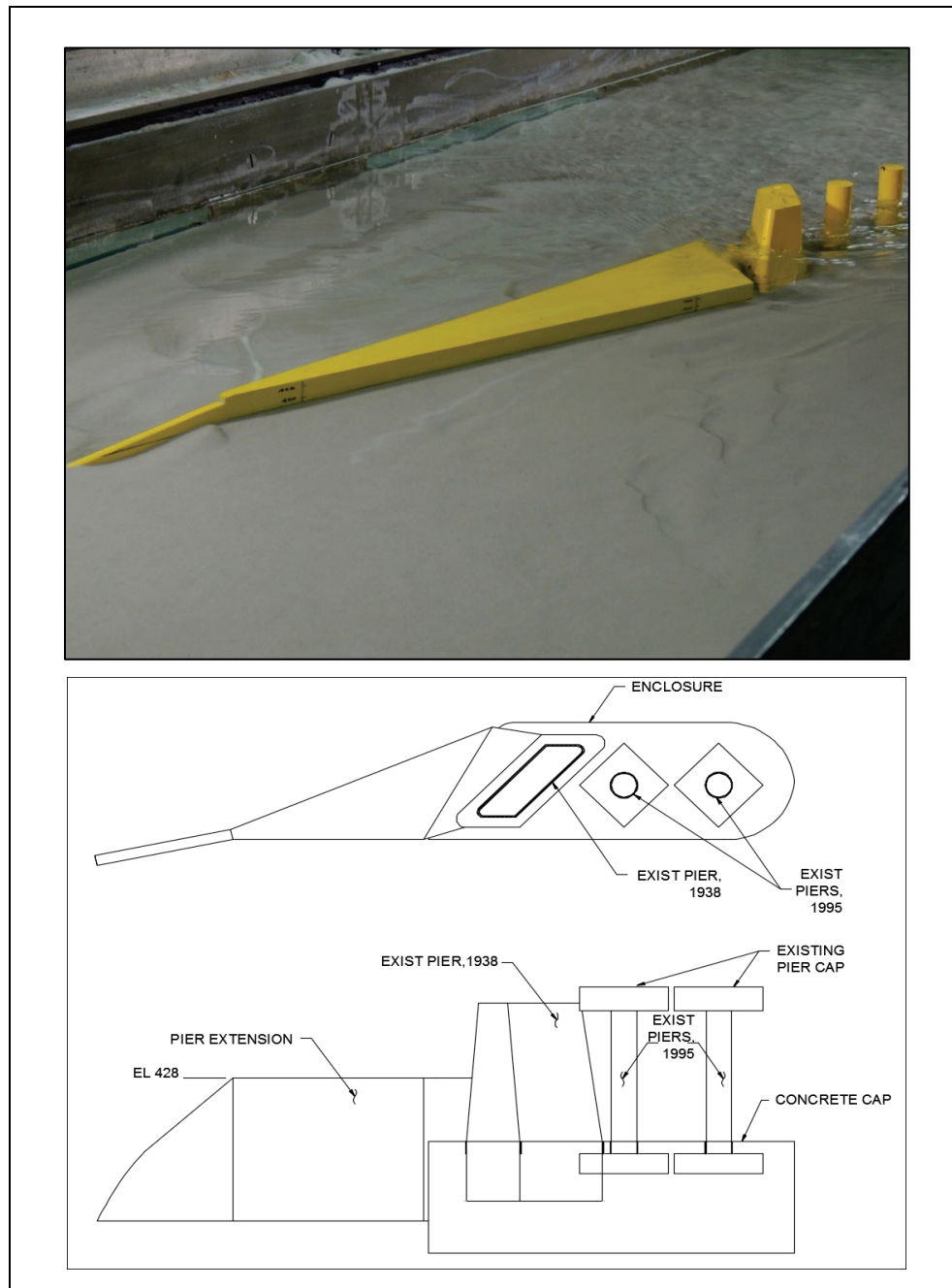
Around the piers and for a range of flows, the 2D numerical model showed an increase in the maximum velocity from existing to proposed conditions, which include the guide walls, the concrete caps, and the pier nose extensions. The increase in maximum velocity ranged from 1 to 6 feet per second (fps) (Sharp and Heath 2014). The 2D numerical model is not capable of simulating local scour at the bridge piers; therefore, a section physical model of a single set of piers (one of the six) was recommended to estimate the difference in local scour at the BNSF railroad bridge piers with and without the proposed concrete cap and pier extensions (see Appendix E).

The intent of the proposed pier extensions is to move local pier scour upstream or away from the BNSF railroad bridge piers and to streamline flow under the bridge. A 1:67 Froude-scaled section physical model of a single set of piers was constructed in a tilting bed flume at the CHL in Vicksburg, MS (Figure 5). Clear-water scour conditions were generated and repeated for multiple tests in the section model. The analysis represents a qualitative evaluation of local scour at pier set 4 of the BNSF railroad bridge and showed potential benefit in reducing the scour depth.

From the section model analysis, it was determined that a general physical model representing all the bridge piers was necessary to provide a quantitative estimate of local pier scour. The general model incorporates the hydraulic interactions of the flow alignment, skewed bridge piers, pier extensions, flow guide walls, and concrete cap and their impact on the scour depth. Additionally, higher-order terms not understood or captured by the 1D and 2D models are captured in the 3D effects of the general physical model. Thus, the SPL elected to pursue the construction and implementation of a general model representing all key hydraulic features at the site. Testing in the general physical model was conducted on the existing conditions, original, and new proposed alternatives. The section-

model proposed alternative was optimized for length, and alignment by the Federal Highway Administration in collaboration with Argonne National Laboratory (Lottes et al. 2015).

Figure 5. Section model of proposed conditions (above) and original pier extension design (below).



## 1.4 Approach

The approach is outlined in Chapter 2, Process and Setup.

## 2 Process and Setup

Three conditions were tested: (1) existing (without project), (2) original proposed (with project) and (3) new proposed (with project), which also included two sensitivity tests. The existing conditions represent the current prototype configuration exposed to potentially larger future dam releases. The original proposed condition includes the ideal pier nose extensions, concrete caps (pile enclosures), and flow guide walls (Figure 4). After the completion of the original proposed conditions, the SPL proceeded with final design. However, within the final design phase, concerns were raised over constructability issues and setback requirements around the existing piers. Thus, a redesign was required that included changes to all three protective components of the original proposed design generating the new proposed design. The sensitivity tests evaluated the impact of long-term channel degradation for both current bathymetry and a modified version for the original design.

As previously demonstrated in the section model (see Appendix D), the intent of the pier extensions is to move scour upstream and/or away from the BNSF railroad bridge piers. Furthermore, the pier extensions and flow guide walls will streamline the flow through the bridge. Additionally, the concrete cap will provide robust protection to the pier footings. The concrete cap will behave similarly to a shallow load-bearing pier footing, where the top of the cap can experience exposure but it stops the scour hole from deepening farther.

### 2.1 Model construction

The general model was constructed as a 1:30 Froude-scaled model of the bridge piers, other related structures, and the adjacent channel. The model was constructed in a 200 × 55 feet (ft) flume at the CHL (Figure 6). The model scale was selected based on the width (55 ft) and depth (3 ft) of the flume. The flume dimensions using a 1:30 scale model provided the correct prototype over bank and approach length distances around the bridge (Figure 7). The floor of the flume was set to a prototype elevation of 392 ft\* and allowed scour to occur to the bottom of the pile caps. A fixed bench mark on the floor of the flume was established for the vertical control. With a channel invert at the bridge of 410 ft, the floor elevation provided 18 ft of available scour depth at this minimum elevation.

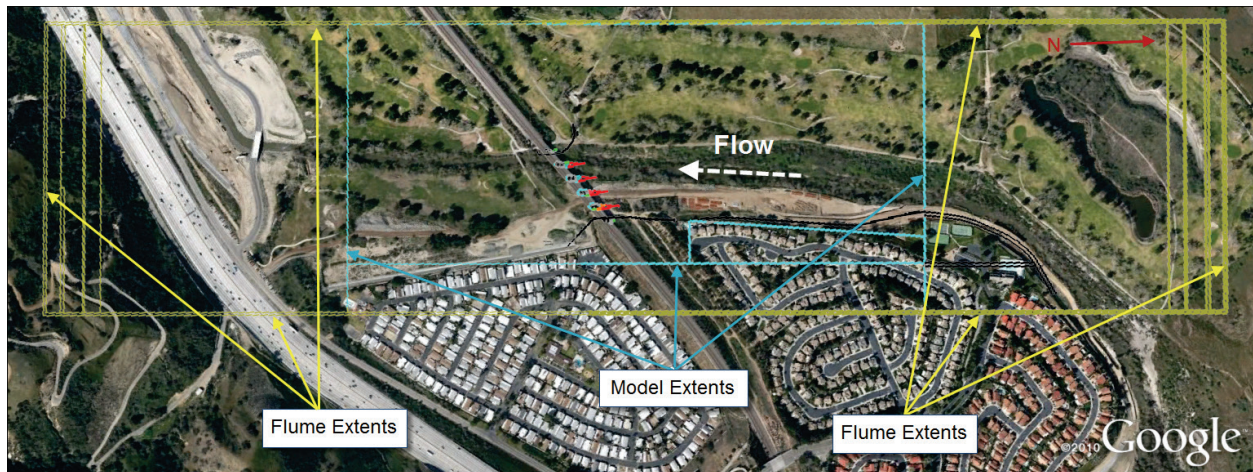
---

\* Elevations are referenced to the National Geodetic Vertical Datum (NGVD) of 1929.

Figure 6. View of flume prior to model construction.



Figure 7. Flume and general model extents overlaid on Google Earth image.



The general model domain length covers 3,200 ft of the Santa Ana River. Approximately 1,300 ft are downstream of the bridge while the approach to the bridge is 1,900 ft (Figure 7). The over banks and channel width are 1,100 and 1,300 ft wide upstream and downstream, respectively. Though flooding could occur beyond this defined width, it would occur primarily on the west side of the channel. The excluded overbank area would have



minimal impact since the flow depth in the over bank area at the maximum dam release is less than 1.5 ft and is primarily water storage.

All key structural features and abutments of the bridge were constructed in the general physical model (Figure 8). In addition to these, the topography and bathymetry of the site were included in the model. While this presented a higher level of difficulty for construction and operation, it provided a more realistic representation of the site. Existing prototype condition cross sections were established every 120 ft with elevation stations at 30 ft increments. This produced a total of 28 cross sections defined within the model domain with the most-upstream and downstream cross sections being fixed plywood templates anchored to the flume floor (Figure 9). These two plywood templates defined and contained the longitudinal extents of the model domain. The lateral extents were defined with the concrete flume wall on the right descending side and a constructed plywood wall on the left descending side. The same cross sections were used for all test configurations with the exception of one of the sensitivity tests, which had a modified channel around two of the pier sets.

Figure 8. Construction of existing pier structures during model construction.

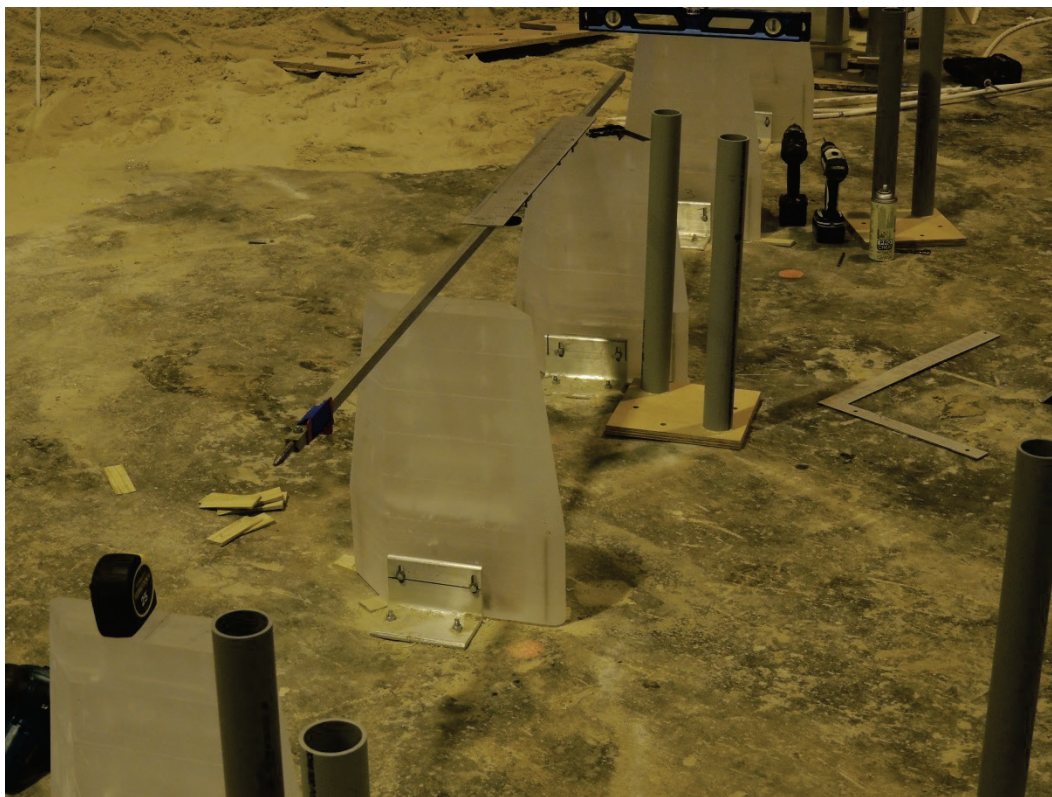
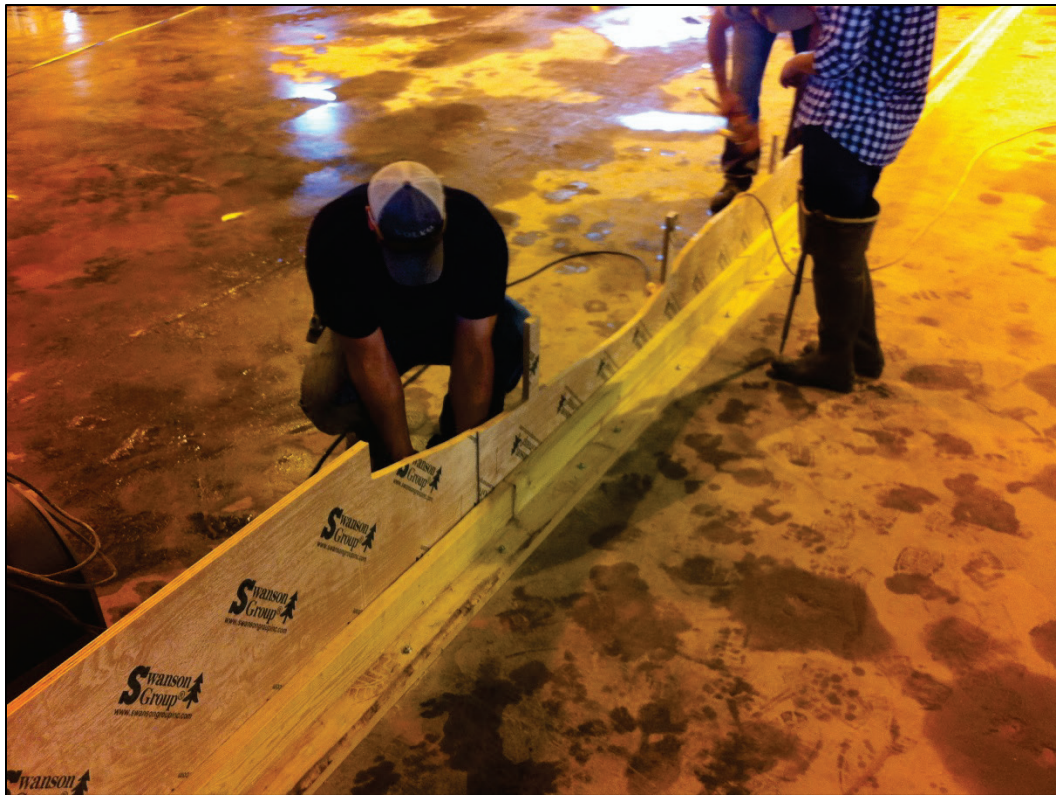




Figure 9. Vertical alignment of fixed plywood template that defines upstream extents.



## 2.2 Lidar

After each test, the domain was remolded to match the existing prototype condition cross sections. To determine changes in the bed geometry, both pre- and post-test lidar scans were taken (Figure 10). To facilitate positioning of the scans, a local coordinate system was established to tie the required multiple scan positions into the same plane. The local system used 21 control points stationed at various elevations around the hangar. Then a MATLAB code was written to scale, translate, and geo-reference the lidar scans into prototype coordinates and units. The lidar scans provided more than 2 million points of coverage and encompassed the entire model domain. The resolution is 0.065 ft horizontally with a vertical error of 0.009 ft, which represents 1.95 and 0.295 ft at prototype. Thus, collected scour depth data will have an error of  $\pm 0.3$  ft at the prototype scale.

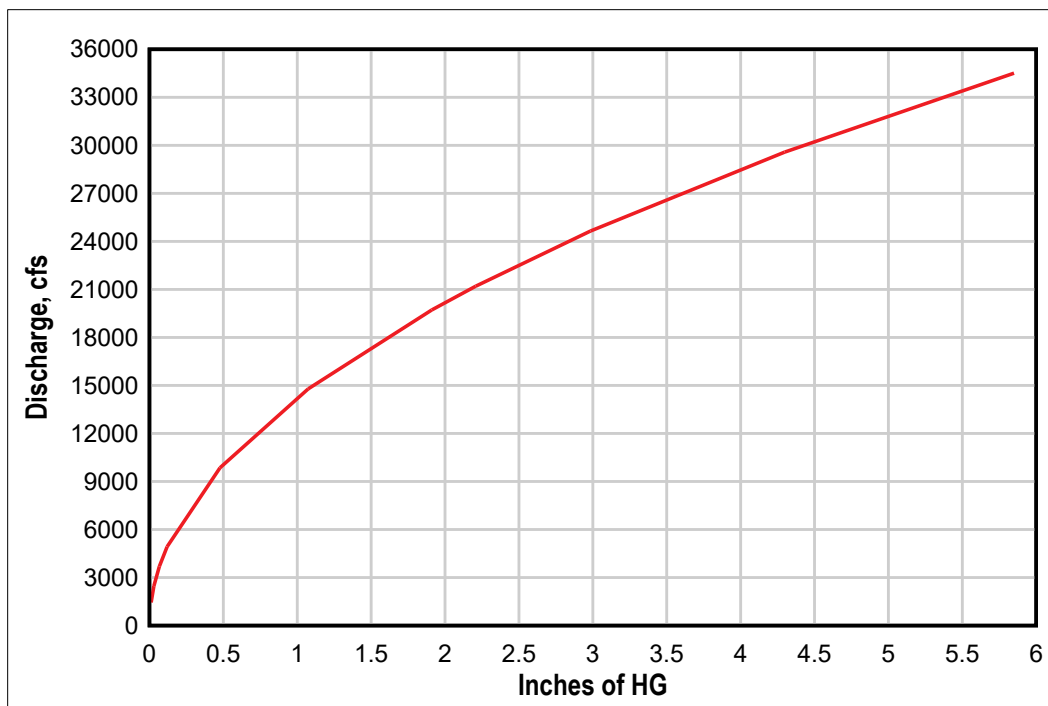
Figure 10. Lidar measurement of the bed post-test.



## 2.3 Boundary conditions

Two steady state flow conditions were simulated in the general physical model. Flow was set with a gate valve and was measured with a differential manometer (the head differential in the meter is measured in inches of mercury [hg]) across a BIF  $12 \times 7.25$  in. Venturi meter (Figure 11). Selection of the two flow cases was made based on the highest design release from Prado Dam and one with a water surface elevation (WSE) corresponding to the height of the proposed pier nose extensions (428 ft): 30,000 cfs and 15,000 cfs, respectively. For the sensitivity tests, only the 30,000 cfs flow was tested, and with the degraded channel, the WSE was near the top of the pier nose extensions. For the new proposed design, only 30,000 cfs flow was tested. These two flow conditions (greatest discharge that has the deepest flow depth and the discharge corresponding to the water surface at the elevation of the top of the pier extension) represented the presumed worst-case flow conditions (see Appendix D). The selection was based on information from the traditional selection criteria (deepest flow depth associated with high flow) and section physical model tests. The section physical model indicated that the worst case might be when the flow is at the top elevation of the pier nose extension.

Figure 11. Head differential for BIF 12 × 7.25 venturi meter.



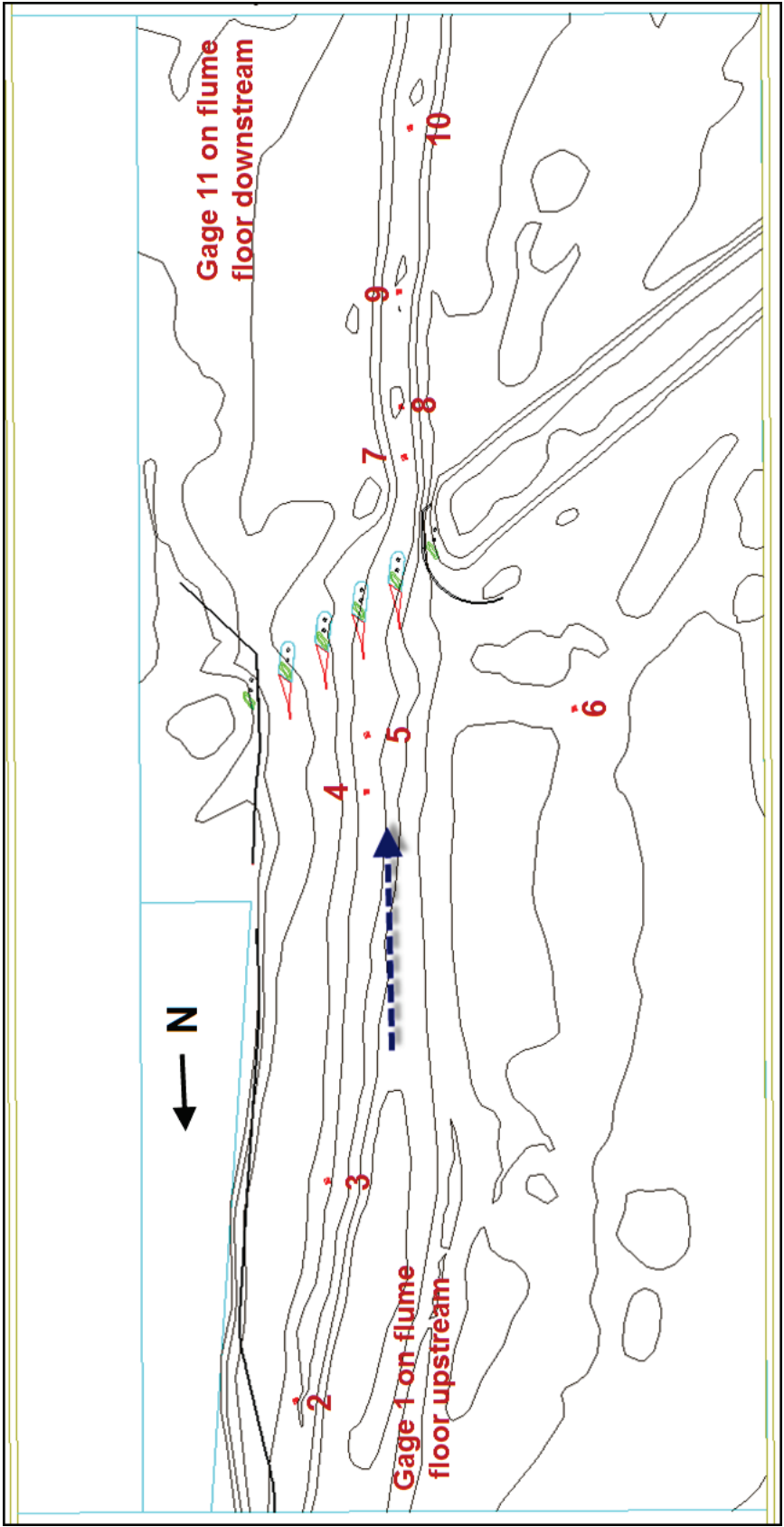
The flow was scaled using the Froude criteria, since the vertical acceleration component is critical for local pier scour. The vertical acceleration can only be satisfied with exact geometric similitude and is only possible through Froude similitude (Julien 2002). In the absence of field data, the Froude number from the numerical models was used (0.27 – 0.34). The Froude number for both the general model flow conditions was 0.29 (30,000 cfs) and 0.28 (15,000 cfs).

The model was configured for clear-water scour conditions, which provided the worst-case scour depth in the shortest amount of run time. Simulation times at model scale for all tests ranged between 600 to 1,400 minutes (2.5 to 7 days at prototype). For both flows, boundary conditions (tailgate settings and flow rates) were defined in the existing conditions configurations. The boundary conditions provided the correct flow depth at the bridge, Froude number, and energy loss through the bridge for the existing conditions. The same settings were then applied for all tests.

## 2.4 Data collection

Multiple longitudinal WSEs were measured during testing with a point gage in a series of stilling wells. Eleven locations were temporally measured and provided the energy loss through the bridge and water surface profiles during testing (Figure 12). The gage farthest downstream, gage 11, was beyond the model domain and provided a control/check for the tests. The boundary conditions were verified for the existing and proposed tests using this same downstream-most stilling well. Additional data collection included relative approach velocities upstream of each pier set, relative velocities between pier sets, velocity profiles, and scour depth measurements. Velocity data were taken with an electromagnetic velocity probe. Scour depth measurements were taken during testing with the model rod and automatic level in addition to pre- and post-test lidar surveys. Furthermore, during some of the tests, an array of single-beam fathometers were used to take scour depth measurements at pier 5. When a change of less than 0.25 ft was observed over a 4-hour run time period, the scour was considered to be at quasi-equilibrium. These measurement methods provided at least two and in some cases three checks on maximum scour depth to check scour hole depth before and after dewatering. Later, a scale factor was applied (Chapter 3 or Sharp et al. [2016]) to the measured values to yield a minimum and maximum scaled scour elevation.

Figure 12. Location of stilling well gages shown with proposed conditions and pre-test bathymetry contours.



## 2.5 Test Outline

- I. Existing conditions (six tests – Tests 1-6) Original proposed concrete caps design, proposed west wall Alternative A, and original proposed pier extensions design (top elevation 428 ft) (four tests – Tests 7–10)
- II. Original proposed concrete caps design, proposed west wall Alternative A, original proposed pier extensions design (top elevation 428 ft), and raised piers (two – five) by a height of 6 inches (in.) (15 ft prototype) (one test – Test 11)
- III. Original proposed concrete caps design, proposed west wall Alternative A, original proposed pier extensions design (top elevation 428 ft), raised piers (two – five) by a height of 6 in., and new bathymetry in the immediate area of piers four and five (one test – Test 12)
- IV. New proposed concrete caps design, proposed west wall Alternative C (top elevation 428 ft), new proposed pier extensions design (top elevation 428 ft), and proposed pier extension enclosure structures (one test – Test 13)
- V. New proposed concrete caps design, proposed west wall Alternative D1 (top elevation 428 ft), new proposed pier extensions design (top elevation 428 ft), and proposed pier extension enclosure structures (one test – Test 14)
- VI. New proposed concrete caps design, proposed west wall Alternative D1 (top elevation 433 ft), new proposed pier extensions design (top elevation 428 ft), and proposed pier extension enclosure structures (one test – Test 15)
- VII. New proposed concrete caps design, proposed west wall Alternative D1 (top elevation 428 ft), new proposed pier extensions design (top elevation 420 ft), and proposed pier extension enclosure structures (one test – Test 16)

### 3 Scale Factor

This chapter contains a description of the process used to generate a scale factor for the general model. A separate flume study was conducted for the scale factor. Data from the scale factor study provides an adjustment for applying documented scour behavior from round piers to a non-typical parallelogram tapered pier and proposed pier nose extension found at the BNSF Railway Bridge. The scale factor establishes the worst-case scour depth for the current bridge configuration and the proposed pier nose extension.

#### 3.1 Introduction

Extensive research has been conducted for local scour around typical pier shapes (round, square, diamond, etc.) with the most commonly studied shape being the round pier. Multiple studies for round piers have been conducted in flumes, as well as field observations (Breusers et al. 1977; Chiew 1984; Kothyari et al. 1992; HEC-18 2012; Melville and Chiew 1999; Lee and Sturm 2009; Mia and Nago 2003; Mueller and Wagner 2005). Multiple predictive equations have been formulated from pier scour studies to provide conservative estimates of maximum scour depth (Laursen and Toch 1956; Shen et al. 1969; Breusers et al. 1977; Jain and Fischer 1979; Melville and Sutherland 1988; HEC-18 2012). The maximum scour depth is then applied in the design of footing depths for bridge piers. The most commonly used equation for calculating maximum scour depth is the HEC-18 equation, but it is only applicable for typical pier shapes (HEC-18 2012). When non-typical complex pier shapes are used, such as those illustrated in Figure 1, the recommended practice is to conduct a physical model study (HEC-18 2012). Thus, the application of historic field and flume data along with the HEC-18 equation is replaced with measurements made in a physical model.

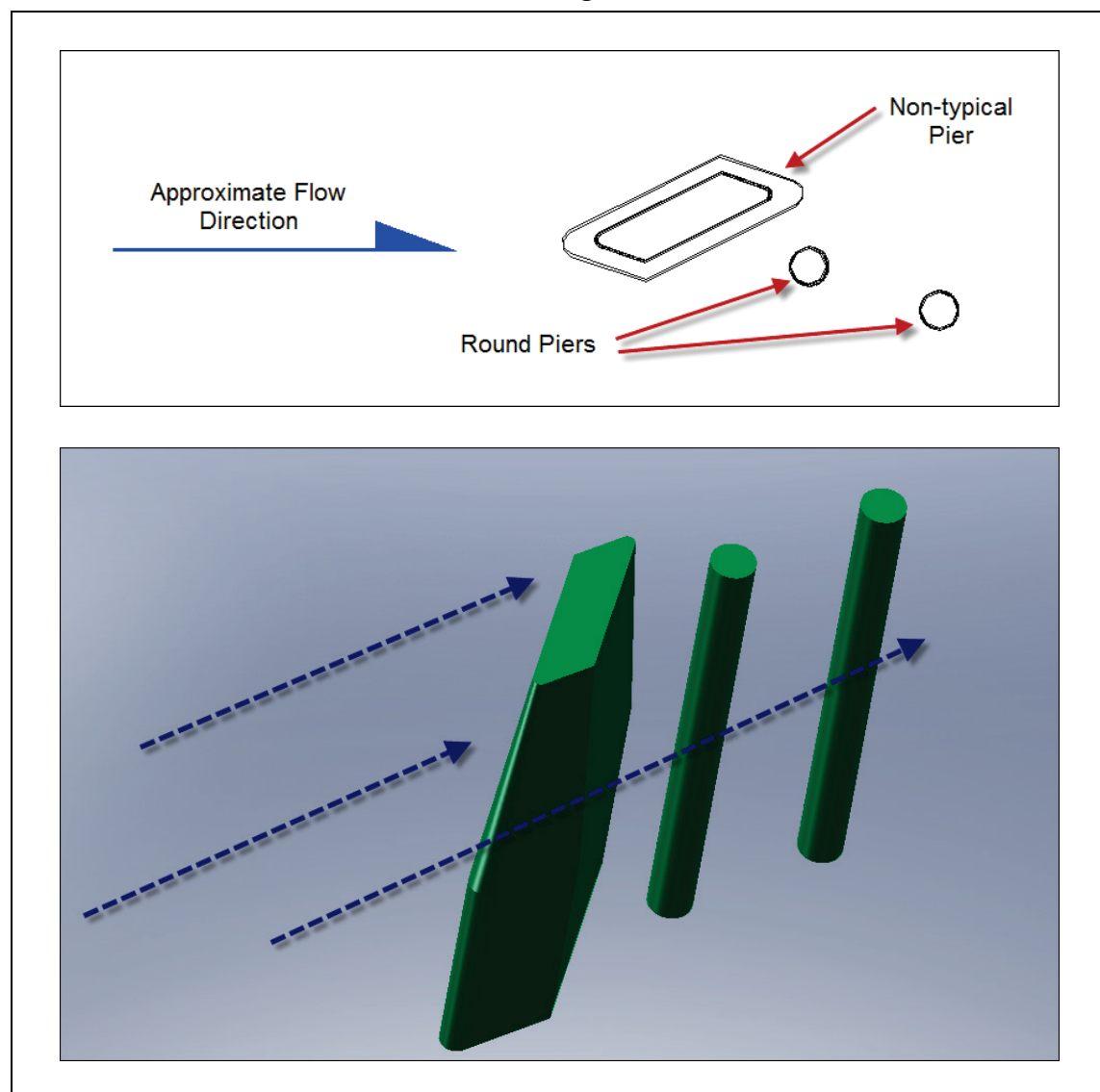
Prior to construction and testing of the 1:30 general physical model of the BNSF Railway Bridge, model scale conversion ratios, domain bounds, and the overall configuration were established. In addition to the typical model scale conversion ratios, a new model scale factor ratio specific to the model bed material (uniformly graded medium sand) at 1:30 scale was formulated for local scour at round piers. The model scale factor ratio for local scour was formulated in this scale test and established a conservative



adjustment for local scour depth for the atypical pier configuration used in the general model.

As formulated here, the scale factor provides a scour depth adjustment comprised of two components. The first component is scale effects due to model issues and is the primary focus of this effort. The second component addresses concerns regarding the safety factor formulated in the HEC-18 equation. In this effort, a scale factor range was produced to provide a minimum and maximum for local pier scour at the BNSF Railway Piers (Figure 13) in the 1:30 general physical model.

Figure 13. Typical configuration of pier sets at the BNSF railroad bridge, plan view above and 3D rendering below.





### 3.2 Process and setup

To incorporate the peer-reviewed data from the literature with the non-typical bridge piers found at the BNSF Railway Bridge (Figure 13), a scale test was formulated. Fundamentally, the scale test is a comparison between the HEC-18 equation for round piers and the trapezoidal-shaped piers found at the BNSF Railway Bridge. The comparison is achieved by setting up a flume test with both typical round piers and the pier sets found at the BNSF Railway Bridge (Figure 14).

The scale test was configured with the same sediment, uniformly graded sand with a  $D_{50}$  of 0.25 millimeter (Figure 15), and scale length ratio of 1:30 used in the general physical model. A flat test section, approximately 32 ft long and 34 to 45 ft wide, was molded to a uniform elevation. Stilling well gages were placed upstream and downstream of the piers. The stilling well gages provided the slope and depth of the flow during the tests. The round piers were spaced 11.25 ft apart. Then, the two pier sets were located between the round piers but 12 ft downstream (Figure 14). This provided an approach and exit length of 10 ft. The spacing of these piers was sufficiently large enough to prevent any interaction of the currents between pier sets.

Boundary conditions were controlled with a gate valve and a tailwater lift gate. Both the head tank and tail tank were located 84 ft upstream and downstream of the test section, respectively. Discharge into the model came from three recirculation pumps with a total capacity of approximately 12.5 cfs. Flow uniformity was checked with an electromagnetic velocity meter and adjusted with upstream baffle blocks. The total discharge was measured by reading the differential from a manometer across a venturi meter and verified with a total discharge calculation from the flow uniformity checks. The WSE was controlled with the adjustable lift gate at the downstream end of the flume.

The test configuration established and maintained clear-water scour conditions, which produced consistent test results. Prior to each test, the tailgate was raised, and the test section was flooded. Once flooded, the flow was adjusted to the desired discharge. Upon setting the discharge, the tailgate was lowered to the chosen height. The height of the gate set the pre-determined flow depth at the piers. The depth was typical of what is expected at prototype scale. The average run time for each test was approximately 18 hours of model time. At various times during testing, the

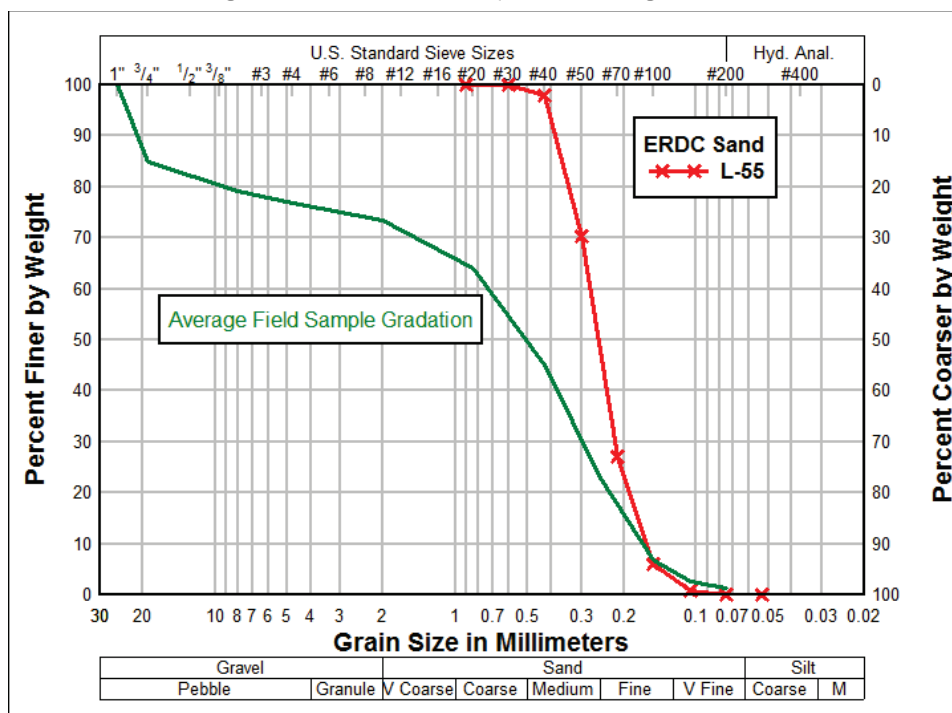
local scour depth was surveyed. Tests were run until the quasi-equilibrium scour depth was reached.

Five tests were conducted to measure the local scour at the piers. Tests 1 and 2 had three round piers. Tests 3 and 3 had three round piers and two pier set configurations like those found at the BNSF Railway Bridge. Test 5 had only two round piers since a higher unit discharge was required and achieved by narrowing the flume from 45 to 34 ft. These five tests provided 14 scour-depth data points for the round piers and 6 for the BNSF pier sets. Collected data included approach velocities and depths, discharge, water-surface slope, and maximum-scour depth. From these five tests, three different flow depths (reported here at prototype scale) were evaluated: 9, 14, and 17 ft. The depth selection was based on mean flow depths expected at prototype. For each test, clear-water scour conditions were generated. At the end of each simulation, the observed scour rates were essentially zero, indicating that a quasi-equilibrium condition had been attained. Sediment transport into the test section was negligible; however, small perturbations upstream (from dye insertion or velocity measurements) caused ripples to form. The measured scour depth is believed to be reasonable for quantitative comparisons between the evaluated configurations. Note that the results are reported in prototype dimensions; thus, the data were scaled undistorted by the length scale ratio of 1:30. Scaling to prototype was done to make direct comparisons between the model results and the actual site.

Figure 14. Test configuration of round piers and pier sets for test 5.



Figure 15. Test and prototype material gradations.



### 3.3 Results and discussion

Test results for round piers showed scour depth increasing as flow depth increased (Table 1 and Figure 16). The flow depth and scour depth correlation of 0.80 for the tests is illustrated in Figure 16 and is expected (Laursen 1953). As stated in ASCE Manual 54 (Vanoni 2006; 38), “the equilibrium (scour) depth appears to depend only on the initial depth of flow and to be independent of both the mean velocity and the sediment characteristics.” Thus, the greatest scour depth for these tests occurred with the 16.9 ft flow depth, and the lowest scour depth occurred with the 9.1 ft flow depth with 6.7 and 3.4 ft of scour respectively (Table 1 and Figure 16).

For the selection of the scale factor, it was decided to use the maximum and minimum from the five tests shown in Table 1, thereby bracketing the 14 scour depth measurements into a scale factor range that would provide the most and least conservative scour depth estimates. Figure 16 shows the results from all the tests.

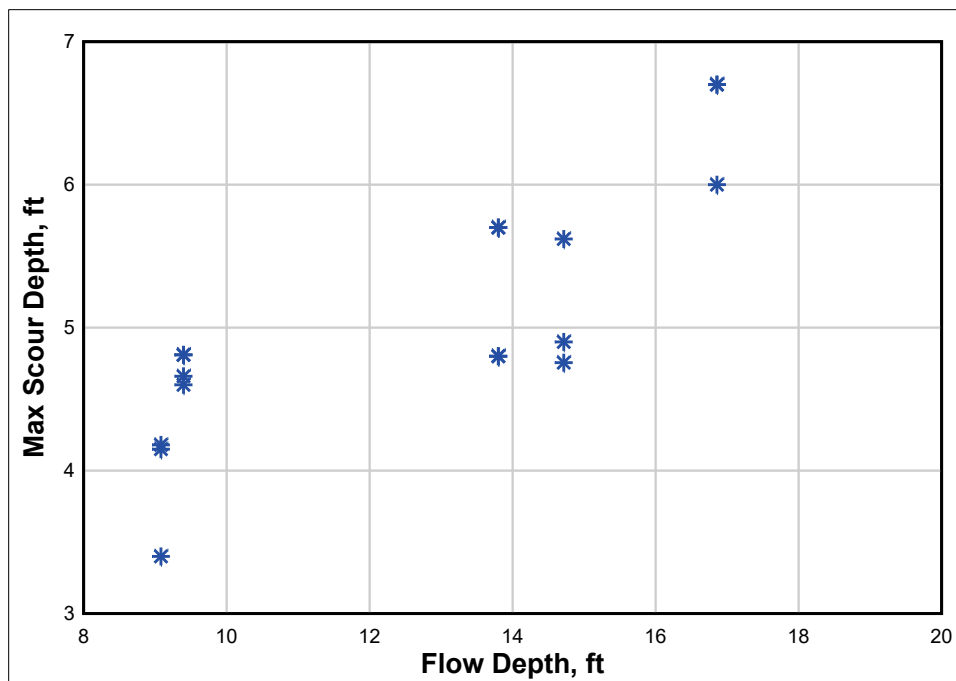
As with the round piers, a similar pattern of increasing scour depth with flow depth was shown with the BNSF bridge pier sets. Since multiple tests with the BNSF pier sets were not conducted, the pier sets are only used in demonstrating the application of the model scale factor ratio for local pier scour.

Table 1. Collected data for round pier tests.

Collected Data from Round Pier Tests						HEC-18 Scour Depth	Scale Factor
	Pier Location	Flow Depth, ft	Scour Depth, ft	Approach Velocity, ft/s	Unit Discharge, cfs/ft		
Test 1	Left	14.7	4.90	2.92	42.99	7.62	1.55
	Center	14.7	5.62	2.87	42.25	7.56	1.35
	Right	14.7	4.76	2.94	43.31	7.64	1.61
Test 2	Left	9.1	4.18	3.18	28.90	7.41	1.77
	Center	9.1	4.15	3.28	29.75	7.50	1.81
	Right	9.1	3.40	3.19	28.94	7.41	2.18
Test 3	Left	9.4	4.66	3.02	28.34	7.27	1.56
	Center	9.4	4.81	3.11	29.22	7.37	1.53
	Right	9.4	4.60	3.02	28.38	7.27	1.58
Test 4	Left	13.8	4.80	3.32	45.79	7.98	1.66
	Center	13.8	5.70	3.44	47.42	8.10	1.42
	Right	13.8	4.80	3.33	45.90	7.99	1.66
Test 5	Left	16.9	6.00	3.58	60.37	8.47	1.41
	Center	16.9	6.70	3.67	61.80	8.56	1.28

Within each test, the variations in scour depth at the different piers are attributed to two main factors. First, there were slight variations in the approach flow depth that is reflected in the small discrepancy in unit discharge. Since scour depth is directly dependent on the approach flow depth (Figure 16), the variation can impact the final scour depth. Second, the test section was molded with an accuracy of +/- 0.5 ft from the assumed initial prototype elevation of 414 ft. For all scour depth measurements, 414 ft was used as the start elevation. Prior to running, the bed was surveyed adjacent to the piers but was not surveyed in the approach. If one pier started at a higher or lower approach bed elevation, then there would be a variation in the approach depth resulting in variations in scour depth.

Figure 16. Maximum scour depth for round pier test.



### 3.4 Application

Two different methods were used to compute the scale factor. The first was application of the HEC-18 equation (Equation (1)). With the HEC-18 equation, the scour depth was calculated based on the flow depth, Froude number, and pier geometry. Then, using the scour depths from the HEC-18 equation (7.3–8.6 ft) and the values measured in the tests (3.4–6.7 ft), a scale factor ( $S_f$ ) ratio was computed with Equation (2). The  $S_f$  ratios ranged from 1.27 to 2.18 and are shown in Table 1.

$$\frac{Y_s}{a} = 2K_1K_2K_3\left(\frac{D}{a}\right)^{0.35} F_r^{0.43} \quad (1)$$

$$S_f = \frac{Y_{sHEC-18}}{Y_{sScale\ Test}} \quad (2)$$

Where  $Y_s$  is scour depth,  $a$  is pier width,  $D$  is flow depth,  $F_r$  is Froude number,  $K_1$  is a correction factor for pier nose shape,  $K_2$  is a correction factor for angle of attack, and  $K_3$  is a correction factor for bed condition (HEC-18 2012).

The second method was based on literature data that are readily available and similar in application. Qualifiers for selected literature data included pier geometry, sand sediment (fine–course sand), flume tests, and hydraulic parameters. A total of 62 data points were applied with 23 in the correct Froude number range as shown in Figure 17. All data were plotted non-dimensionally with the ratio of scour depth to flow depth versus the Froude number as presented in Figure 17. A logarithmic regression was used for each data set. From the logarithmic equations, Equation (2) could be applied to calculate a scale factor (Equation (3)). This provided individual scale factors over the range of all available data (Table 2). The maximum and minimum values for the scale factor are 1.77 and 0.323, respectively. The range verifies that the HEC-18 equation values are reasonable. Thus, the scale factors from the HEC-18 equation formulation are applied as the model scale factors for local scour.

$$Sf = \frac{0.6803 \times \log(Fr) + 3.3135}{0.9082 \times \log(Fr) + 3.4396} \quad (3)$$

Once formulated, the application of the length scale ratio conversion factor for scour is the same as other scale conversion factors. The measured model scour depth is substituted into the equation, in the form of Equation (3) and shown in Table 2, yielding the range of prototype scour depths.

For implementation, the scale factor was applied to the scour depths measured from the pier sets (Table 3). The pier sets scoured less than that of the round piers as shown in Figure 18. This illustrates that the scale factor, by applying it to the measured values of the pier sets, produces a more conservative estimate of the maximum local scour depth.

Figure 17. Literature data as compared to scale factor test data.

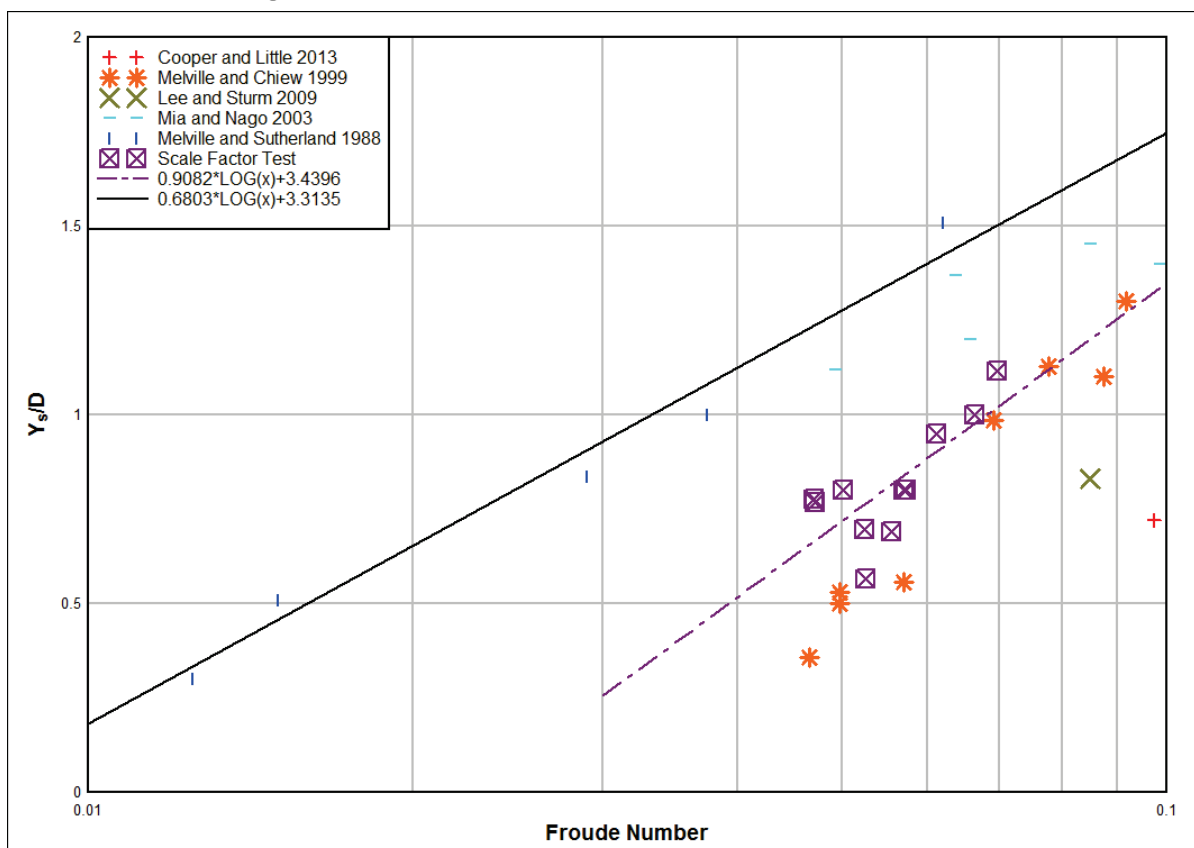


Table 2. Scale factors from literature data and corresponding exponents.

	Scale Factor Ratio (Equation (2))				
Froude Number	Melville and Sutherland (1988)	Lee and Sturm (2009)	Mia and Nago (2003)	Melville and Chien (1999)	Cooper et al. (2016)
0.050	1.77	1.61	1.67	0.68	0.32
0.055	1.66	1.48	1.52	0.76	0.37
0.060	1.58	1.39	1.40	0.82	0.40
0.065	1.52	1.32	1.31	0.86	0.43
0.070	1.47	1.26	1.24	0.90	0.45
Average	1.602	1.413	1.431	0.802	0.395
Standard Deviation	0.121	0.138	0.170	0.085	0.051
Maximum	1.774	1.609	1.673	0.896	0.451
Minimum	1.468	1.261	1.244	0.681	0.323

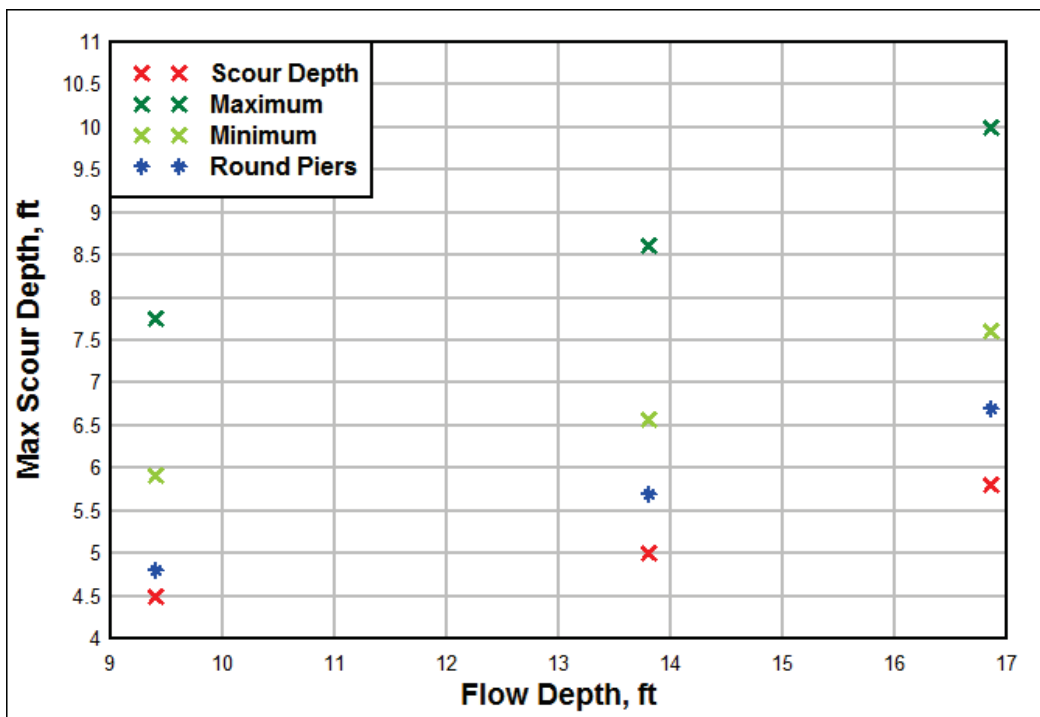
	Scale Factor Ratio (Equation (2))				
Froude Number	Melville and Sutherland (1988)	Lee and Sturm (2009)	Mia and Nago (2003)	Melville and Chien (1999)	Cooper et al. (2016)
	Corresponding x (Equation (3))				
0.050	1.17	1.14	1.15	0.89	0.67
0.055	1.15	1.12	1.12	0.92	0.71
0.060	1.13	1.10	1.10	0.94	0.73
0.065	1.12	1.08	1.08	0.96	0.75
0.070	1.11	1.07	1.06	0.97	0.77
Average	1.138	1.100	1.104	0.934	0.725
Standard Deviation	0.022	0.028	0.034	0.032	0.039
Maximum	1.169	1.140	1.151	0.968	0.766
Minimum	1.113	1.068	1.064	0.887	0.668

Table 3. Scaled and un-scaled BNSF bridge pier set scour depths.

Pier Set Scour and Scaled Scour Depths				
	Flow Depth, ft	Scour Depth, ft	Calibrated Scour Depth, ft	
			$Y_s = LR1.16$	$Y_s = LR1.08$
Test 3	9.40	4.50	7.75	5.91
Test 4	13.80	5.00	8.62	6.56
Test 5	16.86	5.80	9.99	7.61



Figure 18. Scaled and un-scaled BNSF bridge pier set scour depths as compared to round piers.



### 3.5 Recommendation

The scale factor as formulated here is intended only for the use at the BNSF bridge piers. Other locations with complex pier geometry would require a similar test to formulate a site-specific scale factor. The scale factor should be applied to the measured values from the general model to provide confidence that the estimated scour depths are slightly greater than what can be expected at the site. A conservative estimate of local scour depth provides a sufficiently deep protection plan for the pier footings to minimize the risk of potential undermining.

## 4 Uncertainties

There are several uncertainties that if significant in the prototype and not properly captured by the model would directly alter the behavior of the general physical model. The uncertainties outlined here are the only ones currently known. Other undefined conditions or higher order terms might exist which could alter the behavior of the general physical model. The known uncertainties associated with the general physical model testing are the following:

- The model uses uniformly graded sand that represents the critical shear for the D90 at the prototype scale. However, there are sources of larger material capable of armoring the bed. If the larger materials were mobilized, they would migrate to fill the scour hole, and scour could be stopped.
- With the use of uniformly graded sand, there is no consideration for cohesive material. Clay and silt sediment could impact the behavior of the prototype, altering the way local scour forms and behaves. The cohesive nature of clay and silt would increase the critical shear stress required to erode the sediment, resulting in shallower scour depths or altered scour-hole geometry.
- Slick bed conditions were tested in the general model. Currently, the overbanks, banks, and channel are covered with vegetation and other roughness features (Figure 19). This roughness character was not modeled in the general physical model. These vegetative features would alter flow patterns and flow depths. An increase in water depth will increase the scour-hole depth. Alterations in flow patterns could change the scour formation sequence.
- Historically there have been channel alignment changes. Thus, there is potential for channel morphology changes that could alter the behavior of the system. The primary concern is in the flow alignment under the bridge. Any future flow direction alteration is not captured in this effort and could have changes to local scour depth.
- Only steady state flows were simulated during testing. However, the Santa Ana experiences flashy hydrographs. Rapid transitions from dry to wet can cause channel stability issues. The unsteady nature of the hydrograph can change the behavior of sediment transport and scour through the reach. This can result in alterations to local scour and associated depths.

- Natural grade controls could exist under the bed surface, which if exposed during the scour process, could alter flow depths (Figure 20). Alterations in depth would change the scour hole depth potential. Natural grade controls could be revealed through any of the uncertainties described here.
- An entrenched channel downstream of the bridge may influence future channel evolution. Variations in channel evolution could impact the scour depths and their associated locations beyond those provided in this report.

Prior to the formation of any proposed plan, it is necessary to properly vet the perceived performance with the above uncertainties. Slight alterations in the performance at prototype due to the uncertainties listed can have both beneficial and negative consequences. Understanding and maintaining realistic expectations associated with the uncertainties will aid in the proper application of the proposed condition.

Figure 19. Santa Ana River directly downstream of the BNSF Railway Bridge, looking upstream.





Figure 20. Apparent emergent rock downstream of the BNSF Railway Bridge, looking downstream.



## 5 Data and Results

A total of 16 tests were run, 2 for model set-up and adjustments and 14 for analysis. Twelve tests were simulated at 30,000 cfs and four at 15,000 cfs as shown in Table 5. The two tests for adjustments enabled clear-water scour conditions to be met and boundary conditions to be tuned for the existing conditions. The two tests (Test 1 and 3) used to tune and adjust the model still yielded usable data and are included in the results. WSE plots are shown in Appendix A, and relative approach velocity data are shown in Appendix B. Sensitivity tests were conducted for the original proposed conditions to determine the potential impact from long-term degradation. The new proposed condition was tested along with various design alterations for the West Abutment wall.

**Table 4. Test conditions for each test, discharge and approach depth.**

Test Conditions			
	Q (1000 cfs)	Test #	WSE
Existing conditions	30	1	433.44
	30	2	433.47
	30	2L	432.54
	30	2H	434.75
	15	3	428.79
	15	4	429.09
	30	5	433.59
	30	6	433.65
Original proposed conditions	15	7	429.36
	30	8	433.65
	30	9	433.56
	15	10	429.24
Sensitivity conditions	30	11	427.47
	30	12	427.38
New proposed conditions	30	13	433.37
	30	14	433.37
	30	15	433.26
	30	16	433.18



The primary location for the minimum scour elevation (maximum scour depth) occurred around pier set 5 (western-most pier set in the flow). Due to the channel geometry, the flow is focused on this set of piers. Here, the invert of the channel, in the location of scour and prior to testing, started at an elevation between 411 and 412 ft. This variation in start elevation is directly the result in the accuracy of remolding the model. For existing conditions, the minimum scour elevation (maximum scour depth) occurred on the left side of the 1938 pier (parallelogram-shaped) while for the original proposed conditions it occurred there or downstream of the 1995 south pier (circular-shaped). These two locations are denoted in Figure 21 and cover the area enclosed by the two circles in the graphic. Conversely, the maximum scour elevation (minimum scour depth) for the new proposed condition occurred on the right side of the concrete cap. The scour holes are visually represented for existing, original proposed, and new proposed in Figures 22–25.

The bathymetry prior to testing is shown in the pre-test lidar scans illustrated in Figures 26, 27, and 28. The three figures represent the typical starting bathymetry for both the existing, original, and new proposed conditions. Variations in the start bathymetry are the result of hand molding a sand bed model. Figures 29 and 30 show the post-test lidar scans for existing conditions for 15,000 and 30,000 cfs, respectively. Likewise, Figures 31 and 32 are the post-lidar scans for the original proposed conditions. Figures 33–36 are the post-lidar scans for the new proposed conditions. Figures 37–44 are difference plots of pre-lidar minus post-test lidar scans for both existing, original, and new proposed conditions at 15,000 and 30,000 cfs flows. Additional lidar scans are shown in Appendix C. The difference plots show the scour depths where positive values are associated with scour while negative values denote deposition.

Time-series graphs of scour-hole depth for existing, original, and new proposed conditions are shown in Figures 45 and 46. In Figure 45, the 15,000 cfs flow case is shown with Test 3 for existing and Test 7 for original proposed conditions. The 30,000 cfs flow case is shown in Figure 46 with Test 5, Test 8, and Test 14 for existing, original, and new proposed conditions, respectively. As verification on the scour-hole measuring technique, a second method was deployed using an array of single-beam fathometers and checked against the measurements for Test 9 (Figure 47).

As a comparison for all the existing conditions tests, the approach WSE versus the scour elevation was plotted (Figure 48). Results indicated that as the approach WSE increases, the scour elevation decreases, meaning the scour hole deepens. This is further illustrated in Figure 49 where for Test 2 the tailgate was changed  $\pm 1$  ft to determine the sensitivity of the scour depth to the approach depth. It shows that as the approach depth is increased, raising the tailgate 1 ft, the scour hole deepens. Conversely, as the tailgate is lowered, lowering the approach depth 1 ft, the scour hole shallows.

Figure 50 shows the original proposed condition tests as compared to the existing condition tests. As illustrated the original proposed conditions tests improve scour at the bridge. Likewise the new proposed conditions have a similar but less significant improvement on scour at the bridge as shown in Figure 51. Figures 48–51 show the measured and scaled scour elevations for all the tests. Results for all tests are shown in Table 6, where  $S_y$  is the minimum scour elevation.

Figure 21. Location for maximum scour for both new and original proposed and existing conditions.

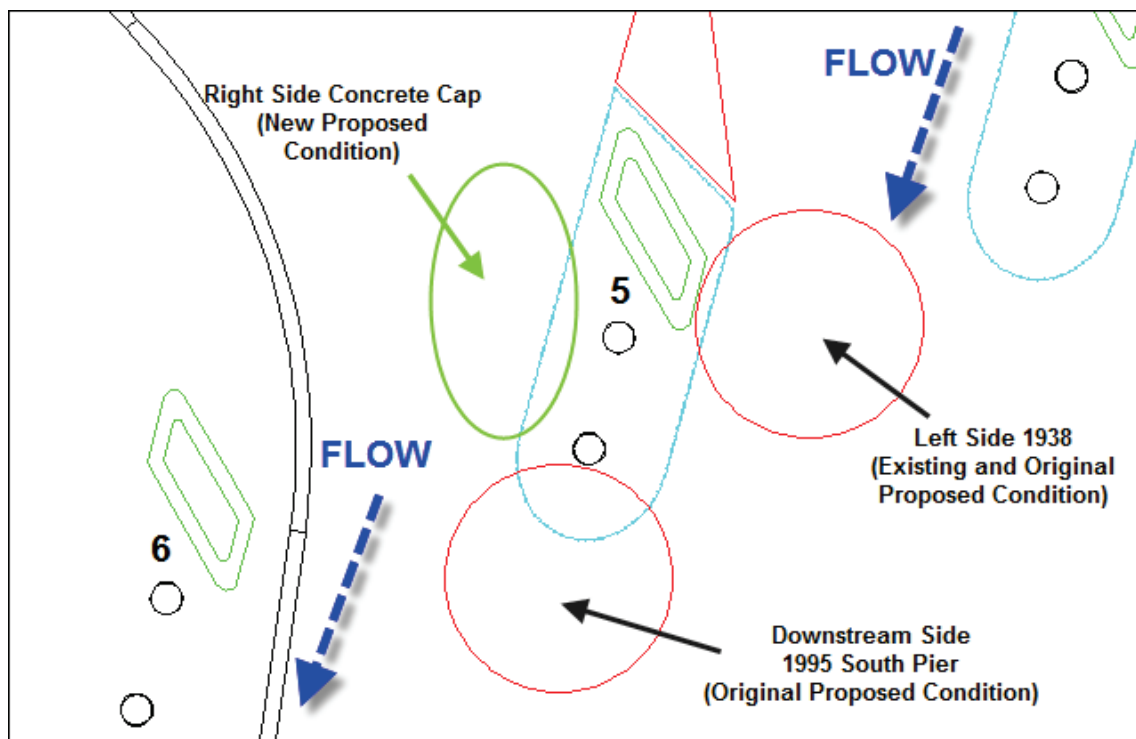


Figure 22. Typical scour at pier set 5 for 30,000 cfs flow test, existing conditions.

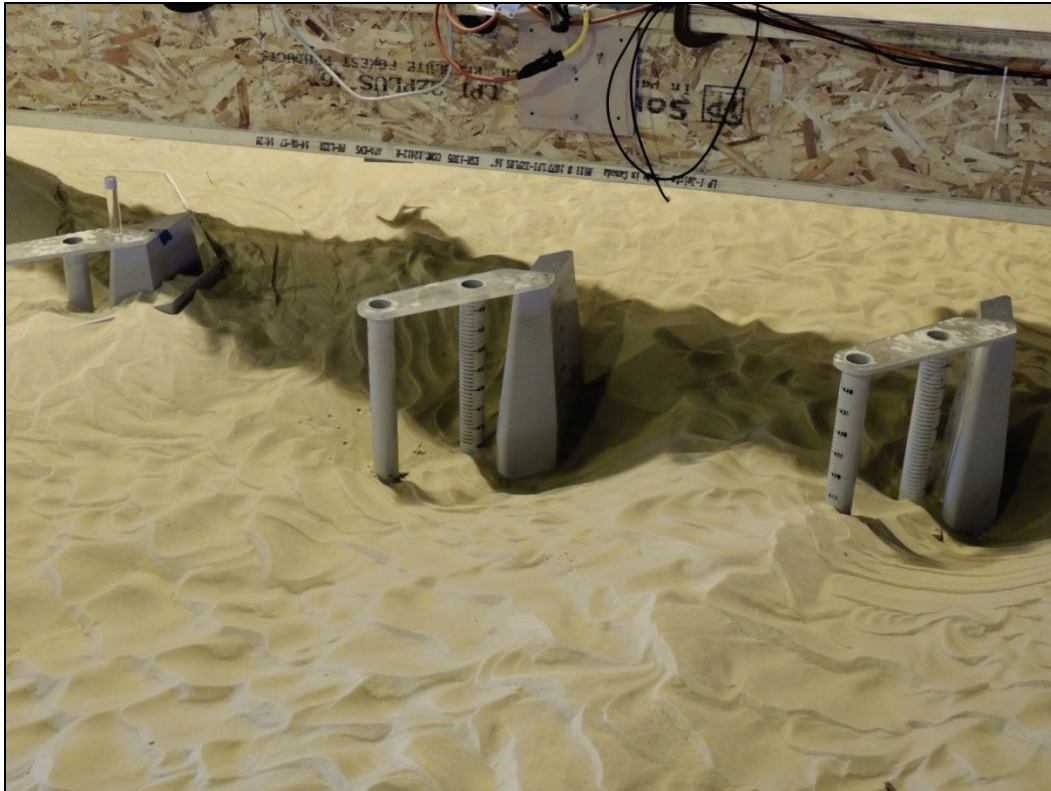


Figure 23. Typical scour at pier set 5 for 30,000 cfs flow test, original proposed conditions.

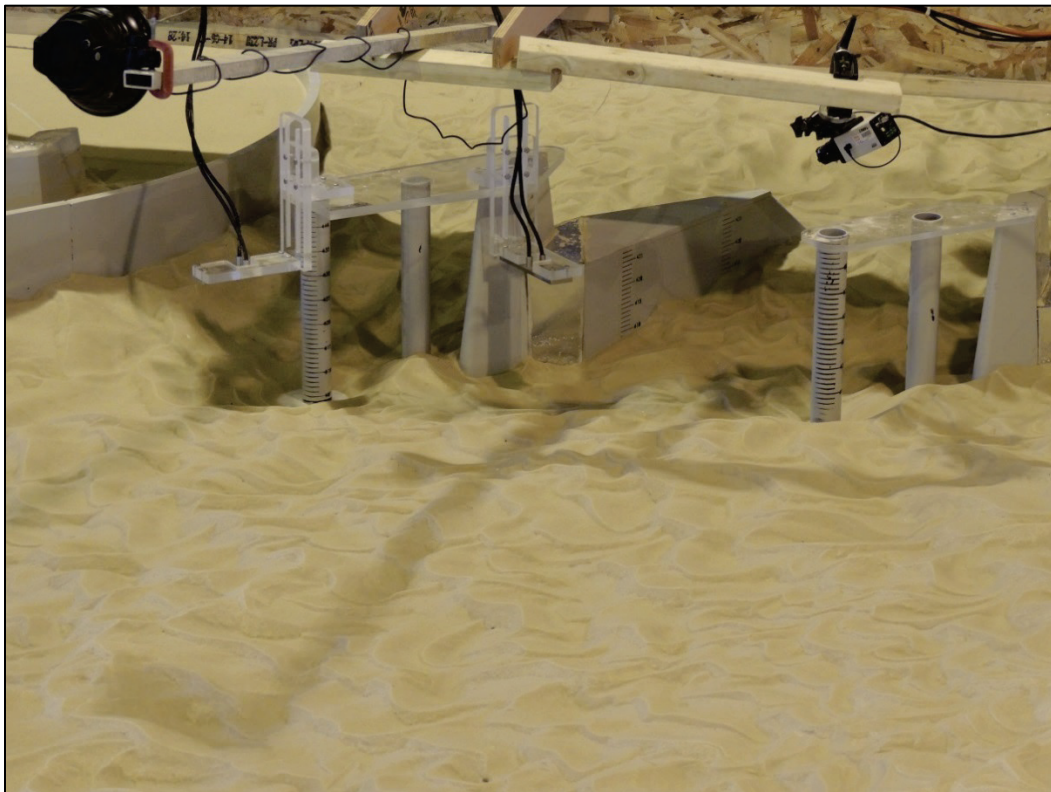




Figure 24. Typical scour at pier set 5 for 30,000 cfs flow test, original proposed conditions.

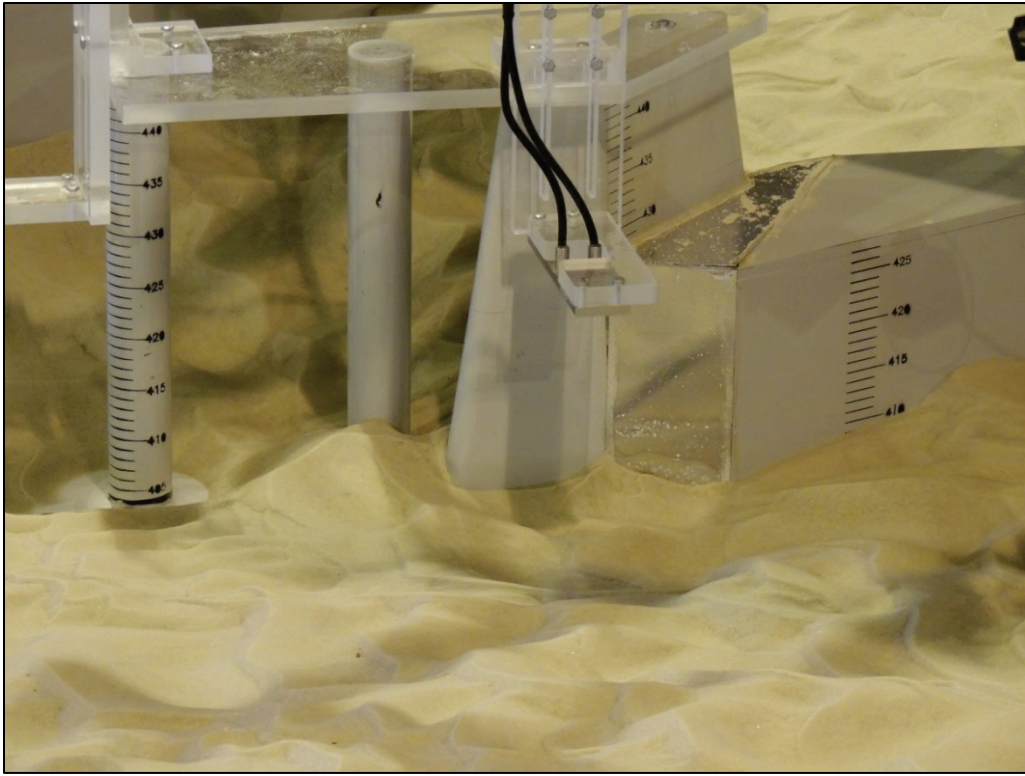


Figure 25. Typical scour at pier set 5 for 30,000 cfs flow test, new proposed conditions.



Figure 26. Test 3 (15,000 cfs existing conditions) pre-test lidar scan (typical).

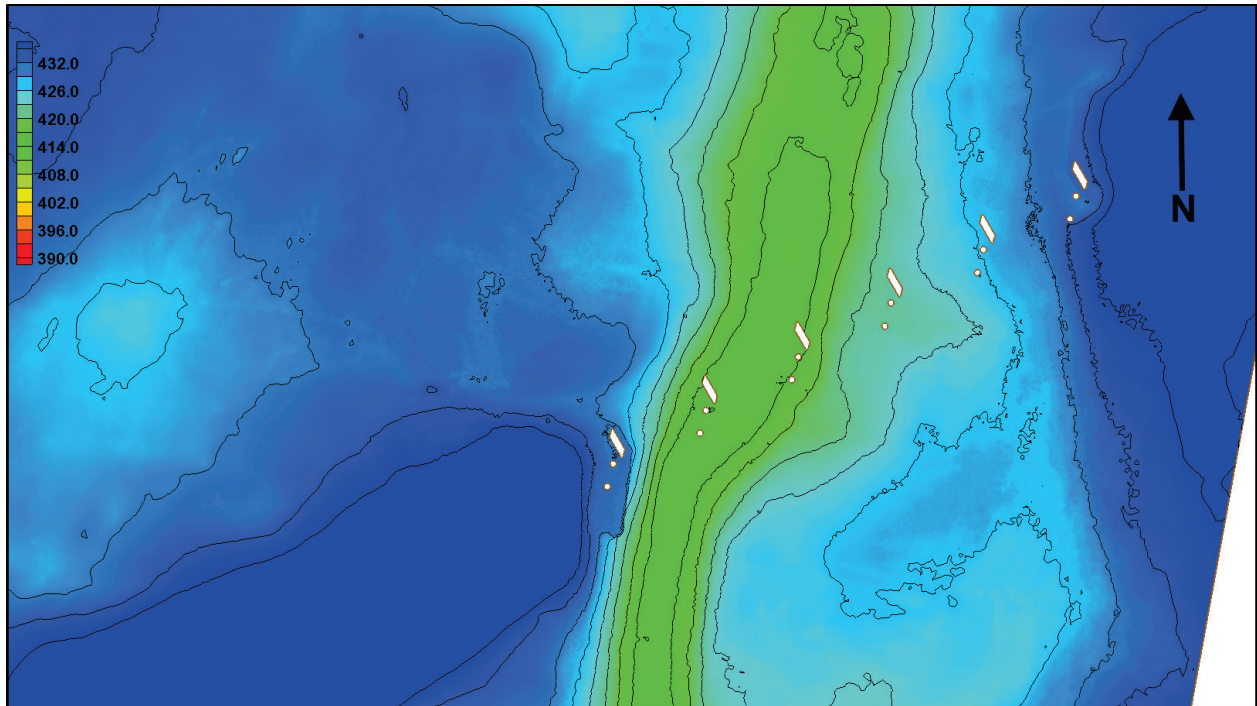


Figure 27. Test 8 (30,000 cfs original proposed conditions) pre-test lidar scan (typical).

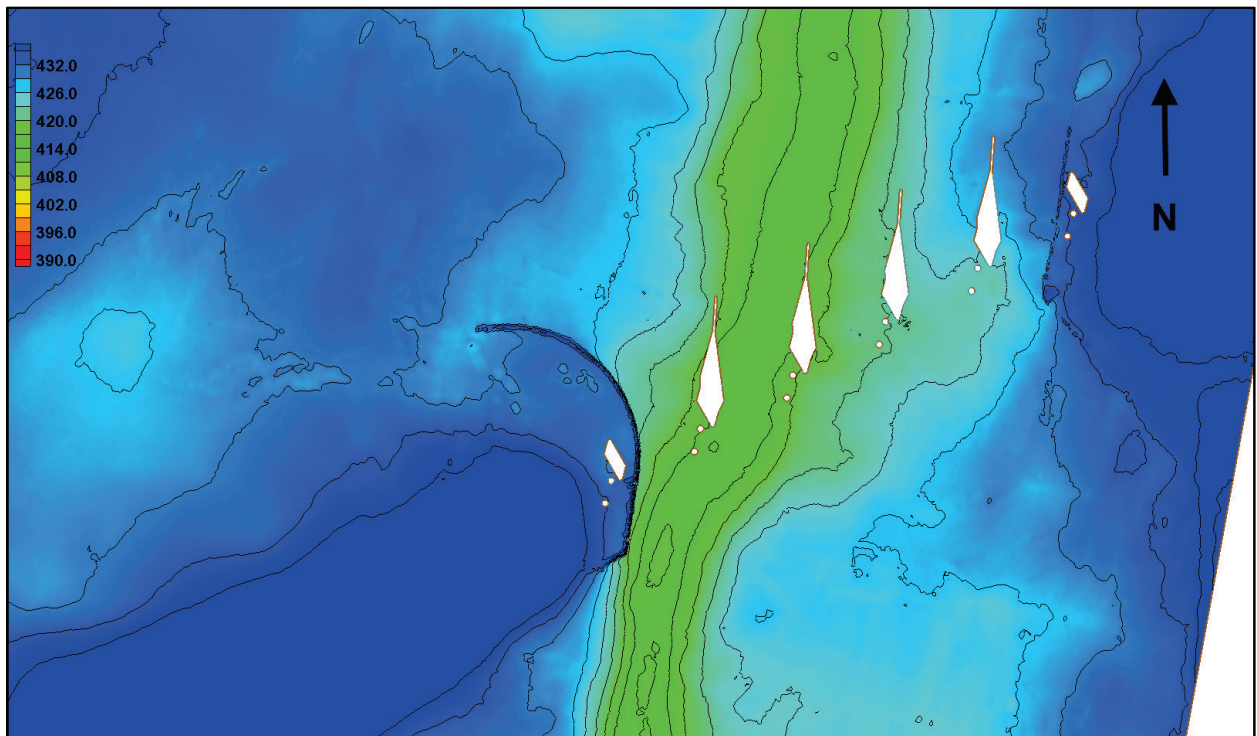




Figure 28. Test 13 (30,000 cfs new proposed conditions) pre-test lidar scan (typical).

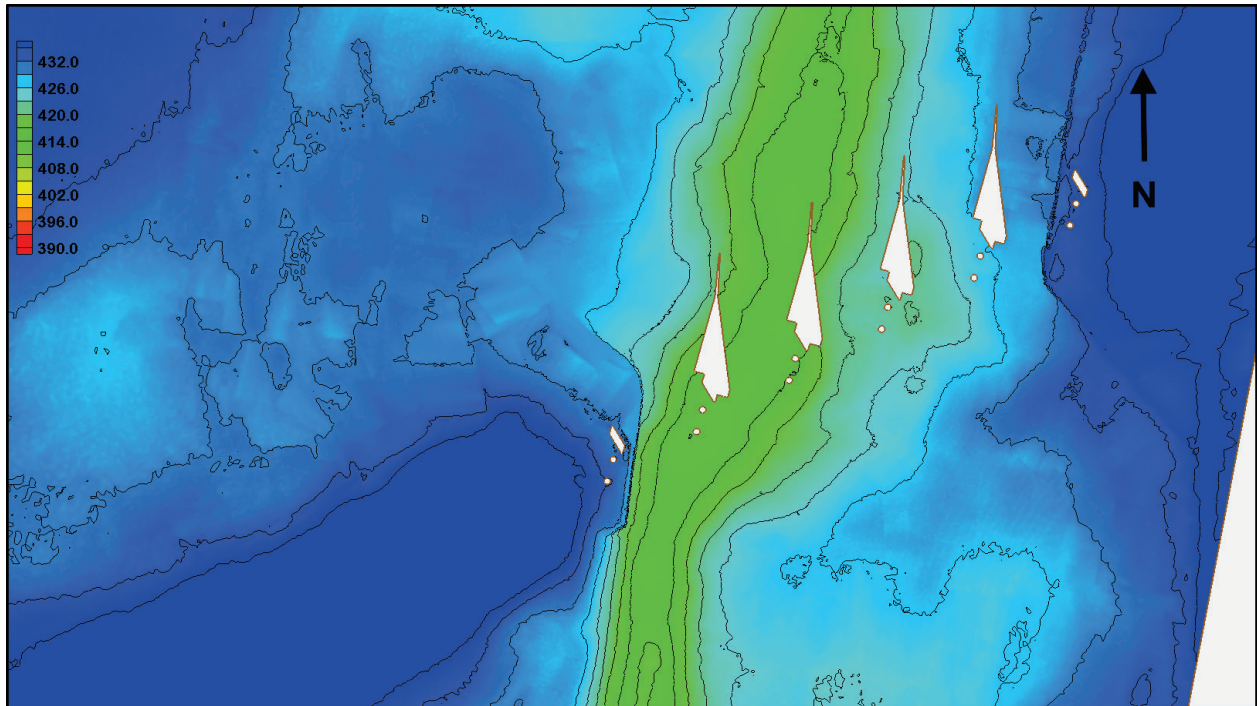


Figure 29. Test 3 (15,000 cfs existing conditions) post-test lidar scan.

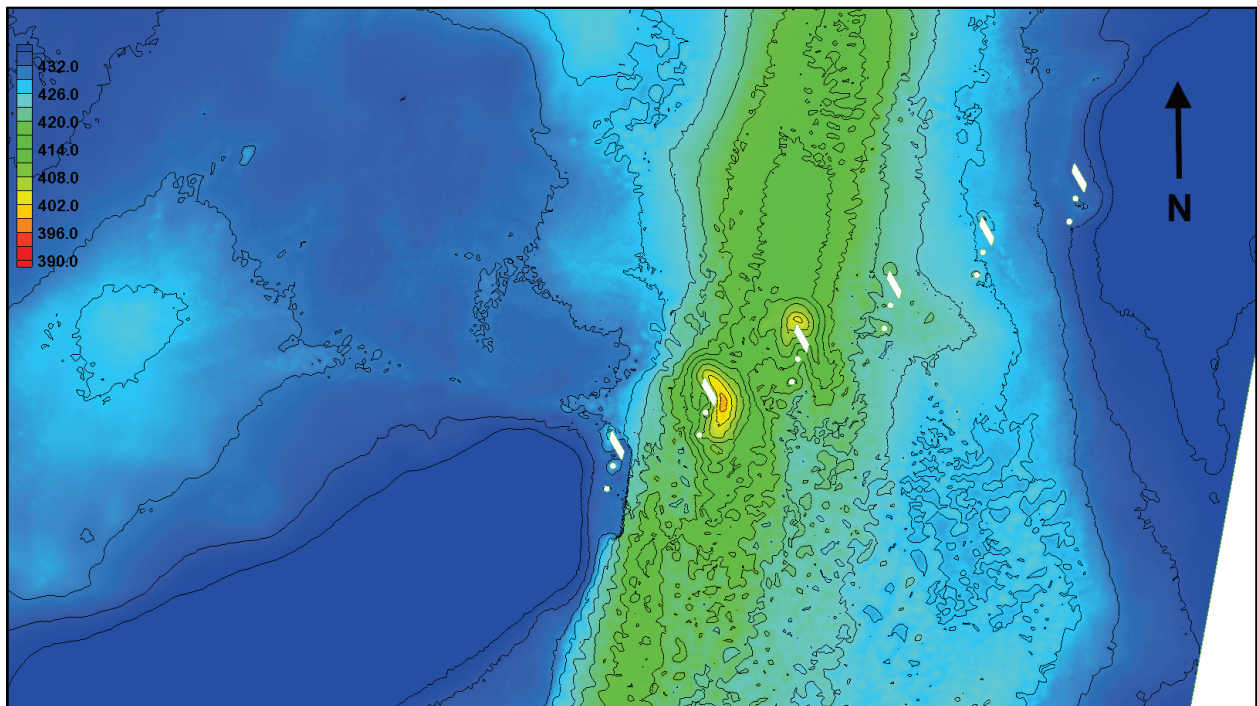




Figure 30. Test 1 (30,000 cfs existing conditions) post-test lidar scan.

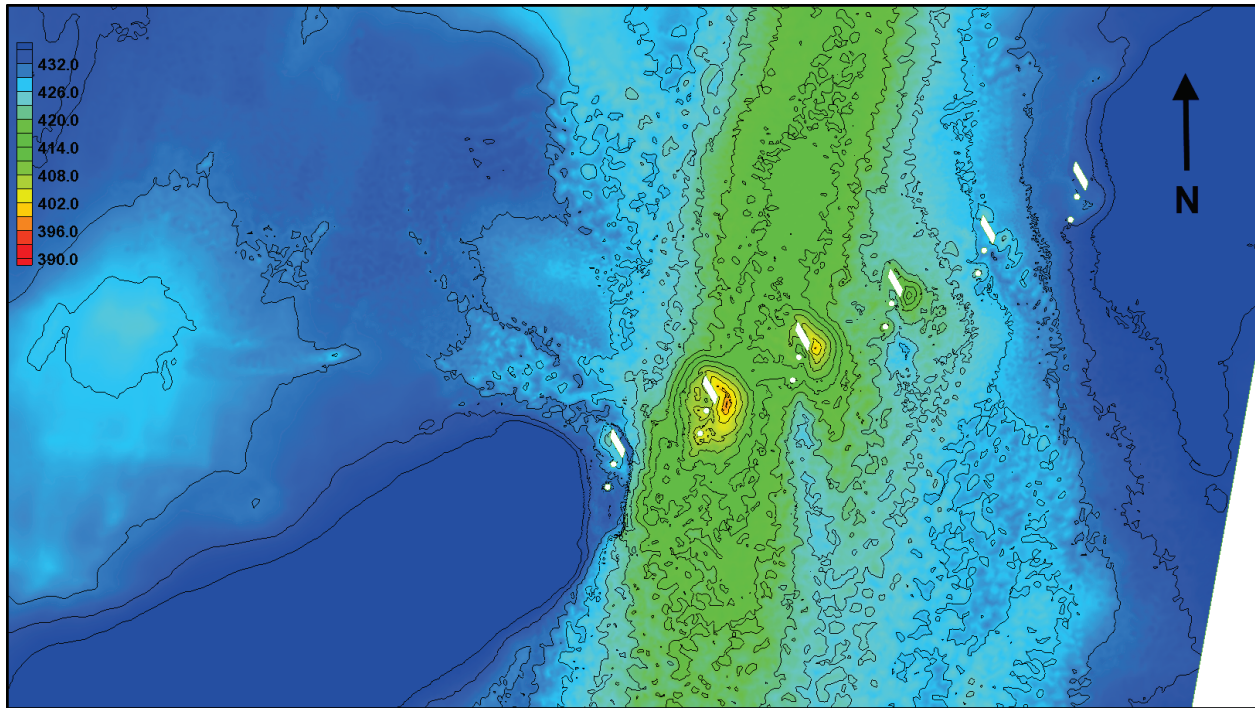


Figure 31. Test 7 (15,000 cfs original proposed conditions) post-test lidar scan.

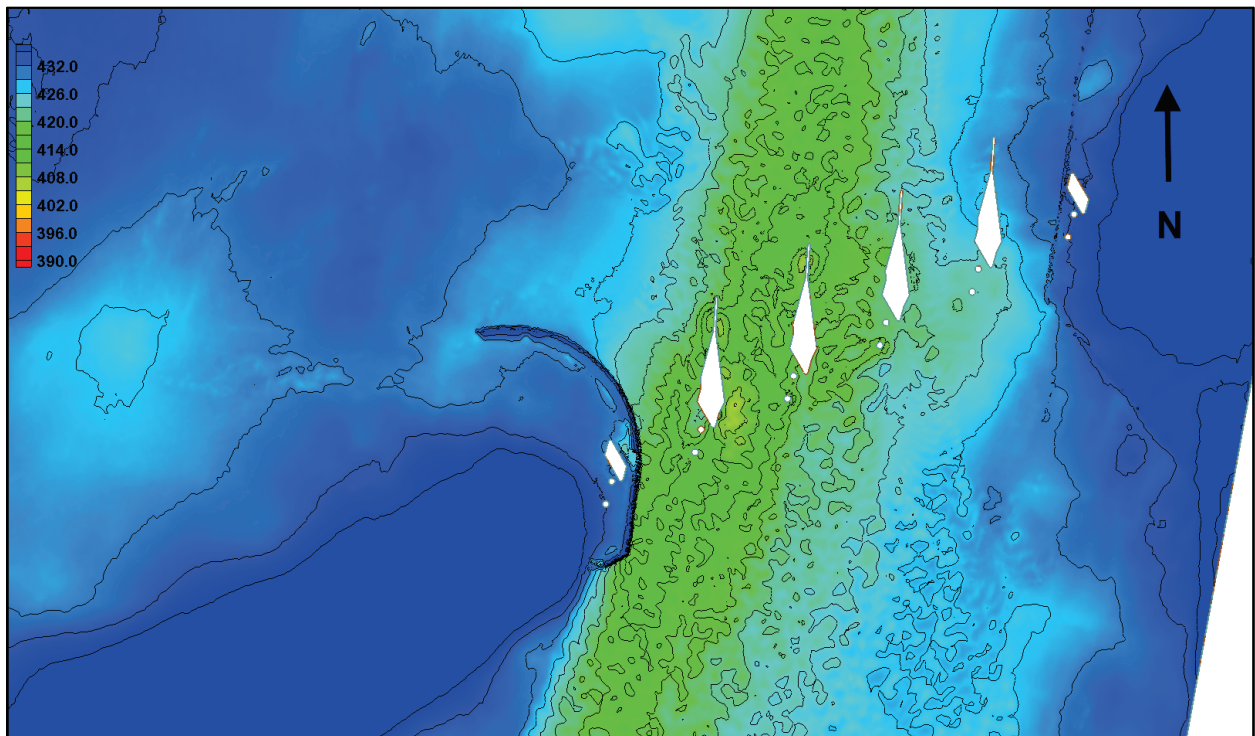


Figure 32. Test 8 (30,000 cfs original proposed conditions) post-test lidar scan.

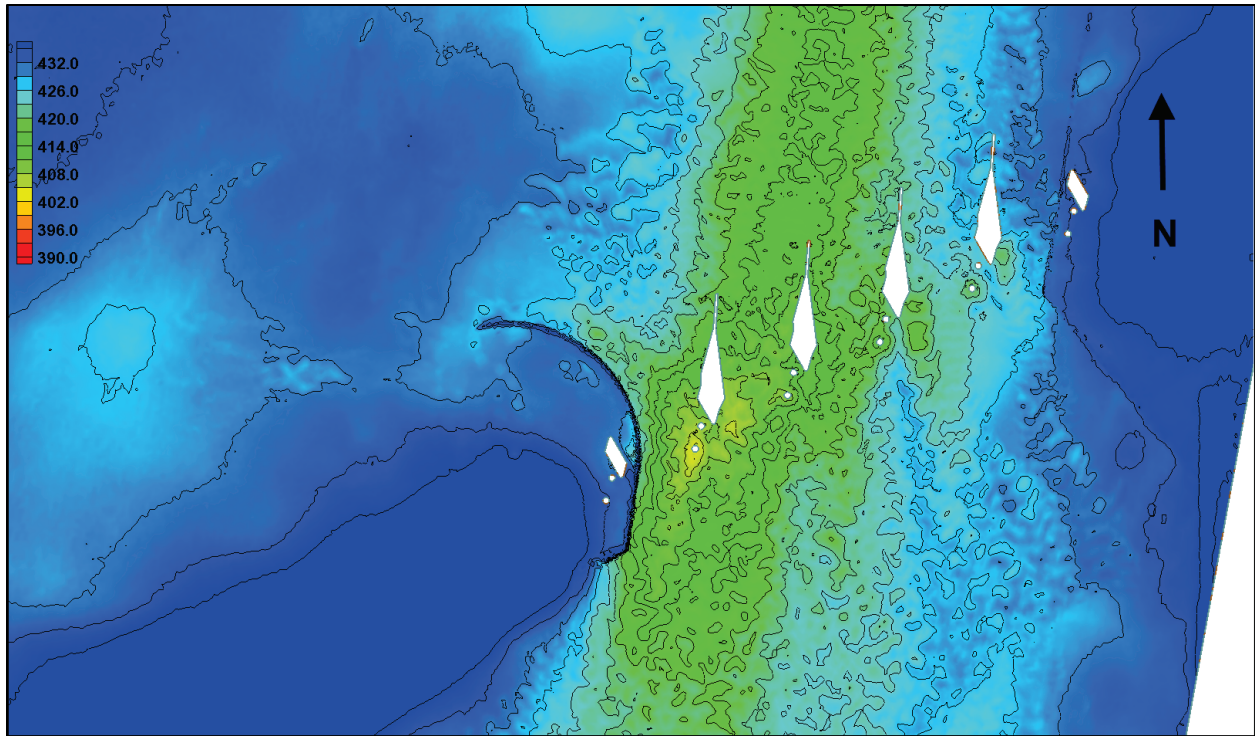


Figure 33. Test 13 (30,000 cfs new proposed conditions) post-test lidar scan.

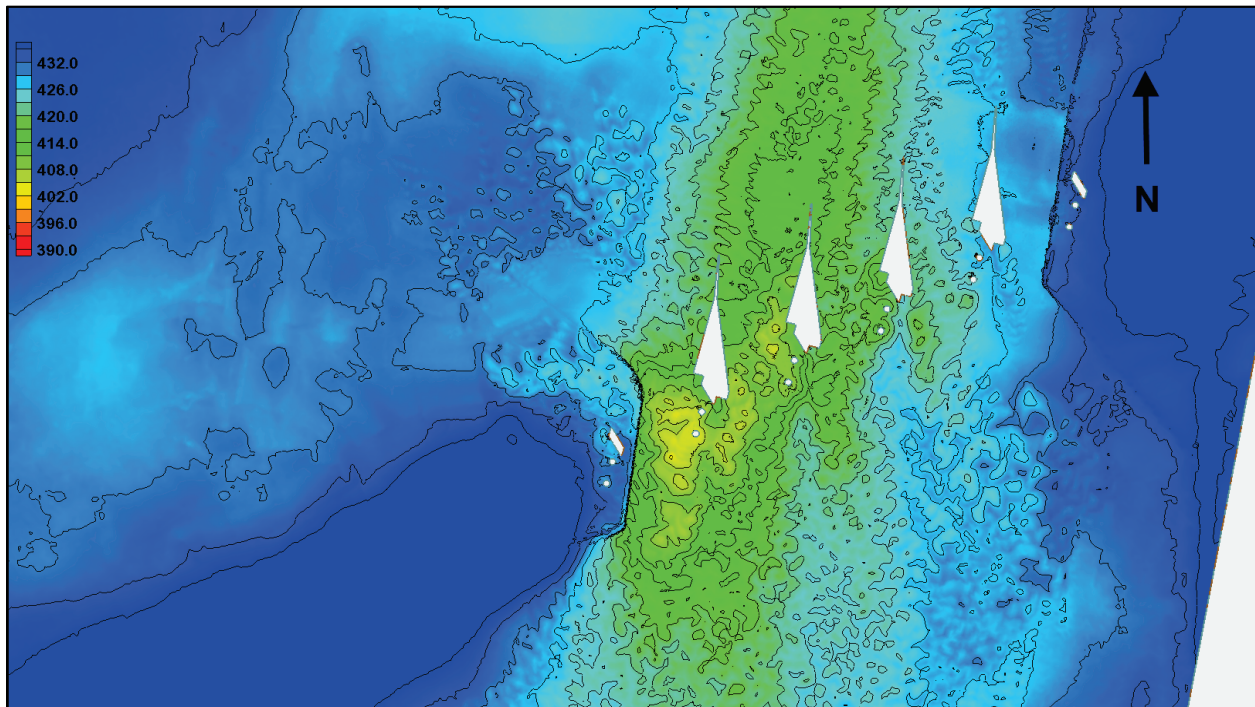




Figure 34. Test 14 (30,000 cfs new proposed conditions) post-test lidar scan.

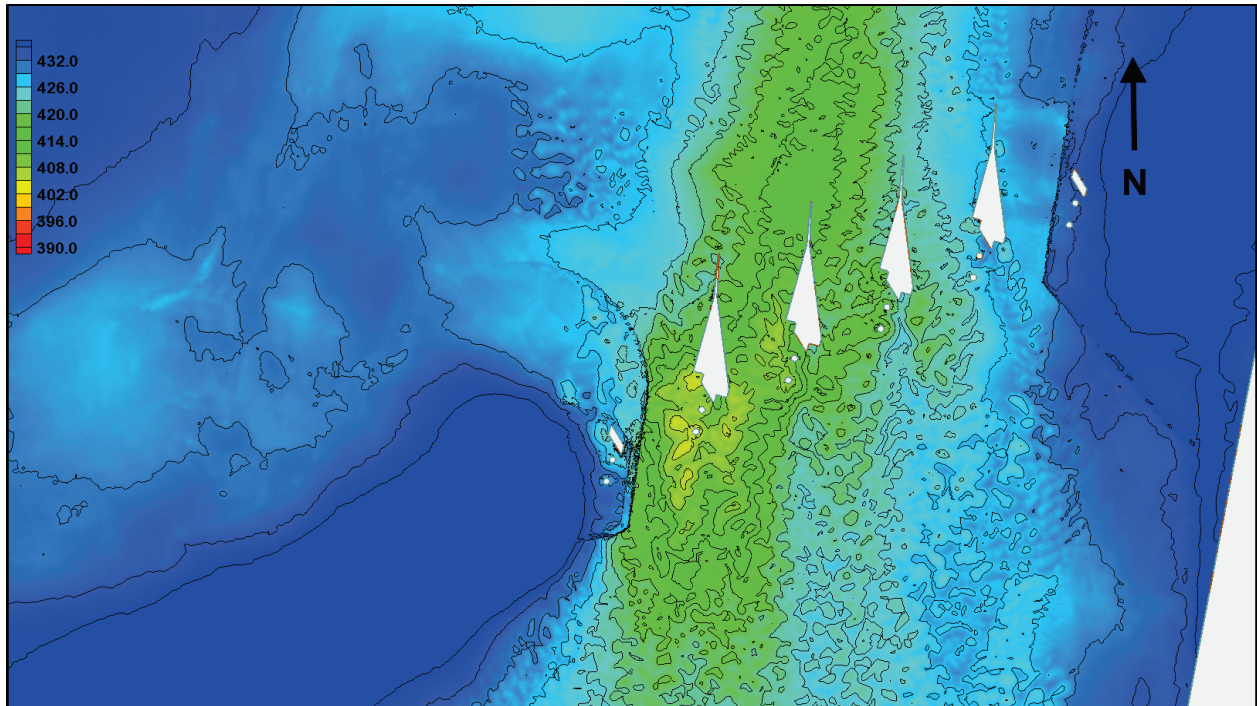


Figure 35. Test 15 (30,000 cfs new proposed conditions) post-test lidar scan.

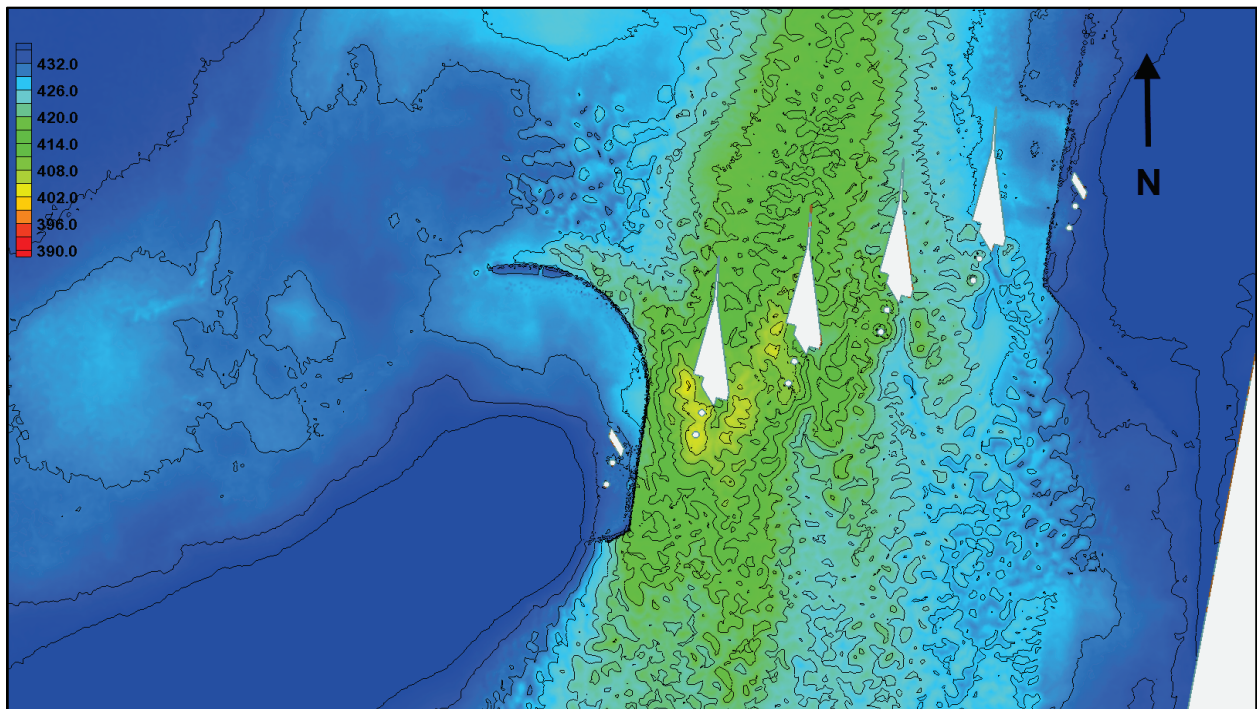


Figure 36. Test 16 (30,000 cfs new proposed conditions) post-test lidar scan.

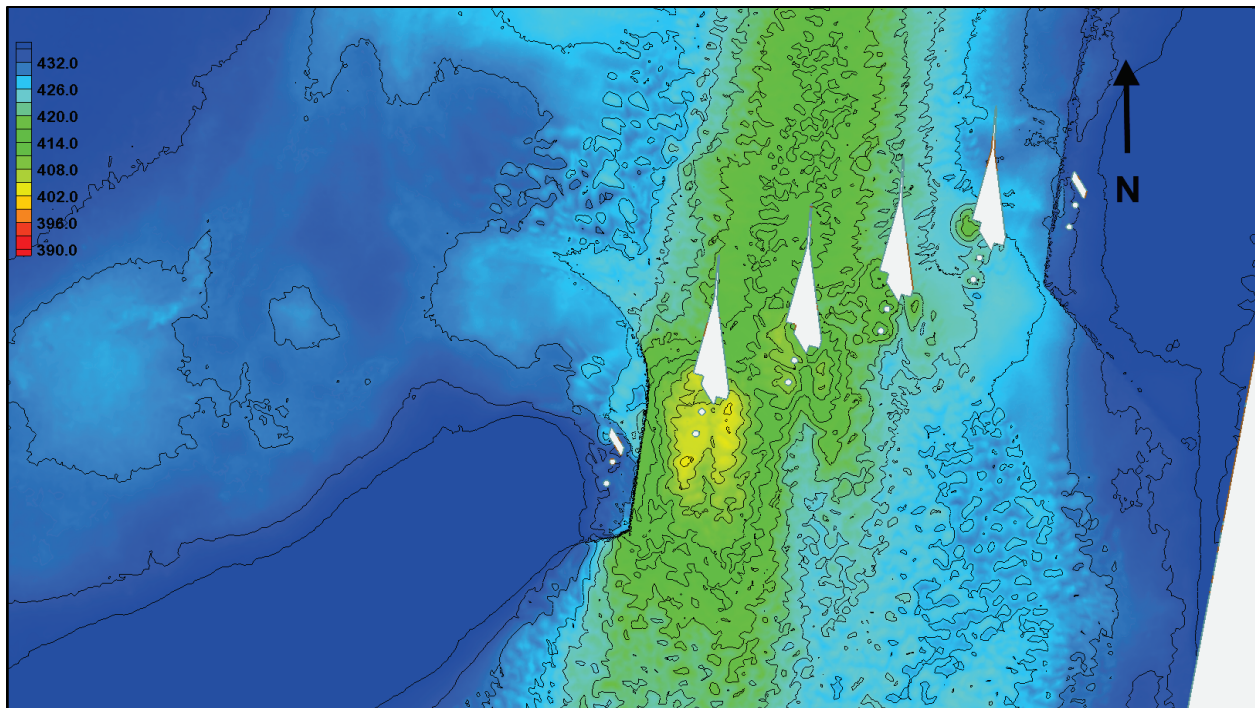


Figure 37. Test 4 (15,000 cfs existing conditions) pre- minus post-test lidar survey.

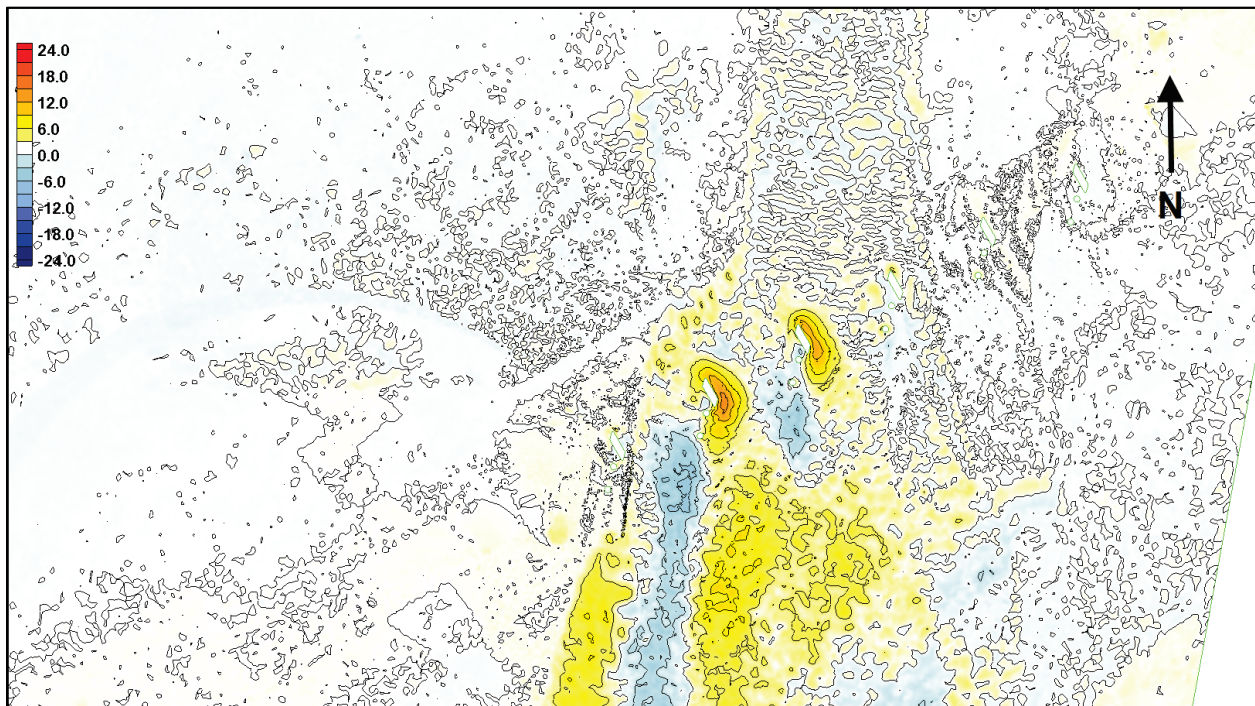




Figure 38. Test 1 (30,000 cfs existing conditions) pre- minus post-test lidar survey.

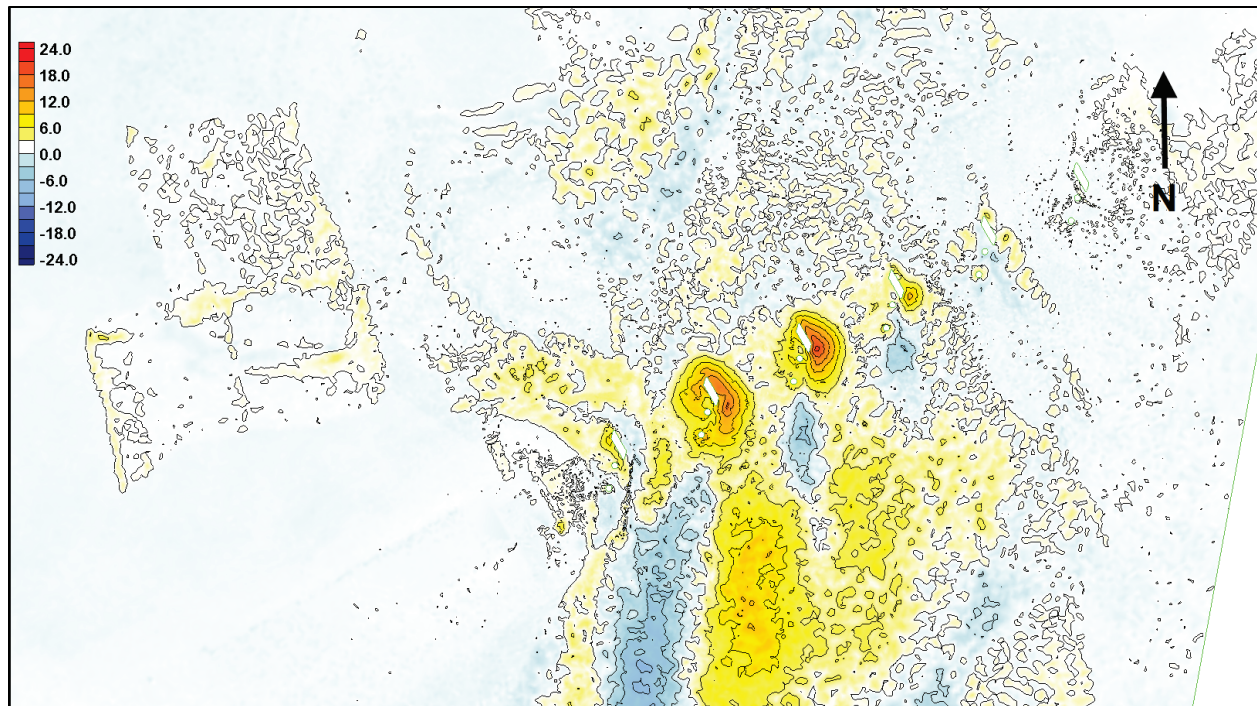


Figure 39. Test 7 (15,000 cfs original proposed conditions) pre- minus post-test lidar survey.

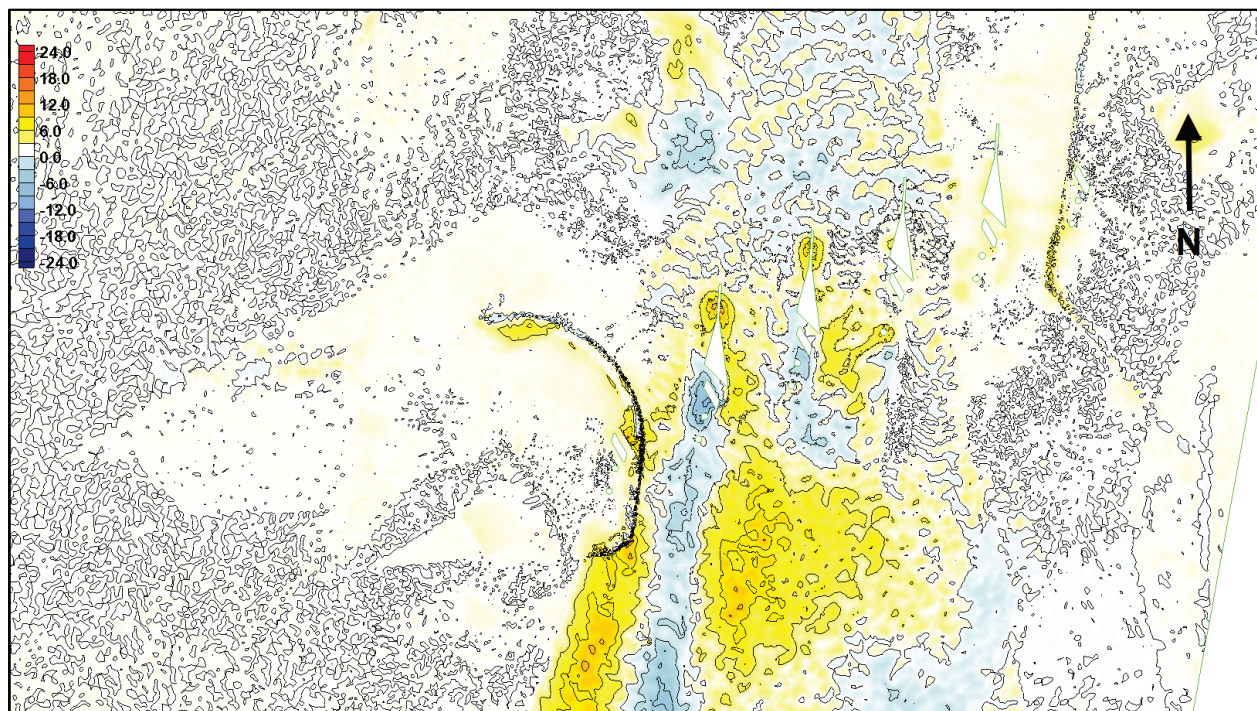




Figure 40. Test 8 (30,000 cfs original proposed conditions) pre- minus post-test lidar survey.

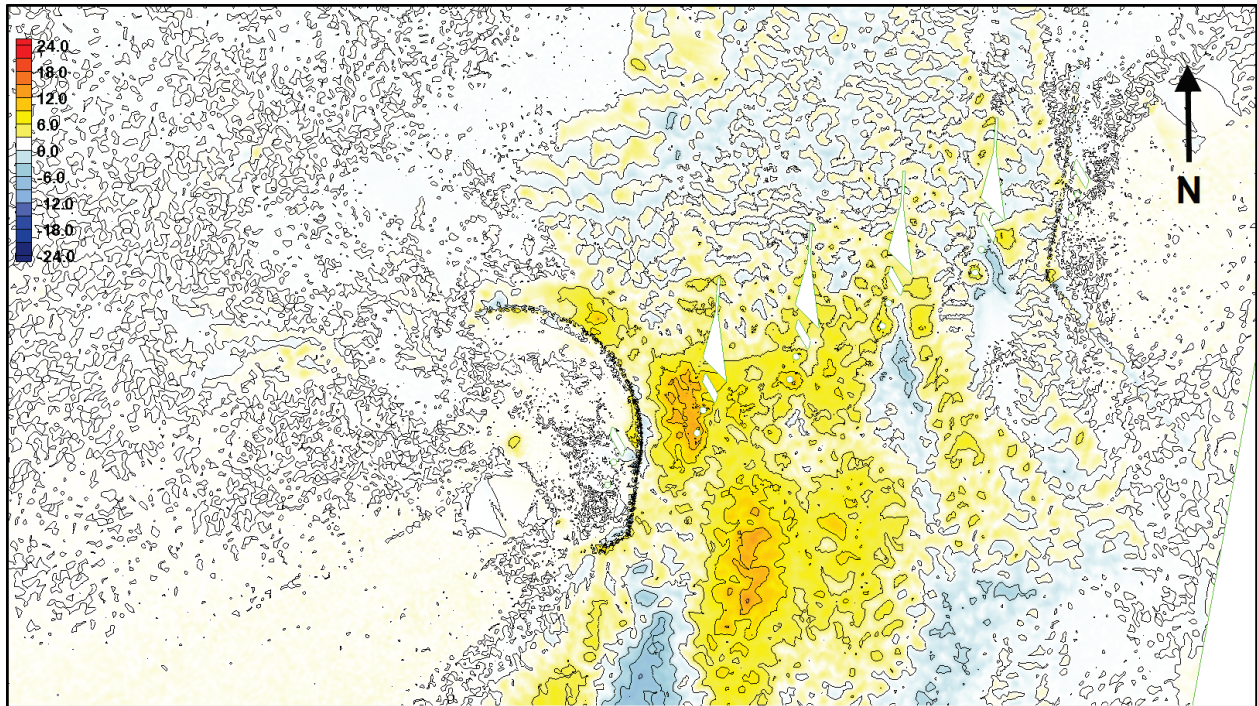


Figure 41. Test 13 (30,000 cfs new proposed conditions) pre- minus post-test lidar survey.

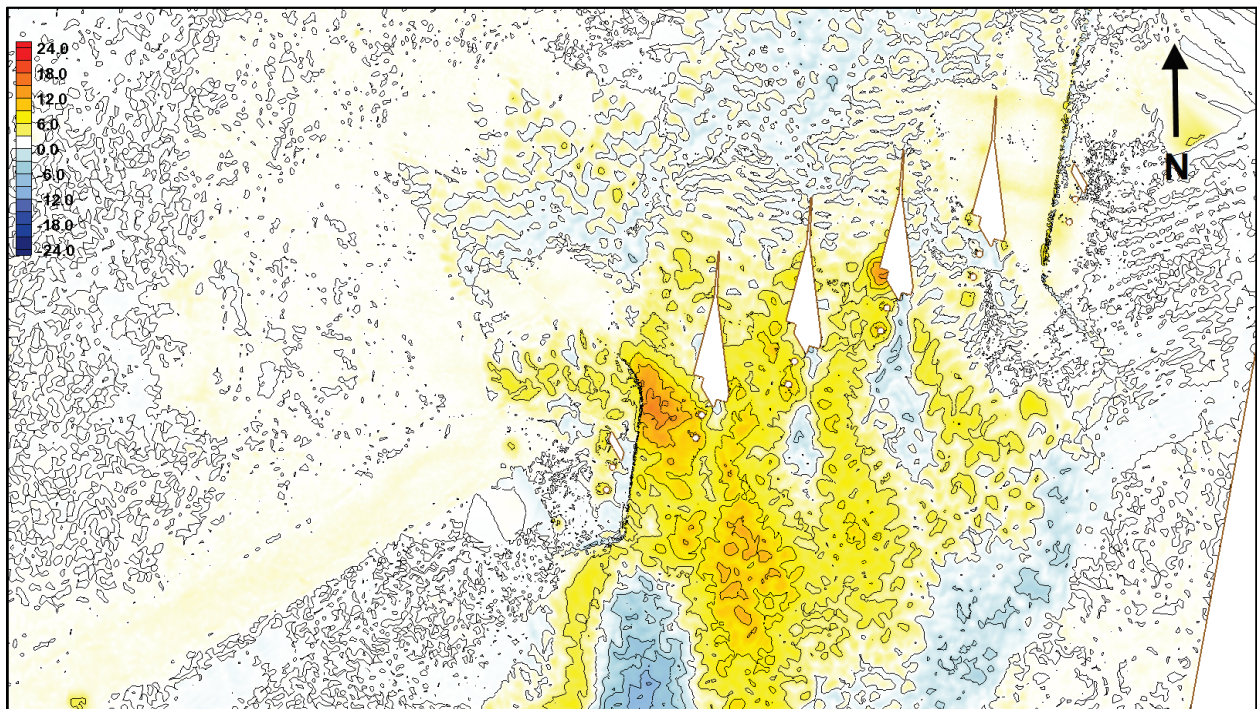




Figure 42. Test 14 (30,000 cfs new proposed conditions) pre- minus post-test lidar survey.

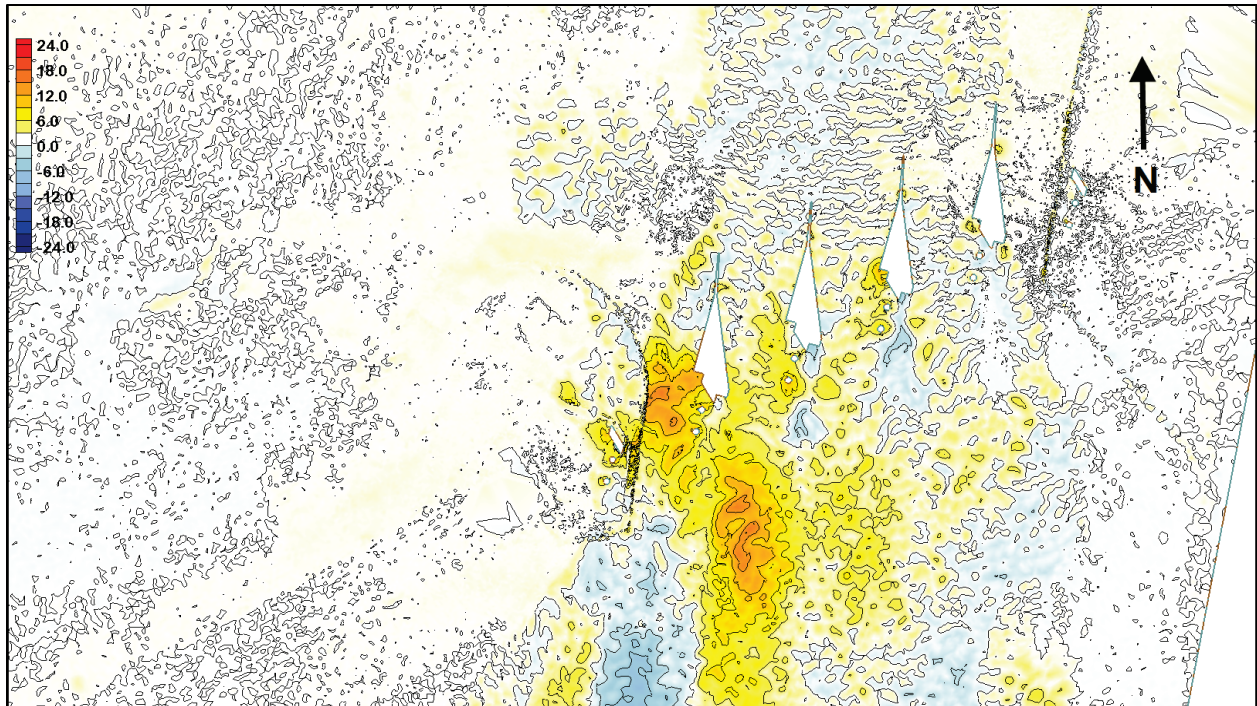


Figure 43. Test 15 (30,000 cfs new proposed conditions) pre- minus post-test lidar survey.

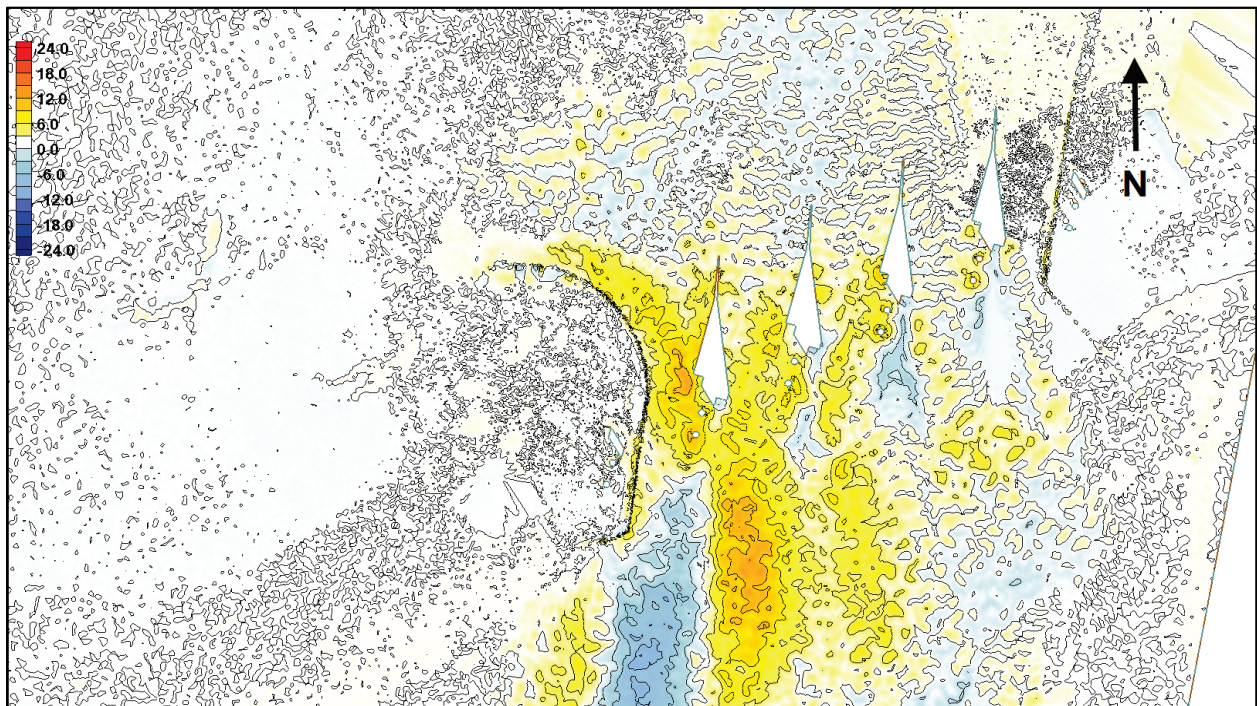




Figure 44. Test 16 (30,000 cfs new proposed conditions) pre- minus post-test lidar survey.

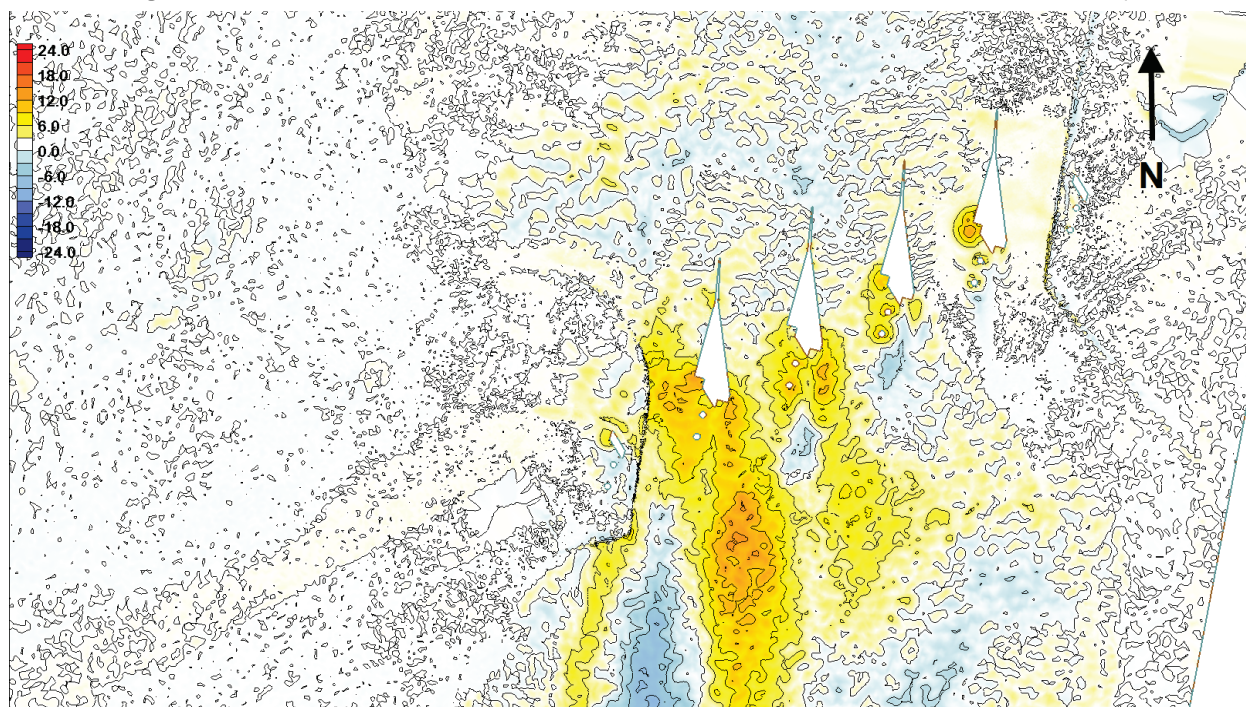


Figure 45. Time series of unscaled scour hole minimum elevation (scour depth) comparison between existing and proposed conditions at 15,000 cfs flow case as measured on left side of 1938 Pier 5 (see Figure 4 for a layout schematic).

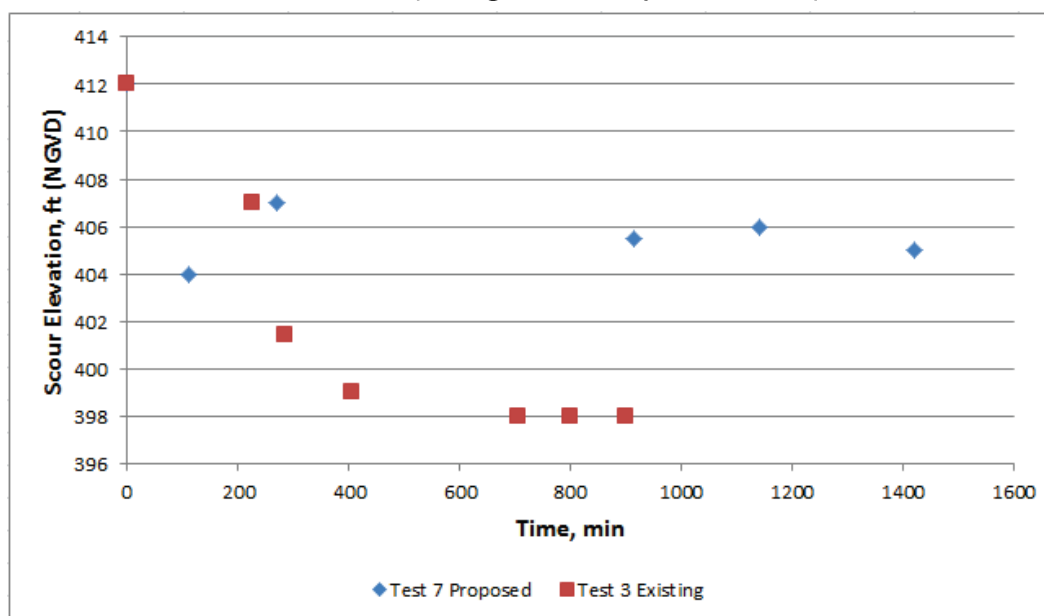


Figure 46. Time series of unscaled scour hole minimum elevation (scour depth) comparison between existing and original and new proposed conditions at 30,000 cfs flow Test 5, 8 and 14.

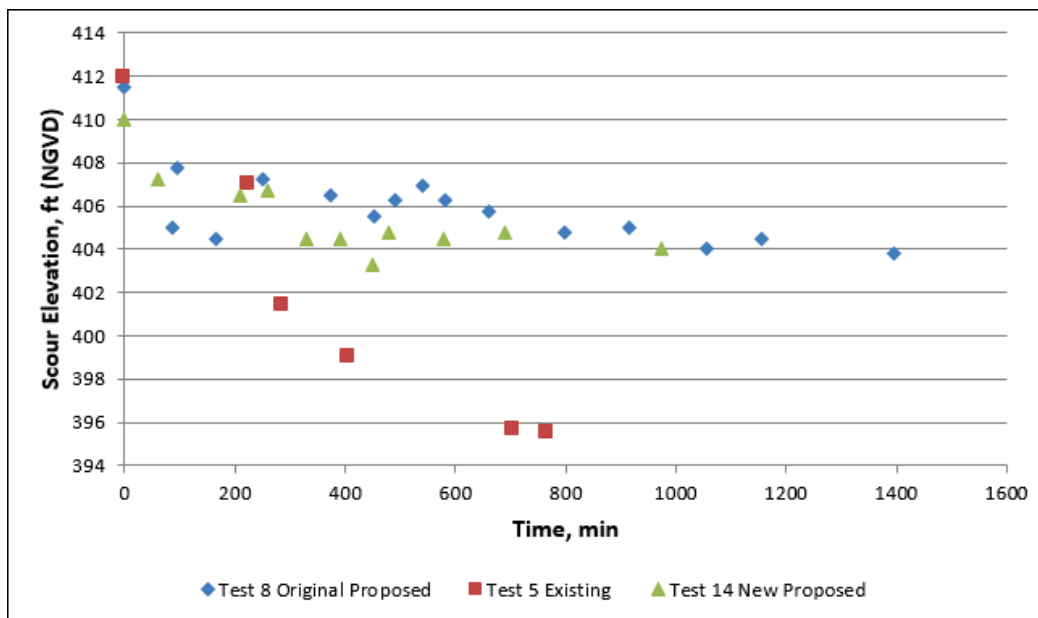


Figure 47. Verification of measuring technique with single beam fathometer array for Test 9 (unscaled results).

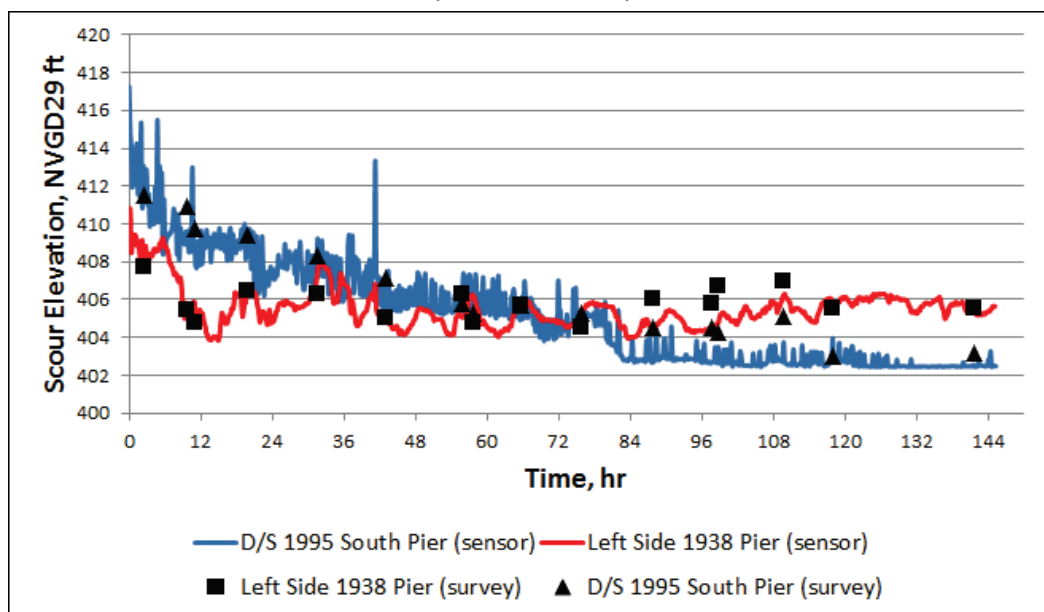


Figure 48. Existing conditions minimum scour elevations (scour depth) at Pier 5 for both measured and scaled at 15,000 and 30,000 cfs flow conditions.

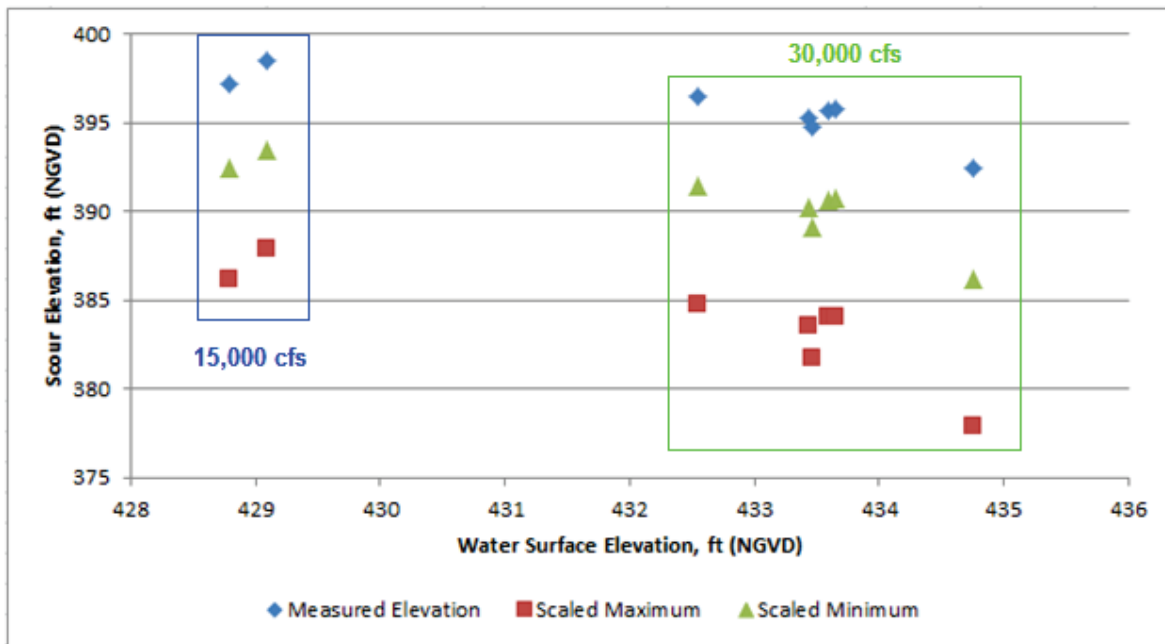


Figure 49. Variations in scour depth with changes in tailwater control at Pier 5 for 30,000 cfs flow case.

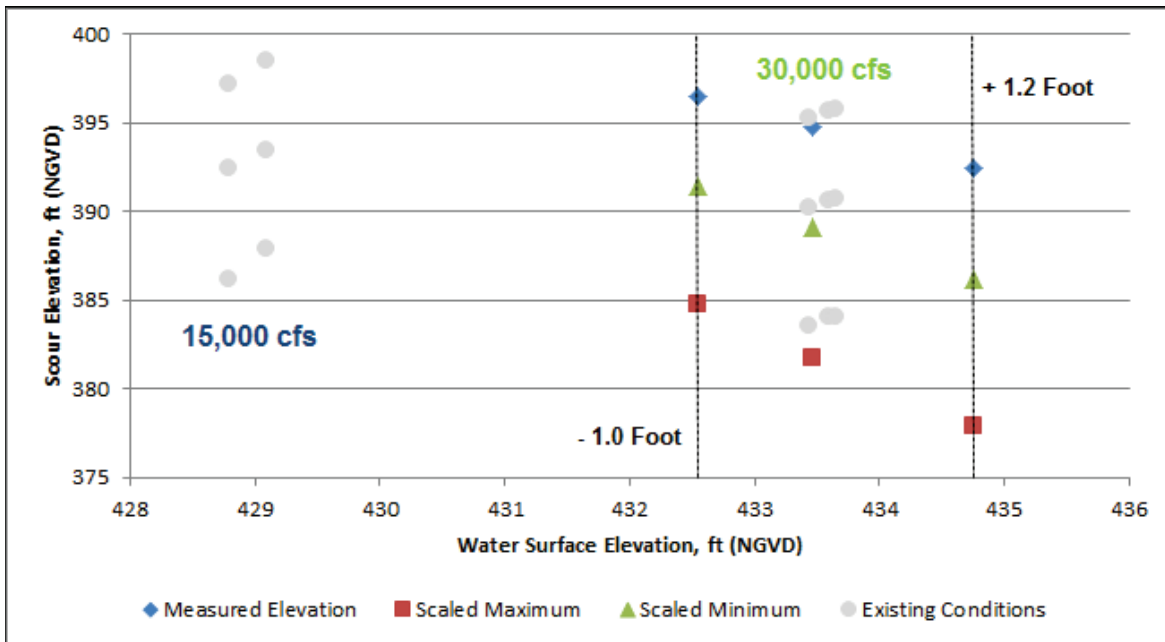


Figure 50. Original proposed conditions (overlaid on existing conditions) minimum scour elevations for both measured and scaled for Pier 5 at 15,000 and 30,000 cfs flow conditions.

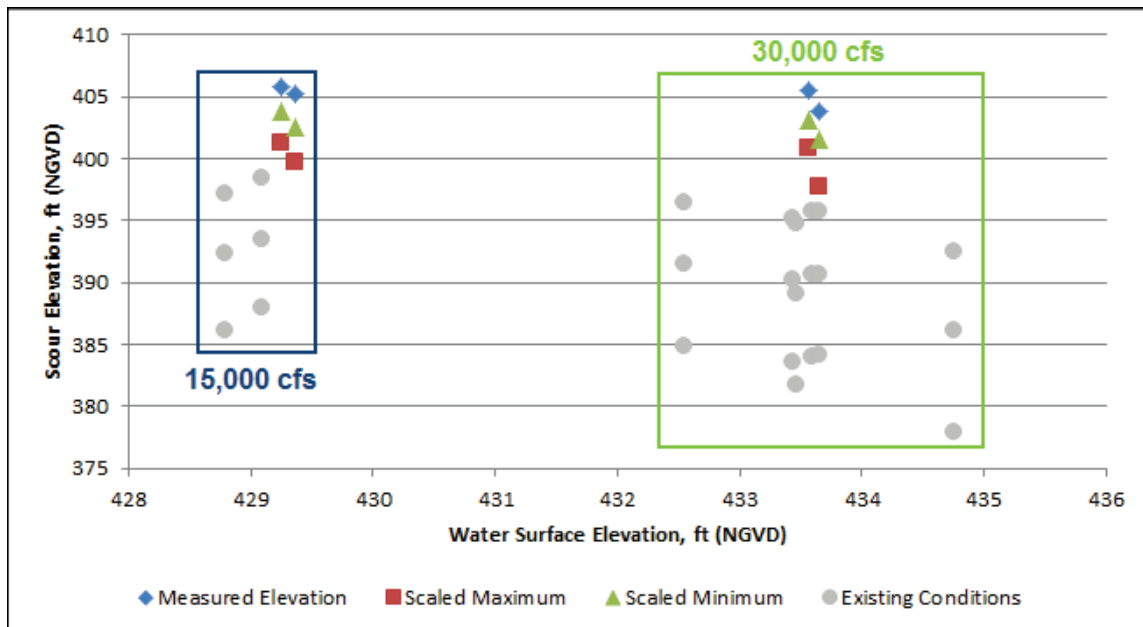


Figure 51. Original and new proposed conditions (overlaid on existing conditions) minimum scour elevations for both measured and scaled for Pier 5 at 30,000 cfs flow conditions.

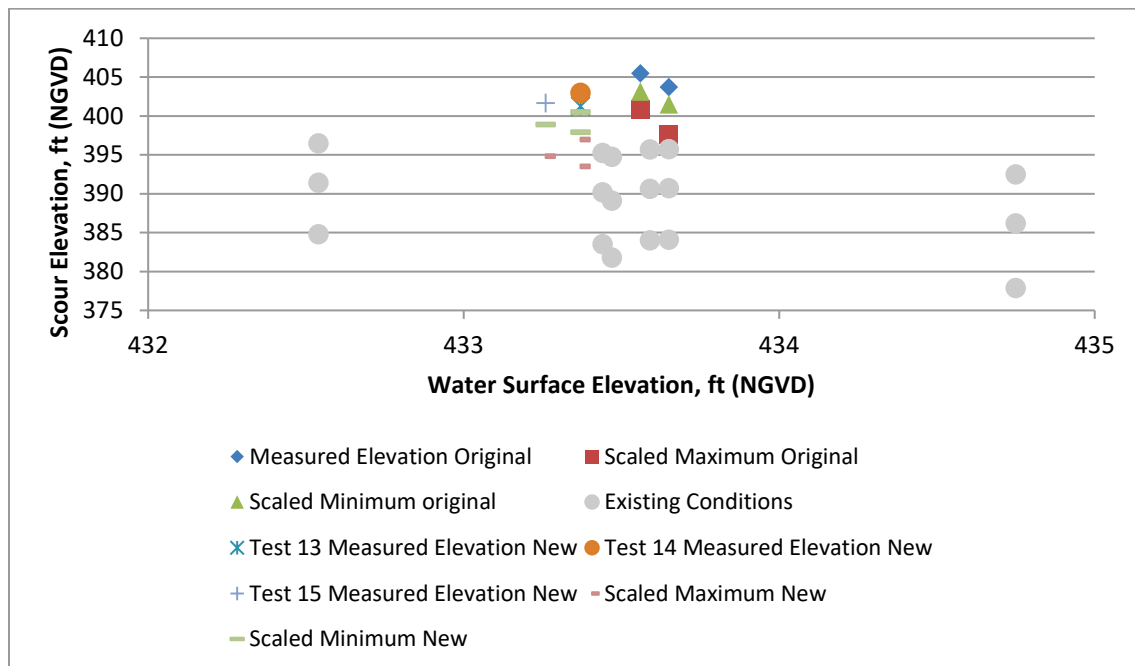


Table 5. Scour data collected from all tests.

		Q cfs	Test #	WSE NGVD 29 (ft)	Left Side 1938 Pier 5				Approach Velocity ft/s	Gage 5 Bed = 414.1		Scour Depth ft	
					Bed Elevation NGVD (ft)	Level Measurement Sy, NGVD 29 (ft)	Lidar Sy	Calibrated, Sy, NGVD 29 (ft)		Flow Depth ft	From 5 to 7 Slope		
								Maximum					Minimum
Existing		30000	1	433.44	411.47	395.25	395.25	383.52	390.18	5.19	19.3	0.00099	16.2
		30000	2	433.47	412.67	394.75	na	381.79	389.15	4.62	19.4	0.00148	17.9
		30000	2L	432.54	412.67	396.50	na	384.81	391.44	5.08	18.4	0.00153	16.2
		30000	2H	434.75	412.67	392.50	392.5	377.91	386.19	4.14	20.7	0.00104	20.2
		15000	3	428.79	412.47	397.20	397.2	386.15	392.42	3.34	14.7	0.00129	15.3
		15000	4	429.09	411.12	398.50	397.67	387.93	393.46	4.23	15.0	0.00124	12.6
		30000	5	433.59	411.85	395.70	na	384.02	390.65	4.42	19.5	0.00173	16.2
		30000	6	433.65	411.85	395.75	na	384.11	390.72	4.68	19.6	0.00143	16.1
Original proposed		15000	7	429.36	411.56	405.25	404.72	399.78	402.59	4.43	15.3	0.00153	6.3
		30000	8	433.65	411.53	403.75	403.89	397.70	401.50	4.71	19.6	0.00134	7.8
		30000	9	433.56	410.53	405.50	404.92	400.80	403.17	5.26	19.5	0.00129	5.0
		15000	10	429.24	411.90	405.75	na	401.30	403.83	4.43	15.1	0.00104	6.1
Sensitivity conditions		30000	11	427.47	405.60	398.50	398.41	388.81	394.31	5.07	19.4	0.00129	7.1
		30000	12	427.38	405.60	395.50	394.28	383.64	390.37	3.38	19.3	0.00089	10.1
New proposed	Wall C 428	30000	13	433.37	411.9	401.25*	402.7	393.55	397.92	4.41	19.3	0.00113	10.7
	Wall D1 428	30000	14	433.37	411.9	403.25**	402.98	396.99	400.55	4.32	19.3	0.00129	8.6
	Wall D1 433	30000	15	433.26	411.9	402^	401.7	394.84	398.90	4.22	19.2	0.00183	9.9
	P.E. 420	30000	16	433.18	411.9	401*	401.12	393.12	397.59	4.29	19.1	0.00199	10.9

\* Scour hole downstream of concrete cap: \*\* Scour hole on the right side of the south 1995 pier: ^ Scour hole on right side of 1938 pier.

## 6 Discussion

Clear-water scour conditions were generated and repeated for multiple tests in the general physical model. Tests reached quasi-equilibrium (a point where changes in the scour hole were not measurable) within the test run time of 600 to 1,400 minutes. At the end of each test, the observed scour rates were essentially zero, indicating that a quasi-equilibrium condition had been attained. Sediment transport into the test section was minimal; however, perturbations upstream (from stilling pipes, flow entry, bathymetric setups, etc.) caused ripples to form. The estimated maximum scour depth is believed to be reasonable for a qualitative and quantitative comparison between the existing and proposed configurations.

### 6.1 Maximum scour depth

The maximum scour for all tests occurred for the 30,000 cfs flow cases. At this discharge and its associated approach WSE, the average measured scour elevation for the existing conditions was 395.4 ft with the scaled maximum and minimum being 383.4 ft and 390.2 ft respectively, as presented in Table 6. The scaled maximum and minimum values were calculated from estimated distorted scale factors. These scale factors were formulated from a flume study and are discussed in Chapter 3. For the 30,000 cfs original proposed condition flow test, the scaled maximum scour elevation was 399.3 ft and was an improvement of almost 16 ft. A similar trend was shown for the 15,000 cfs flow case. Both the 15,000 and 30,000 cfs flow cases represent a 55% and 60% improvement, respectively, in reducing the scour depth with the original proposed conditions configuration, Table 6.

The new proposed conditions showed less improvement than the original proposed conditions configuration. Prior testing has clearly illustrated that the 30,000 cfs flow case is the worst case for scour. Thus, no 15,000 cfs flow tests were conducted for the new proposed conditions. For the 30,000 cfs new proposed condition flow test, the scaled maximum scour elevation was 397.0 ft to 393.1 ft. This range of scour is directly attributed to the west abutment wall design, Alternative D1. Of the four new proposed conditions tests, Test 14 had the least amount of scour (Figure 52; Table 7). Test 14 showed a 46% improvement.



Table 6. Percentage Improvement from original proposed to existing conditions test.

Percentage Improvement, Proposed/Existing				
	Level Measurement			
Sy	30K cfs Existing	30K cfs Proposed	15K cfs Existing	15K cfs Proposed
Average	395.4	404.6	397.9	405.5
Standard deviation	0.40	0.88	0.65	na
Scour depth	16.6	6.4	13.9	6.3
% Improvement		61%		55%
	Scaled Maximum			
Average	383.4	399.3	387.0	400.5
Standard deviation	0.93	1.55	0.89	na
Scour depth	28.6	11.8	24.8	11.0
% Improvement		59%		55%
	Scaled Minimum			
Average	390.2	402.3	392.9	403.2
Standard deviation	0.63	0.84	0.52	na
Scour depth	21.7	8.7	18.9	8.4
% Improvement		60%		56%

Figure 52. Location and elevation of unscaled scour depths.

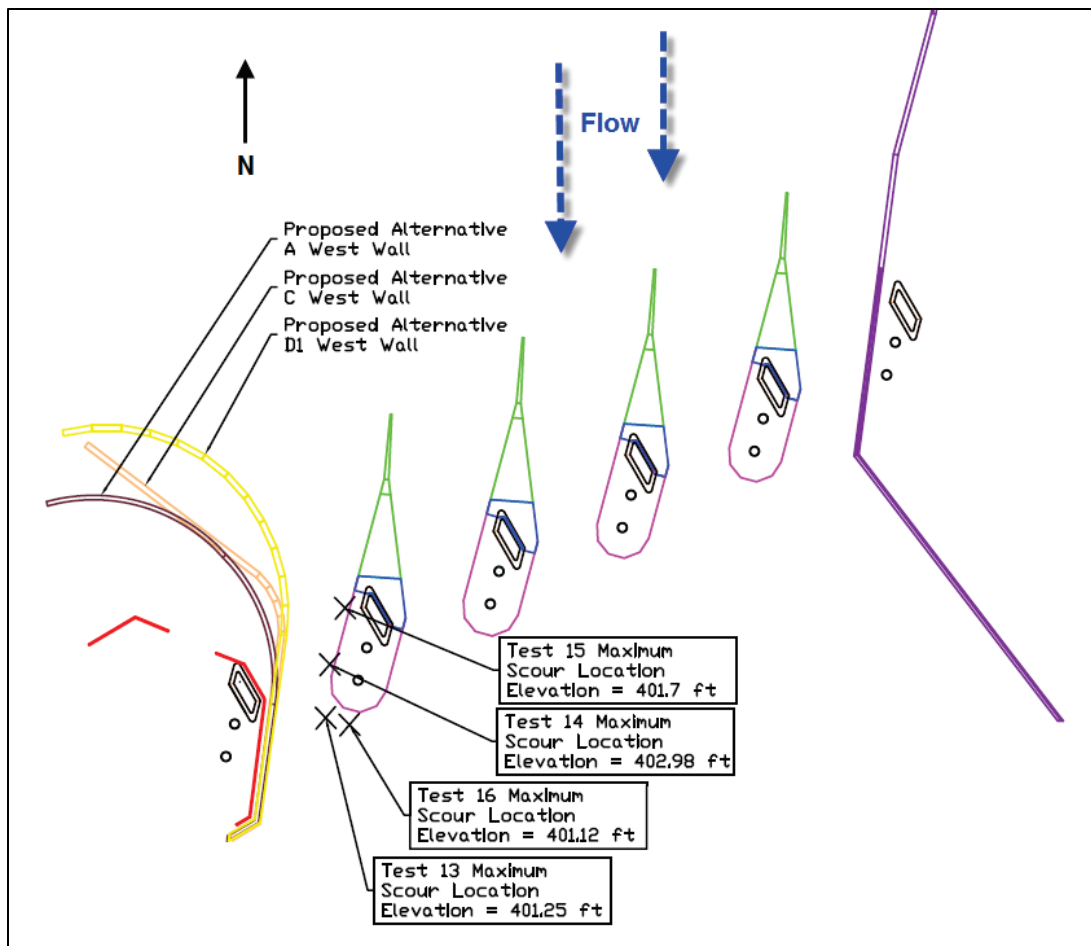


Table 7. Percentage Improvement from new and original proposed to existing conditions test for 30,000 cfs flows only.

Percentage Improvement, Proposed/Existing						
	Level Measurement					
Sy	30K cfs Existing	30K cfs Original Proposed	Test 13 New Proposed	Test 14 New Proposed	Test 15 New Proposed	Test 16 New Proposed
Average	395.4	404.6	401.3	403.0	401.7	401
Standard deviation	0.40	0.88	na	na	na	na
Scour depth	16.6	6.4	10.7	8.9	10.2	10.9
% Improvement		61%	36%	46%	39%	34%
	Scaled Maximum					
Average	383.4	399.3	393.5	397.0	394.8	393.1
Standard deviation	0.93	1.55	na	na	na	na
Scour depth	28.6	11.8	18.4	14.9	17.1	18.8
% Improvement		59%	36%	48%	40%	34%
	Scaled Minimum					
Average	390.2	402.3	397.9	400.5	398.9	397.6
Standard deviation	0.63	0.84	na	na	na	na
Scour depth	21.7	8.7	14.0	11.4	13.0	14.3
% Improvement		60%	35%	47%	40%	34%

## 6.2 Correlation and comparison

Correlation calculations were made to determine the dependence of various variables as related to one another. Since there was only one flow rate used in the new proposed conditions, there were no correlation calculations made for the new proposed conditions. Scour depth, approach velocity, WSE, Froude number, Reynold's number, and discharge were used in the correlations. Table 8 lists the correlation values for the most pertinent variable sets for both the existing, proposed, and both. As shown in Table 8 and illustrated in Figures 53 and 55, there is a strong inverse correlation between scour depth and WSE. This was initially illustrated in Figures 48–51. While correlated, it is slightly less for the proposed than it is for the existing (Table 8). The reduction in correlation indicates the beneficial nature of the original proposed plan. Conversely, there is little correlation between scour depth and velocity for existing conditions (Figure 54). However, there is no correlation between scour depth and velocity for the proposed conditions (Figure 56). This is an additional indicator that the original proposed plan has changed the flow field around the piers. The change is beneficial for the proposed conditions as related to maximum scour depth.

Velocity measurements were taken between the pier sets for the purpose of determining relative changes in velocities. Between each pier, three evenly spaced velocity measurements were made and averaged. The measurements were taken when the scour hole reached maximum depth. A percentage change between the proposed and existing was calculated and is listed in Table 9. As shown, the velocity typically increases between the piers from existing to proposed conditions. This is as expected, but as the correlation data illustrated, the increased velocity has no impact on the maximum scour depth from existing to proposed conditions. A decrease in velocity was shown for the 30,000 and 15,000 cfs flow cases between piers 2 to 1 and piers 3 to 2, respectively. Although not measured, this indicates the original proposed condition changes the overall conveyance putting more flow in the main channel, piers 6–4.

An additional comparison was made between the time-series scour elevation and the head loss through the bridge. As the scour hole deepens, the total head loss through the bridge decreases. This was shown to be the case for both the 30,000 and 15,000 cfs flow cases (Figures 57 and 58).

The addition of the concrete caps, pier nose extensions, and flow guide walls have decreased the amount of scour depth at the piers, as shown in Figures 59 and 60. While the flows tested were the perceived worst-case scenarios in the prototype, unaccounted uncertainties, as listed in Chapter 4, could contribute to changes in the local pier scour.

**Table 8. Correlation of various variables.**

Correlated Variables			Correlation Value		
			Existing	Proposed	Both
$Y_s$	and	V	-0.175	-0.004	0.173
$Y_s$	and	WSE	-0.850	-0.578	-0.430
$Y_s$	and	Fr	0.247	0.846	0.486
Re	and	$Y_s$	-0.553	-0.361	-0.158
WSE	and	V	0.580	0.810	0.542
Q	and	V	0.714	0.819	0.615
Q	and	WSE	0.963	1.000	0.976
Q	and	$S_y$	-0.724	-0.562	-0.431

$Y_s$ : scour depth, ft

V: velocity, ft/s

WSE: Water Surface Elevations, NGVD 29 ft

Re: Reynolds number

Q: Discharge, cfs

Figure 53. Correlation of scour depth vs. WSE for existing condition tests.

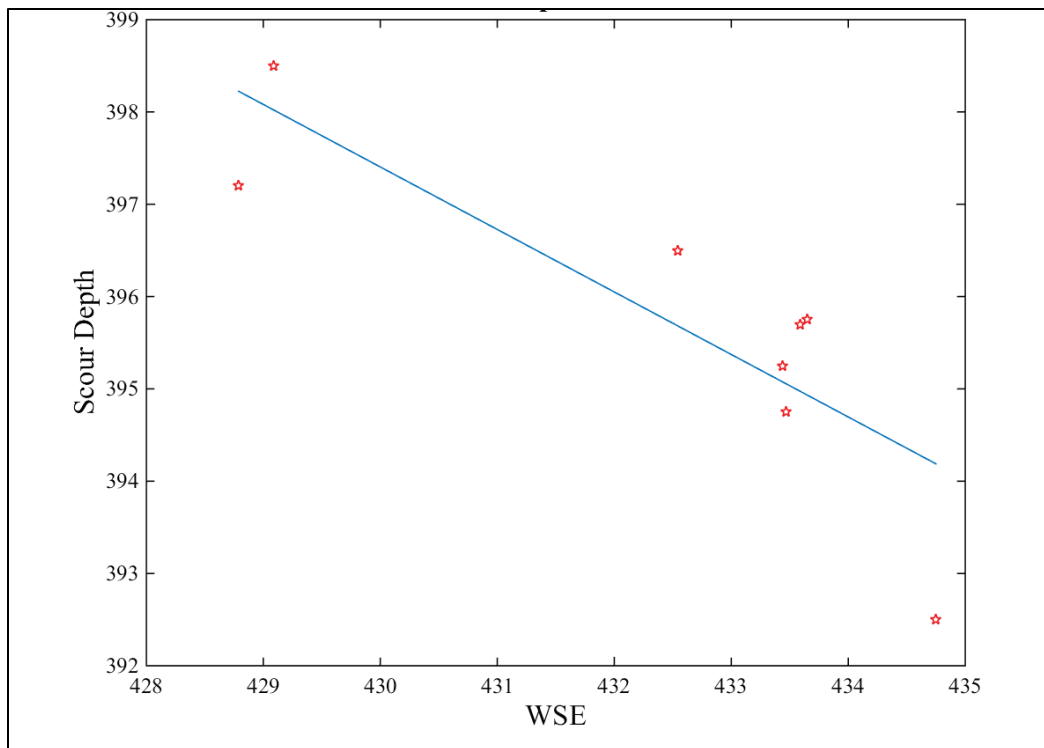


Figure 54. Correlation of scour depth vs. velocity for existing condition tests.

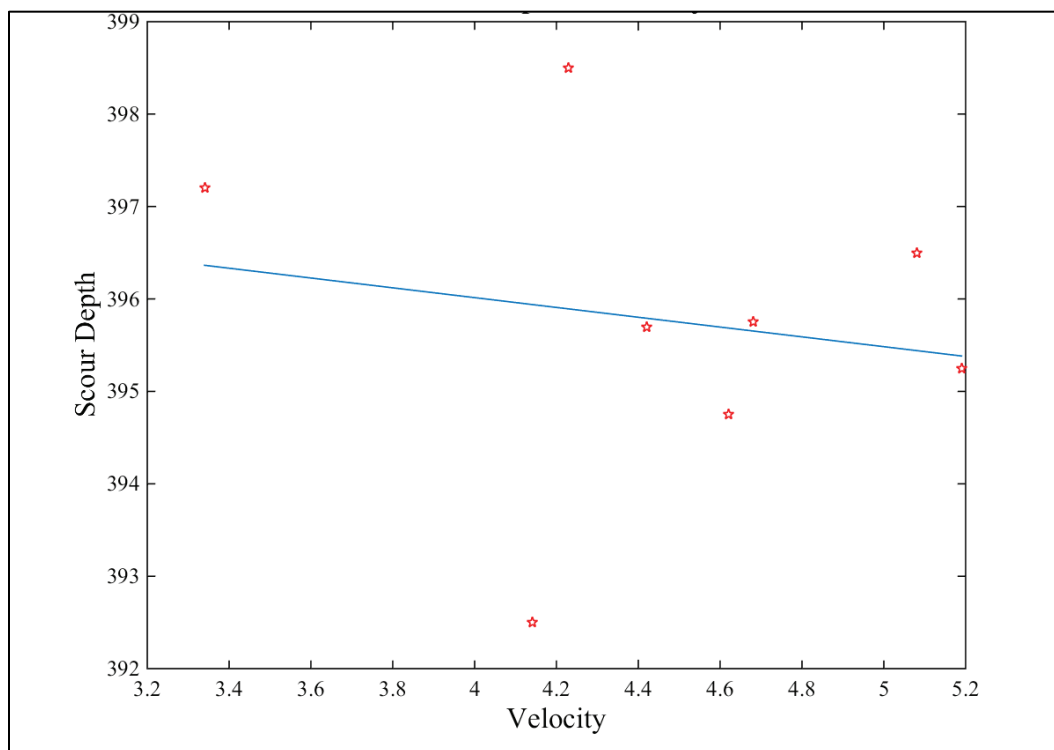


Figure 55. Correlation of scour depth vs. WSE for original proposed condition tests.

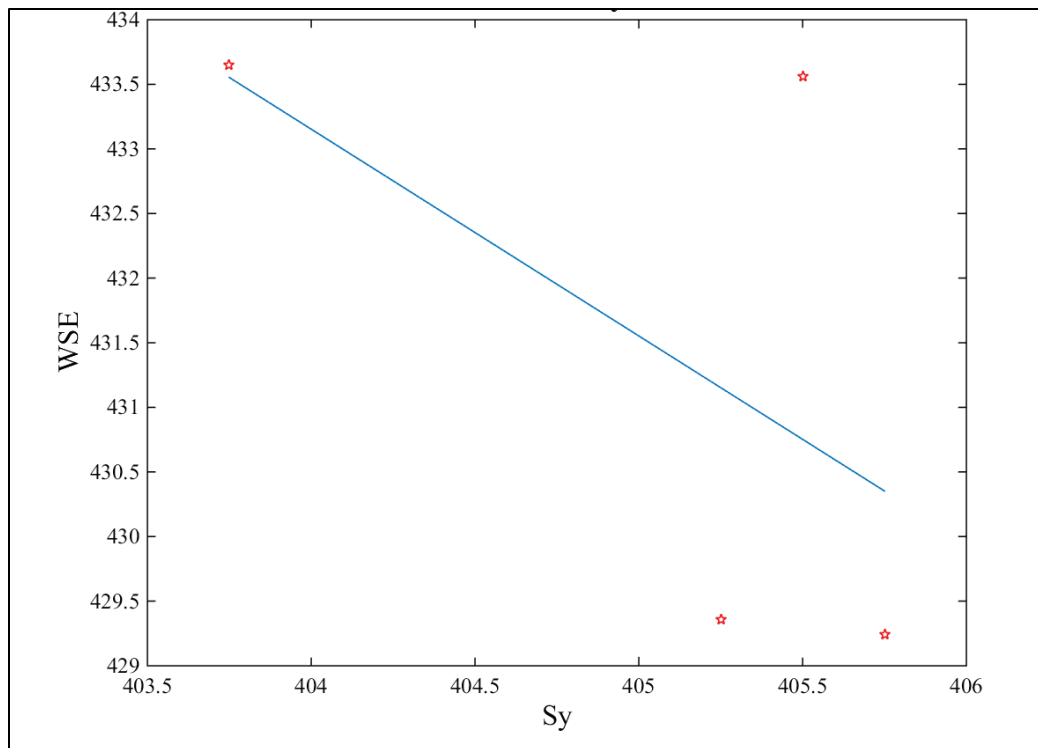


Figure 56. Correlation of scour depth vs. velocity for original proposed condition tests.

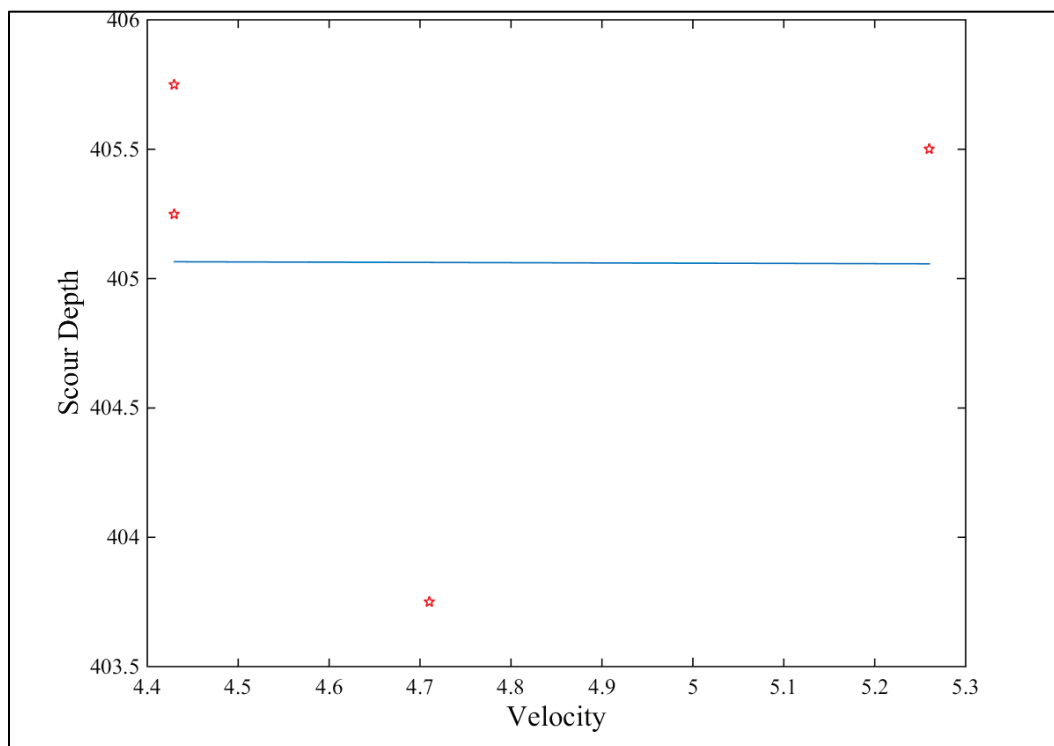




Table 9. Percentage increase above existing conditions in velocity between the piers.

Pier location	% Change in Average Velocity (Proposed–Existing)/Existing	
	30,000 cfs	15,000 cfs
6 to 5	40.8%	17.1%
5 to 4	13.0%	15.5%
4 to 3	28.8%	15.0%
3 to 2	12.5%	-27.6%
2 to 1	-42.1%	NA

Figure 57. Comparison of total head loss through the bridge and scour elevation for 15,000 cfs flow case.

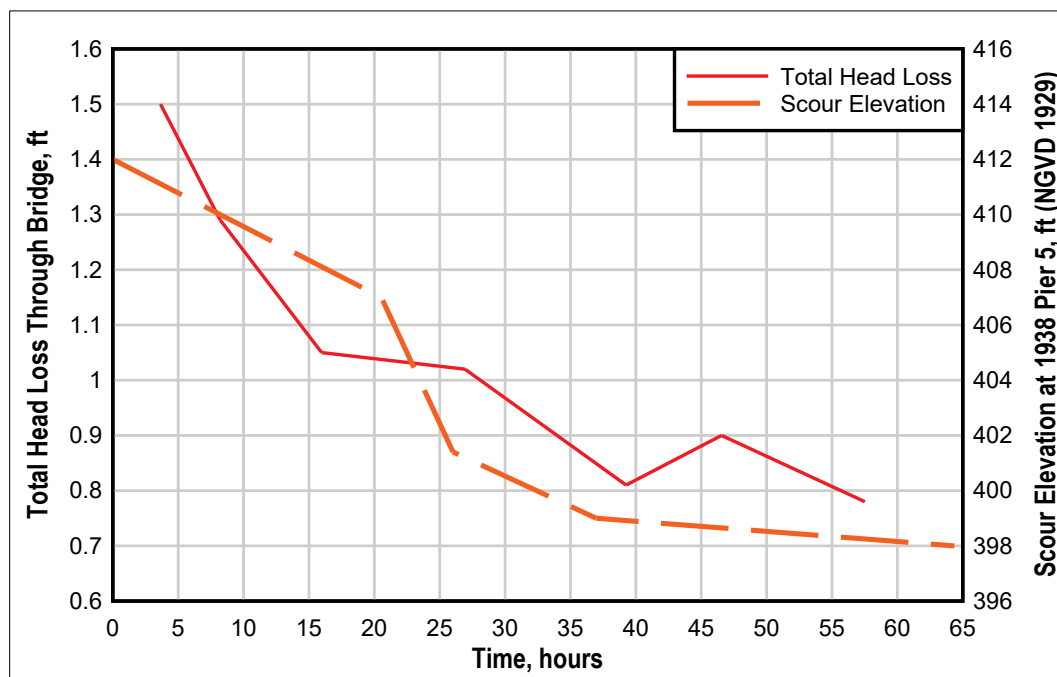


Figure 58. Comparison of total head loss through the bridge and scour elevation for 30,000 cfs flow case.

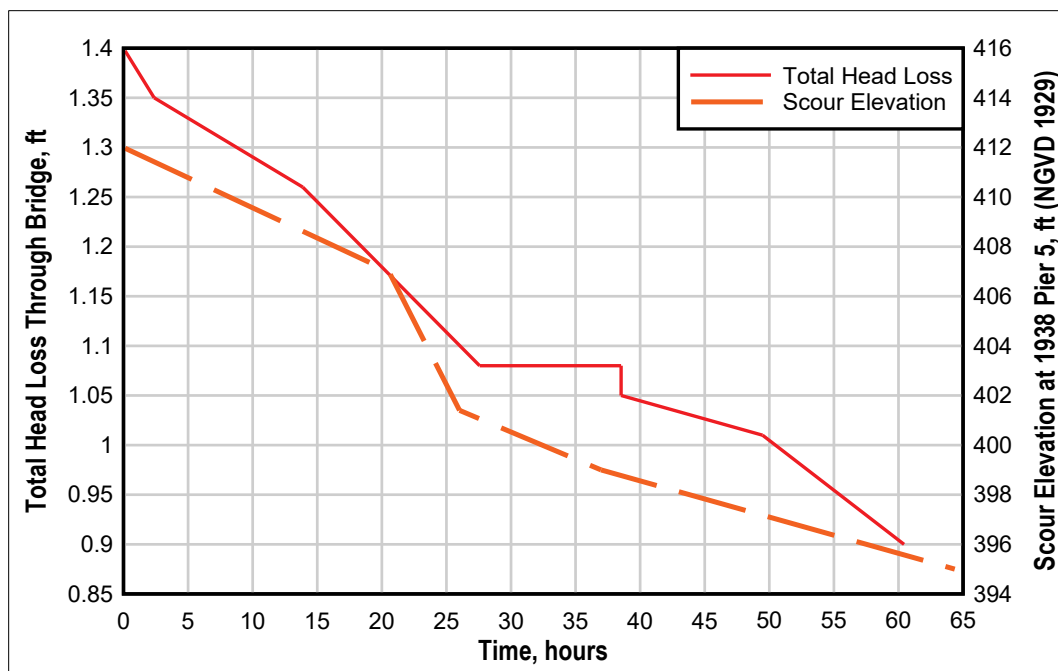




Figure 59. Cross section at bridge through scour holes for existing and original proposed minimum elevation for all tests at 30,000 cfs (un-scaled values and no channel degradation, circle represents location of maximum scour).

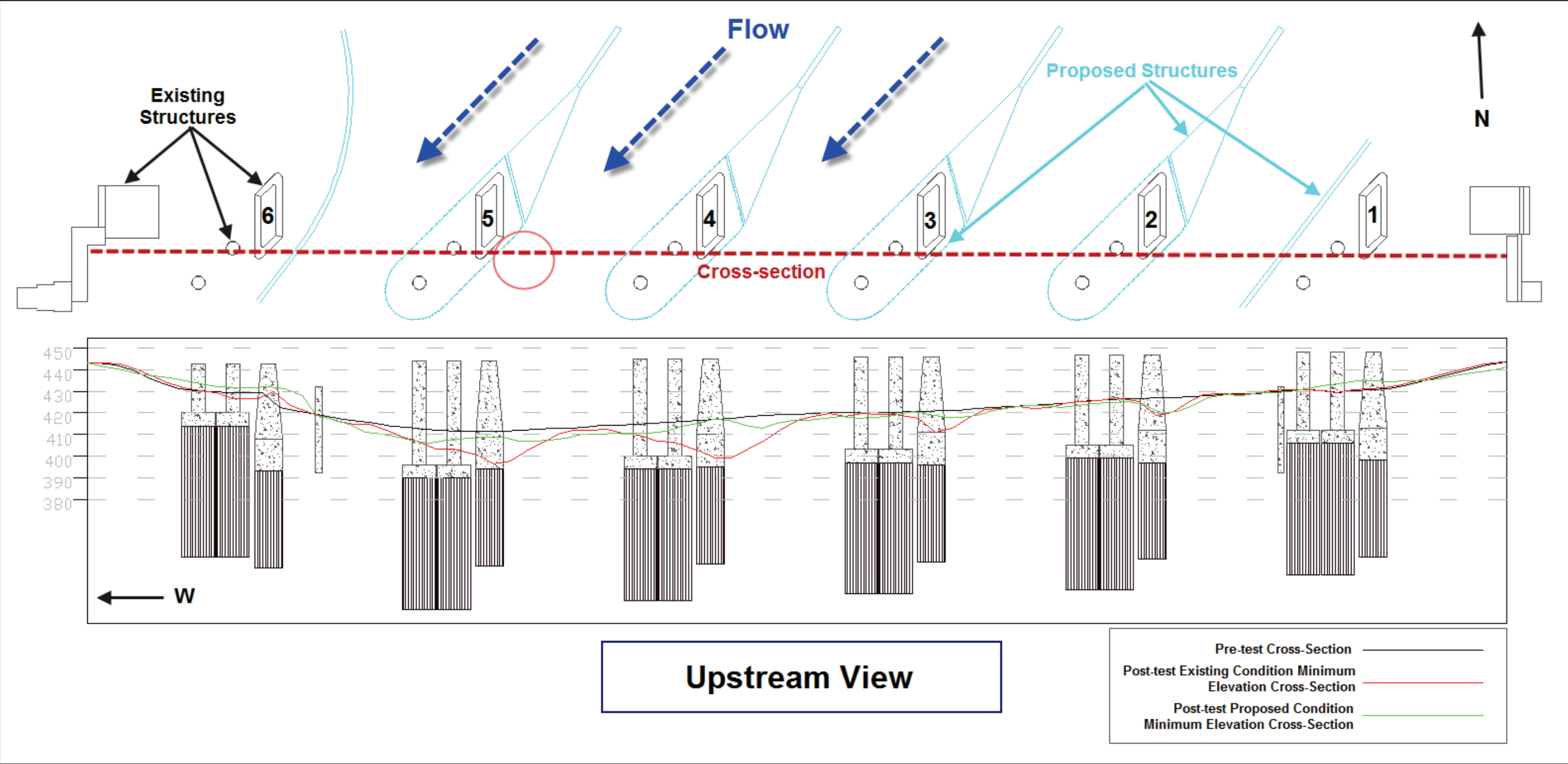
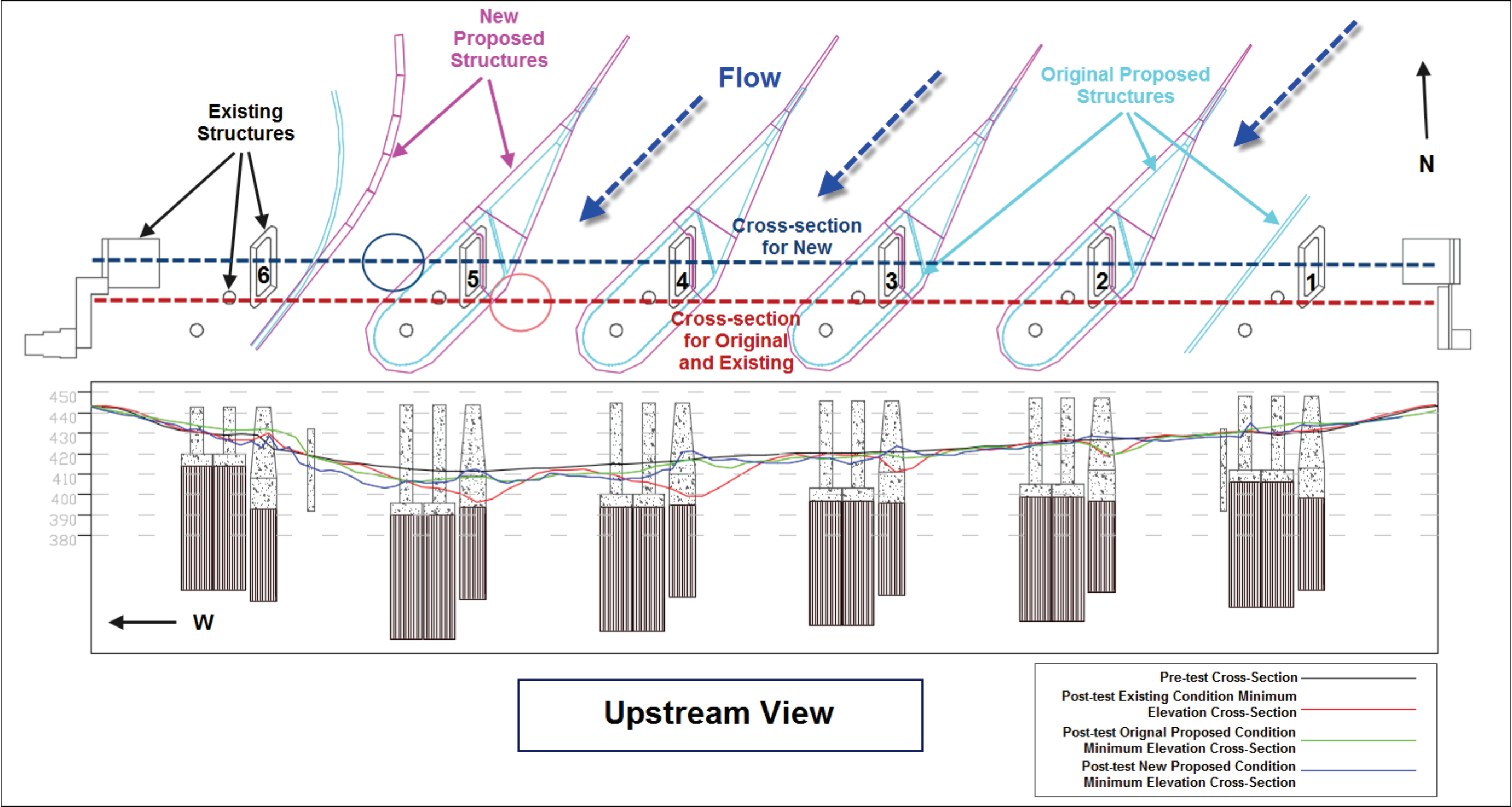


Figure 60. Cross section at bridge through scour holes for existing, original and new proposed minimum elevation for all tests at 30,000 cfs (un-scaled values and no channel degradation, circles represent the maximum scour).



### 6.3 Sensitivity testing

Tests 11 and 12 were done as sensitivity tests for evaluating long-term channel scour conditions. Test 11 simulated 6 ft of long-term channel and overbank scour (Figure 61). In addition to the configuration for Test 11, Test 12 had modified bathymetry around pier sets 4 and 5 (Figure 62). When the 6 ft of channel degradation was added back into the scour depth for Test 11, the scour depth was similar to the scour depths measured in Tests 8 and 9. However, Test 12 had modified bathymetry, which changed the invert at the scour hole to a lower start elevation. This naturally caused an increase in flow depth resulting in a greater scour depth. When the 6 ft of channel degradation was added back into the scour depth for Test 12, the increased scour depth was an additional 3 ft from Tests 8 and 9 (Figures 63–64). Then, Figures 65 and 66 show the pre- minus post-test conditions for Tests 11 and 12, respectively. Both tests were conducted with the same downstream control. As the channel scours, the downstream will also lower resulting in a lower flow depth at the bridge and reduced scour.

Figure 61. Test 11 (30,000 cfs original proposed conditions) pre-test lidar scan.

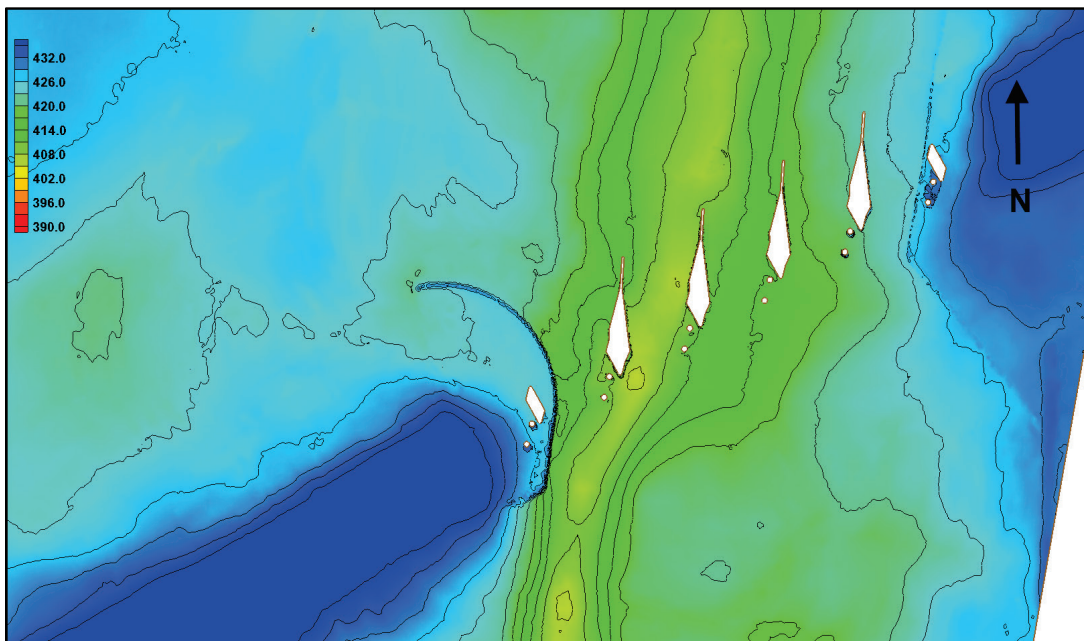




Figure 62. Test 12 (30,000 cfs original proposed conditions) pre-test lidar scan.

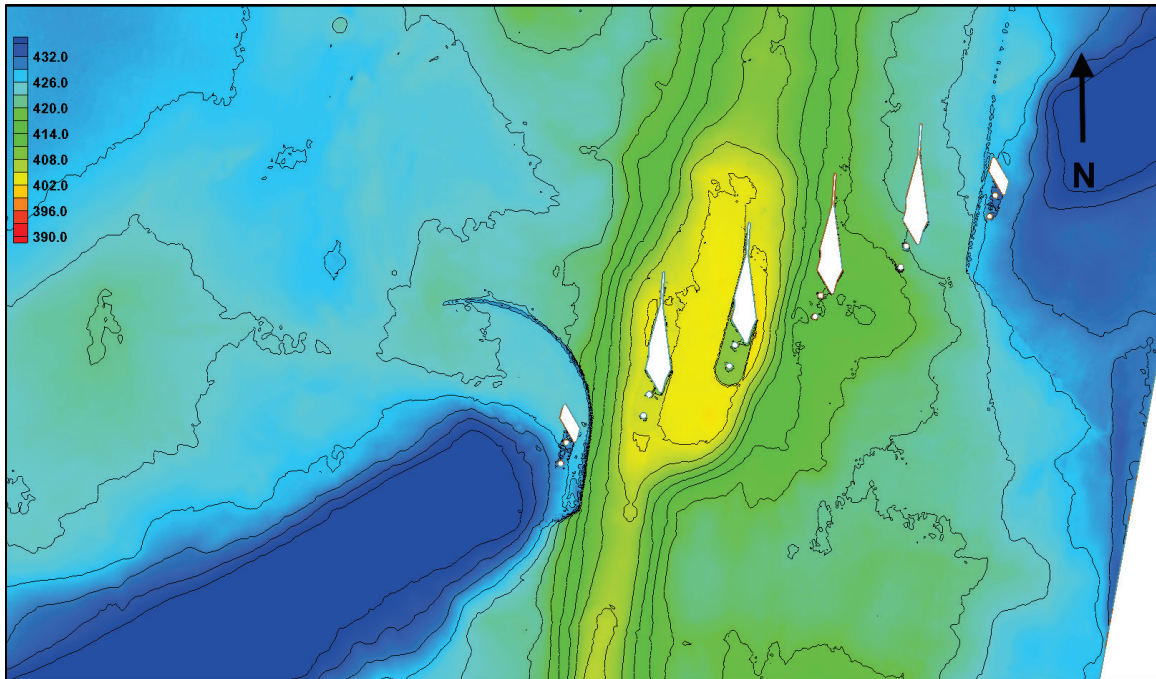


Figure 63. Test 11 (30,000 cfs original proposed conditions) post-test lidar scan.

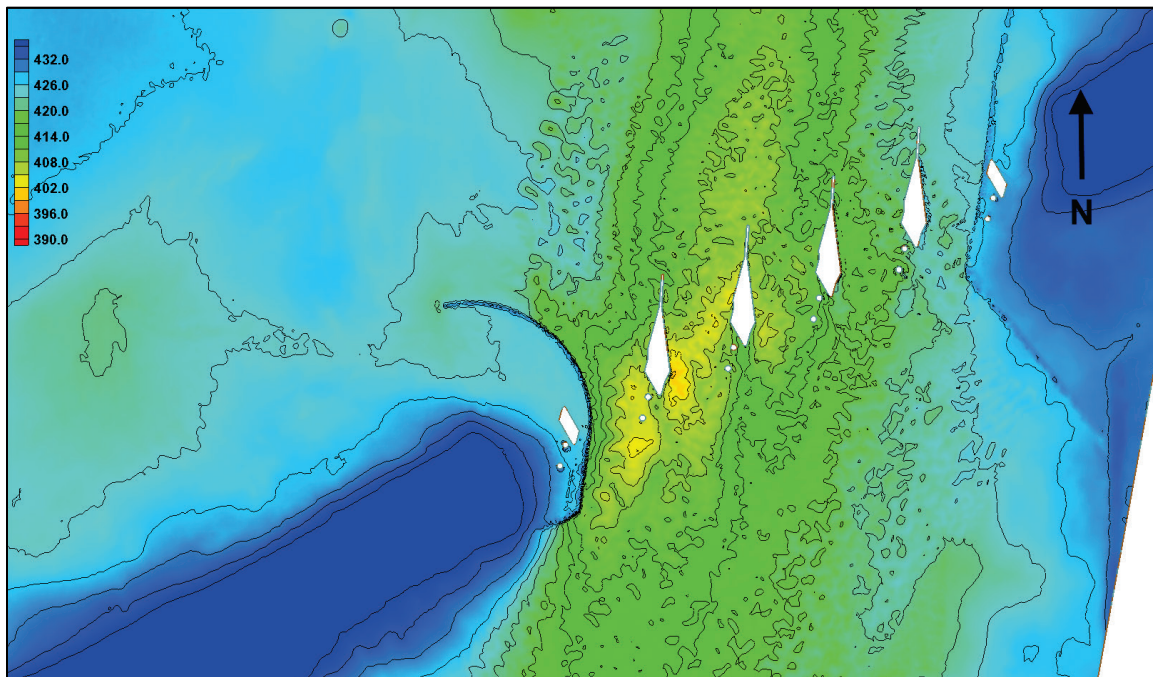


Figure 64. Test 12 (30,000 cfs original proposed conditions) post-test lidar scan.

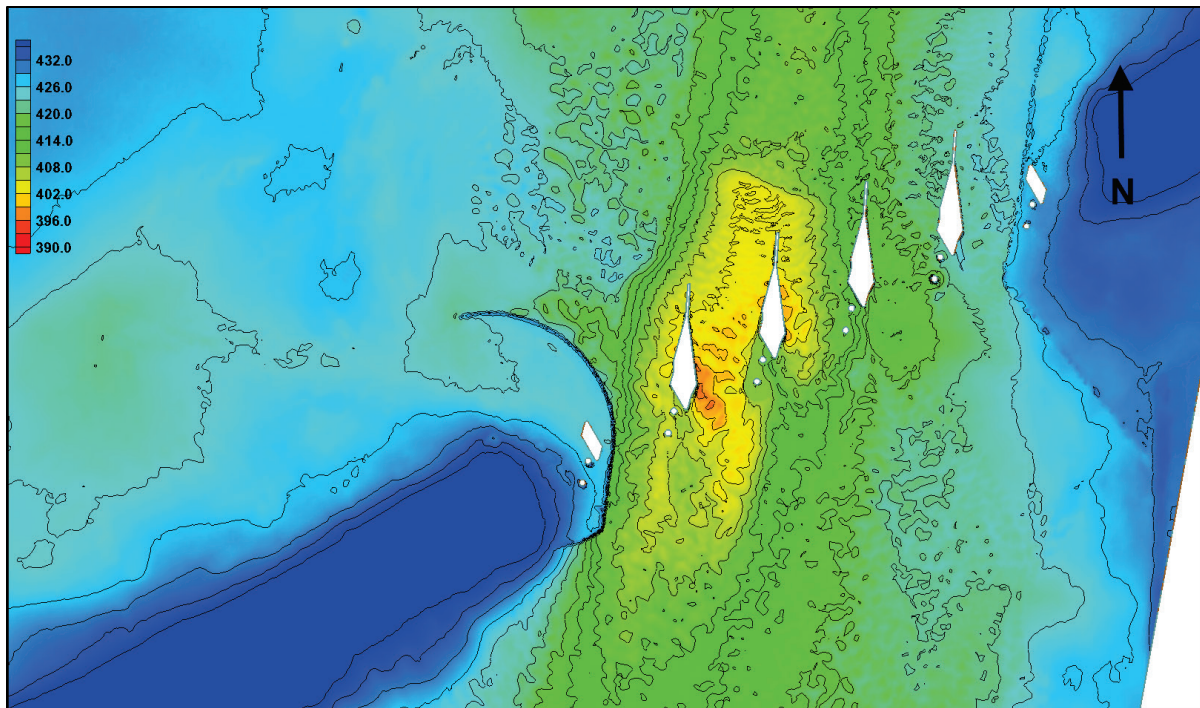


Figure 65. Test 11 (30,000 cfs original proposed conditions) pre- minus post-test lidar survey (blues indicate deposition and yellows/reds indicate scour).

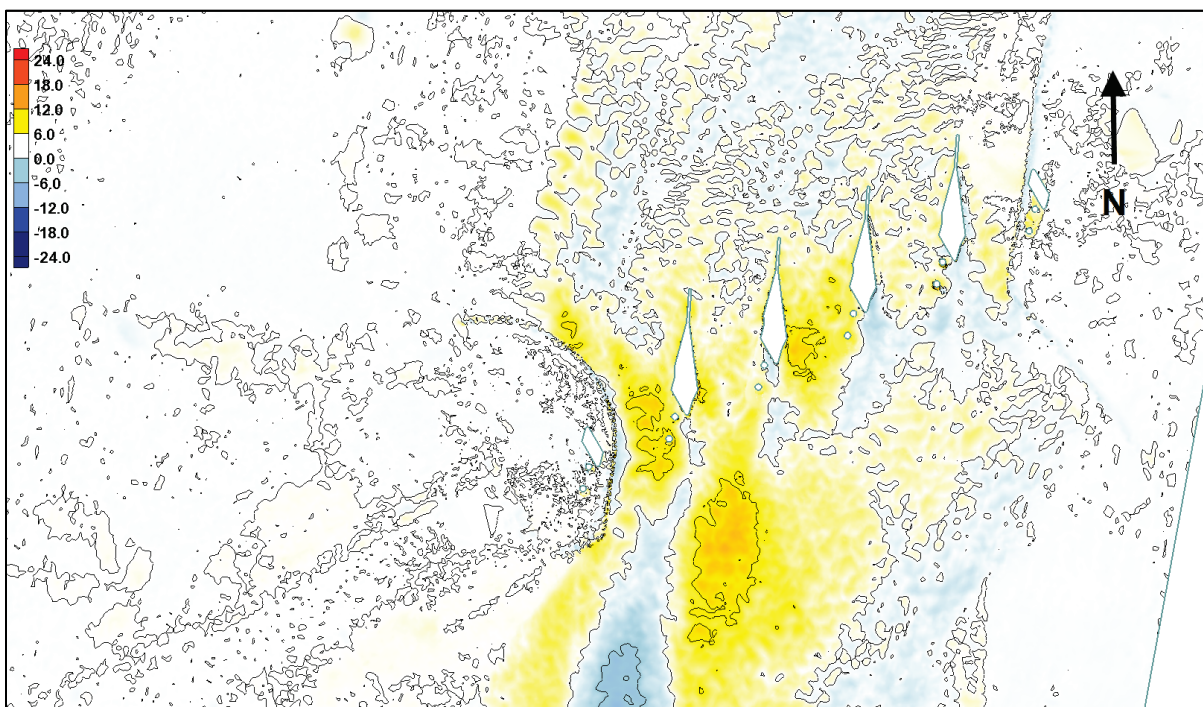
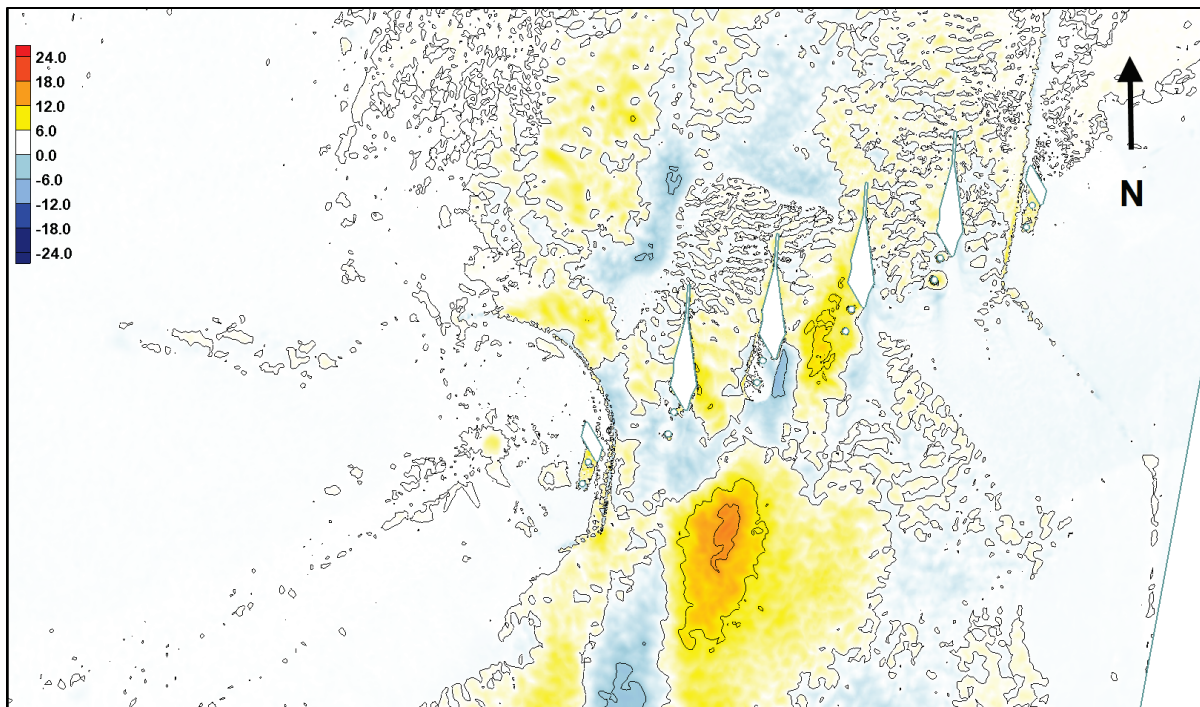




Figure 66. Test 12 (30,000 cfs original proposed conditions) pre- minus post-test lidar survey (blues indicate deposition and yellows/reds indicate scour).



## 7 Conclusion and Recommendation

The test results show the proposed concrete cap (pile enclosure), guide walls, and pier extensions, under the presumed worst-case flow conditions, to effectively and significantly reduce local scour, resulting in less scour than the existing configuration. These findings provide evidence that the original and new proposed conditions are a benefit to reducing scour at the bridge. However, careful consideration should be given to the selected scour elevation used in the final design. Note that long-term scour is not considered in the modeling and should be accounted for to derive total scour.

As the flow depth increases so does the scour depth. The dependency of flow depth to scour depth is shown in the data where there is a direct correlation. However, the correlation is reduced when evaluated for the original proposed condition indicating a direct impact on the local scour behavior. The testing indicates that reducing flow depth in the prototype will reduce scour depth in the prototype. Consideration of this relationship should be made for future projects on the Santa Ana River where any change would potentially affect the flow depth at the bridge.

While the facility is available, ERDC recommends any additional desired testing be conducted with the general physical model. Currently, the scour values reported include local, abutment, and contraction. Thus, it would also be beneficial to isolate a single set of piers, pier extensions, and concrete cap at the 1:30 scale to determine the local pier component of the scour. This separation of scour components would allow for a more refined application of the scale factor from Sharp et al. (2016). Furthermore, any proposed additions to the bridge such as the additions of new piers should be evaluated in the model to ensure they do not interfere with the benefit observed with the proposed configuration. Finally, if capturing changes in velocity between piers from existing to proposed conditions is desired, then additional testing should be conducted. More precise methods for velocity measurement capable of capturing undistorted velocities would be implemented.

## References

- Breusers, H. N. C., G. Nicollet, and H. W. Shen. 1977. "Local Scour around Cylindrical Piers." *J. Hydr. Res.* 15(3): 211–252.
- Chiew, Y. M. 1984. *Local Scour at Bridge Piers*. Rep. No. 355. Auckland, New Zealand: School of Engineering, Univ. of Auckland. <http://hdl.handle.net/2292/2520>.
- Deborah R. Cooper, Charles D. Little, Jr., Julie Cohen, Brendan Yuill, Johannes Wibowo, Bryant Robbins, Raymond Reed, Maureen K. Corcoran, and Kevin S. Holden. 2016. *Application of Bridge Pier Scour Equations for Large Woody Vegetation*. ERDC TR-16-10. Vicksburg, MS: U.S. Army Engineer Research and Development Center.
- HEC-18. 2012. *Evaluating scour at bridges*. Hydraulic Engineering Circular No. 18, Rep. No. FHWA-HIF-12-003. Washington, DC: U.S. Dept. of Transportation. <http://www.fhwa.dot.gov/engineering/hydraulics/pubs/hif12003.pdf>.
- Jain, S. C., and E. E. Fischer. 1979. *Scour around Circular Bridge Piers at High Froude Numbers*. Rep. No. FHWA-RD-79-104. Washington, DC: Federal Hwy. Administration.
- Julien, P. Y. 2002. *River Mechanics*. Cambridge, UK: Cambridge University Press.
- Kothyari, U. C., R. J. Garde, and K. G. Ranga Raju. 1992. "Temporal Variation of Scour around Circular Bridge Piers." *J. Hydraul. Eng.* 118(8): 1091–1106.
- Laursen, E. M. 1953. "Observations on the Nature of Scour." In *Proceedings of Fifth Hydraulic Conference, Bulletin 34, University of Iowa, Iowa City, Iowa, June 9–11, 1952*, 179–197. <http://ir.uiowa.edu/uisie/34>.
- Laursen, E. M., and A. Toch. 1956. *Scour around Bridge Piers and Abutments*. Bull. No. 4. Ames, IA: Iowa Hwy. Res. Board. <http://publications.iowa.gov/id/eprint/20237>.
- Lee, S., and T. Sturm. 2009. "Effect of Sediment Size Scaling on Physical Modeling of Bridge Pier Scour." *J. Hydraul. Eng.* 135(10): 793–802. [https://doi.org/10.1061/\(ASCE\)HY.1943-7900.0000091](https://doi.org/10.1061/(ASCE)HY.1943-7900.0000091).
- Lottes, S. A., N. Sinha, C. Bojanowski, and K. Kerenyi. 2015. *Three Dimensional Analysis of Pier Extension and Guide Wall Design Alternatives to Mitigate Local Scour Risk at the BNSF Railroad Bridge Downstream of the Prado Dam*. ANL/ESD-15/7. Argonne National Laboratory. <http://www.ipd.anl.gov/anlpubs/2015/03/113580.pdf>.
- Melville, B. W., and A. J. Sutherland. 1988. "Design method for local scour at bridge piers." *J. Hydr. Engrg. ASCE* 114(10):1210–1226.
- Melville, B. W., and Y. M. Chiew. 1999. "Time scale for local scour at bridge piers." *J. Hydraul. Eng.* 125(1): 59–65.
- Mia, Md. F., and H. Nago. 2003. "Design Method of Time-Dependent Local Scour at Circular Bridge Pier." *J. Hydraul. Eng.* 129(6): 420–427.

- Mueller, D. S., and C. R. Wagner. 2005. *Field observations and evaluations of streambed scour at bridges*. (No. FHWA-RD-03-052).  
<http://www.fhwa.dot.gov/publications/research/infrastructure/hydraulics/03052/03052.pdf>.
- Sharp, J. A., R. E. Heath, H. E. Park, and T. O. McAlpin. 2016. *Scale Factor Study for 1:30 Local Scour Model*. ERDC/CHL CHETN-VII-15. Vicksburg, MS: U.S. Army Engineer Research and Development Center.
- Shen, H. W., V. R. Schneider, and S. Karaki. 1969. "Local scour around bridge piers." *Journal of the Hydraulics Division, Proceedings of the American Society of Civil Engineers*, ASCE 95(6): 1919–1940.
- Vanoni, V. A. 2006. *Sedimentation Engineering*. ASCE Manuals and Reports on Engineering Practice No. 54. Reston, VA: American Society of Civil Engineers.  
<http://dx.doi.org/10.1061/9780784408230>.



## Appendix A: Water Surface Data

Figure A-1. Test 2 average WSE for various tailgate settings.

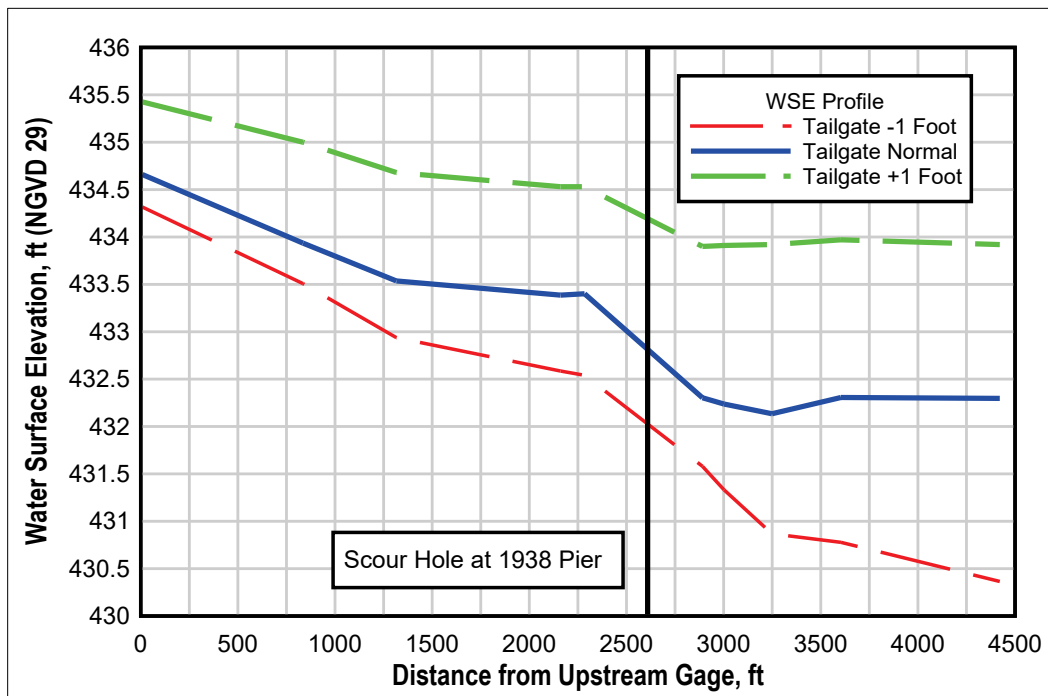


Figure A-2. Test 2 existing conditions minus 1 ft on tailgate for 30,000 cfs.

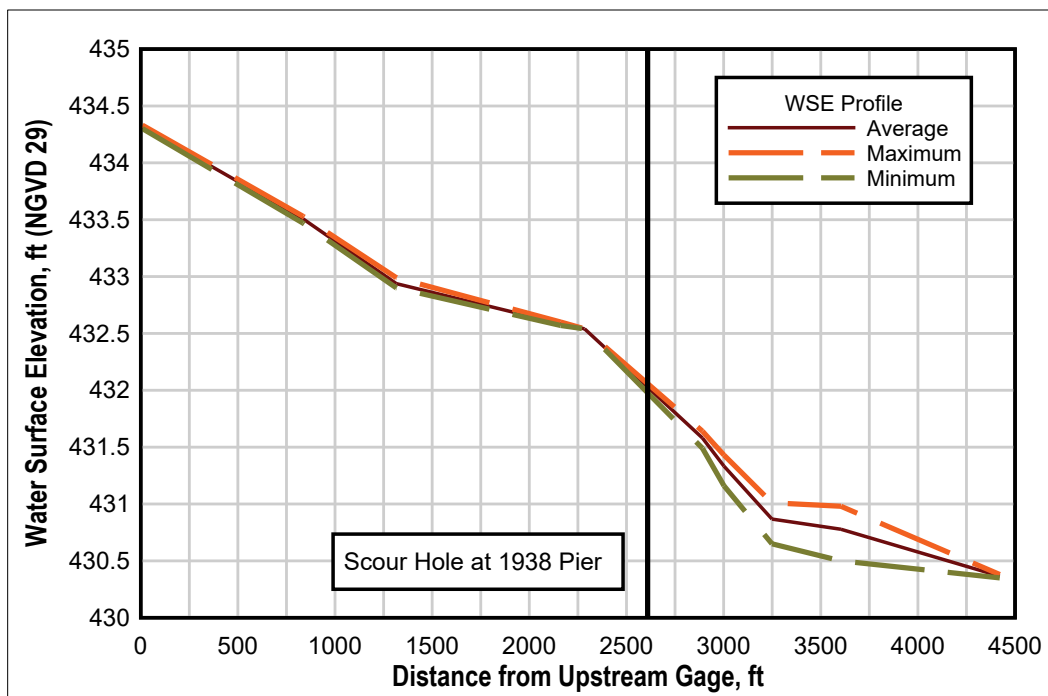


Figure A-3. Test 2 existing conditions 30,000 cfs.

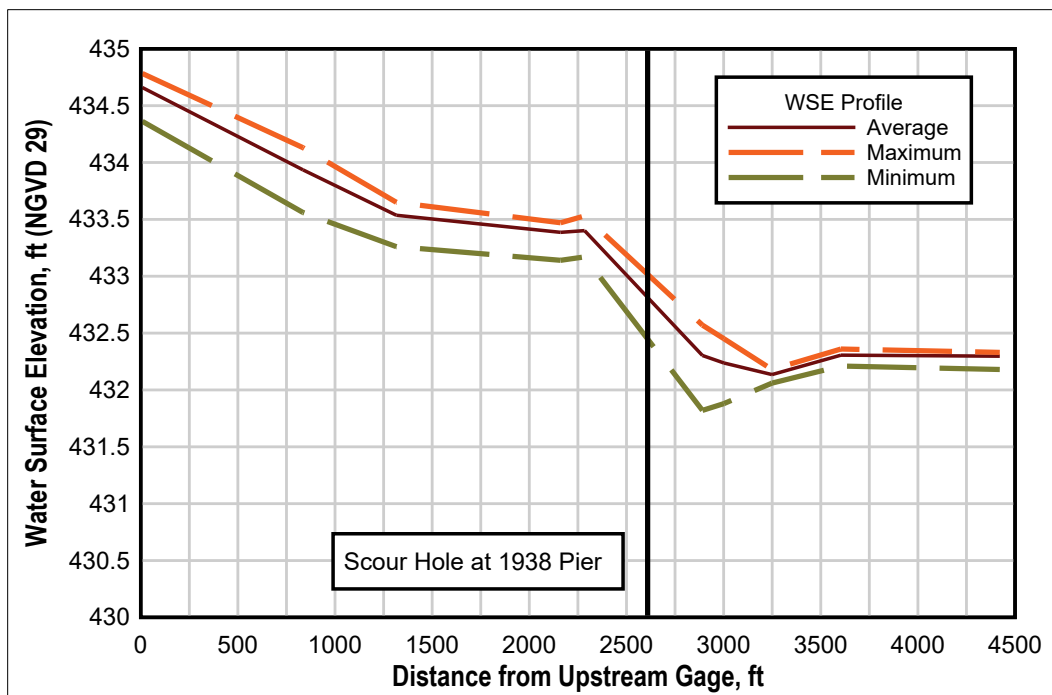


Figure A-4. Test 2 existing conditions plus 1 ft on tailgate for 30,000 cfs.

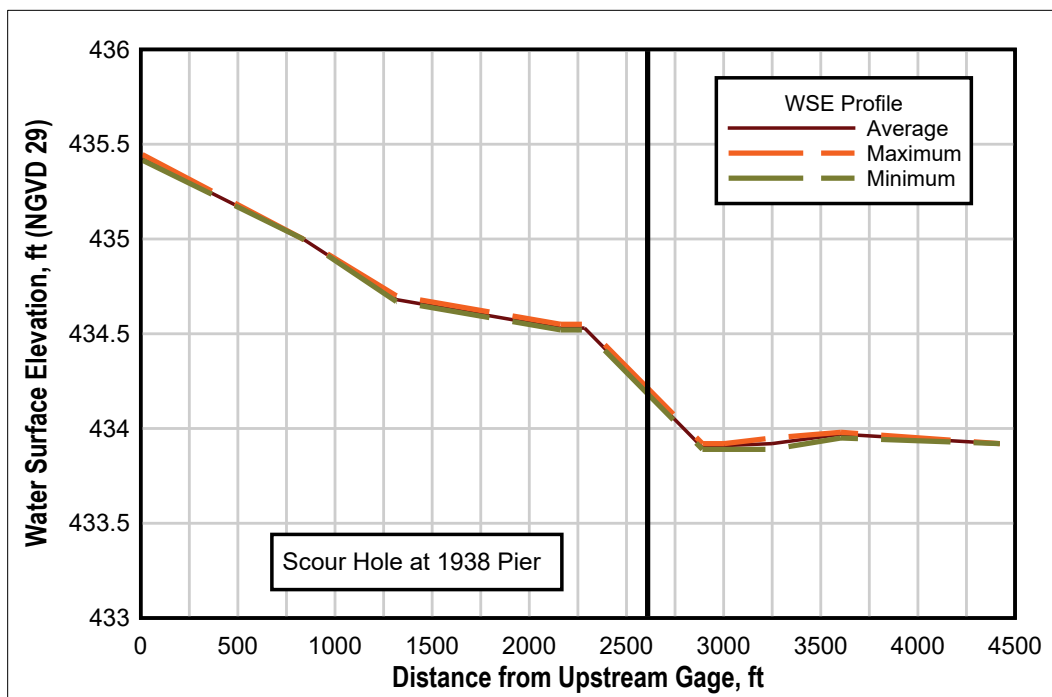


Figure A-5. Test 3 existing conditions 15,000 cfs.

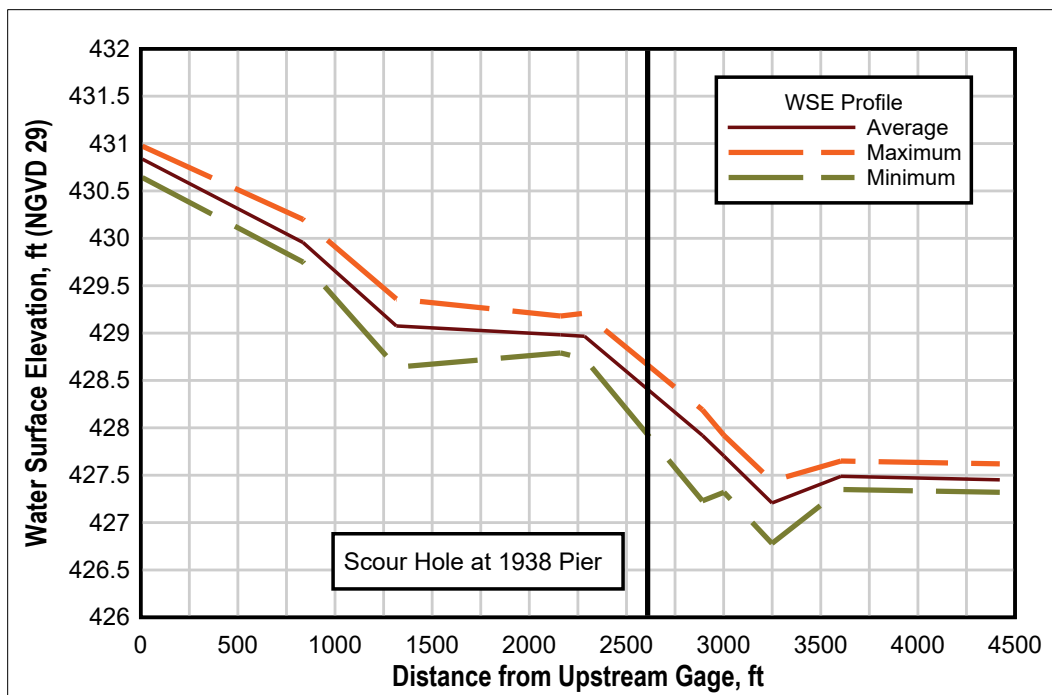


Figure A-6. Test 4 existing conditions 15,000 cfs.

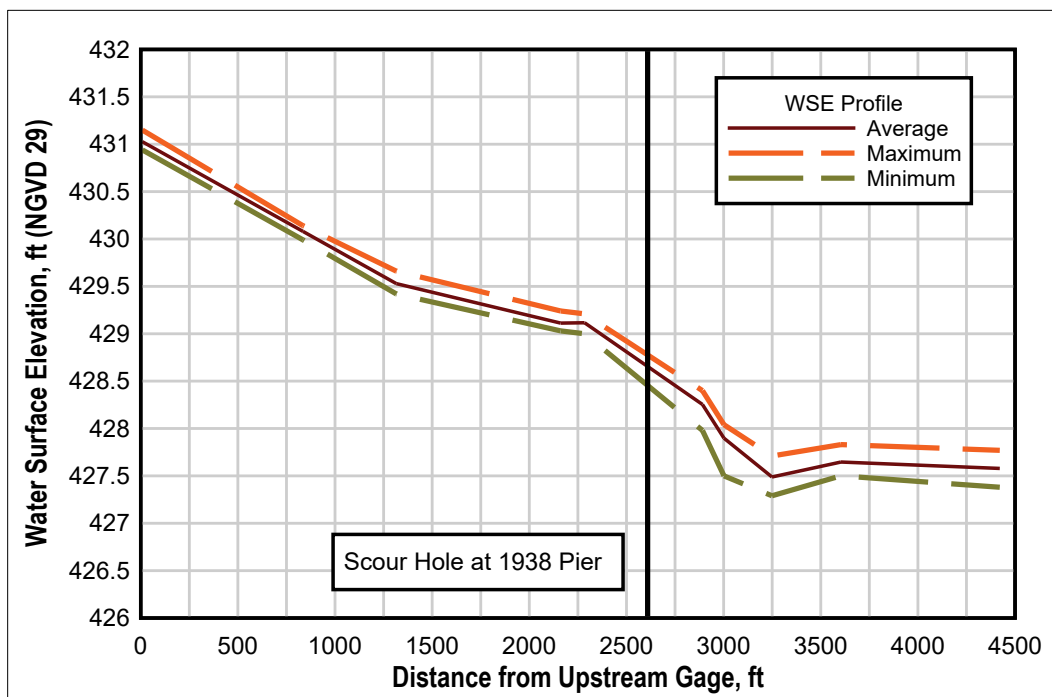


Figure A-7. Test 5 existing conditions 30,000 cfs.

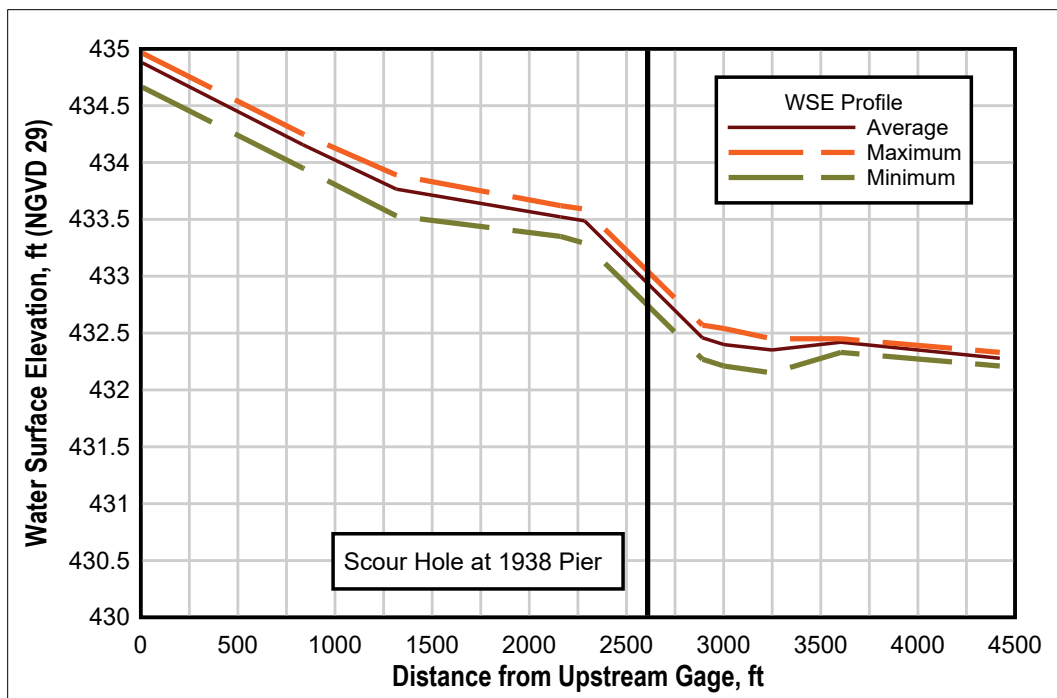


Figure A-8. Test 6 existing conditions 30,000 cfs.

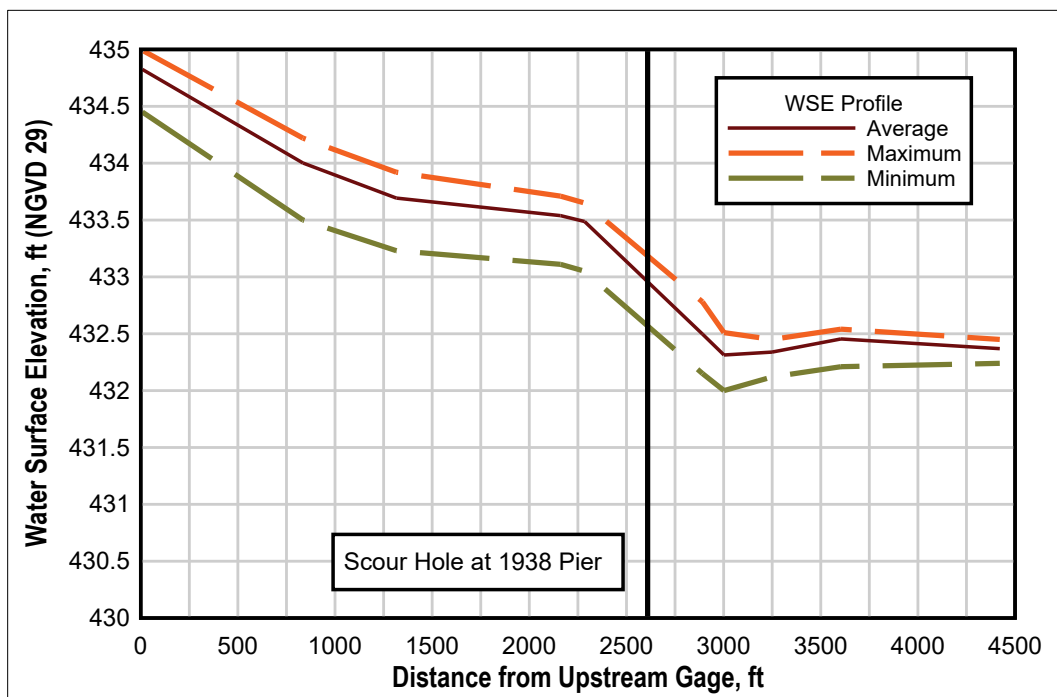


Figure A-9. Test 7 original proposed conditions 15,000 cfs.

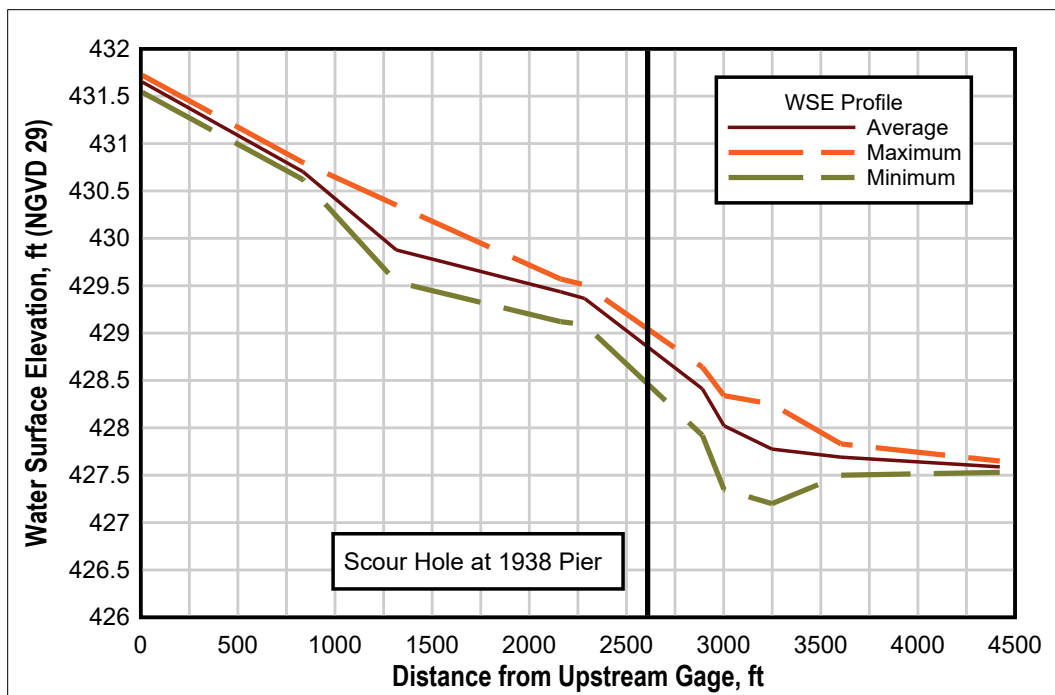


Figure A-10. Test 8 original proposed conditions 30,000 cfs.

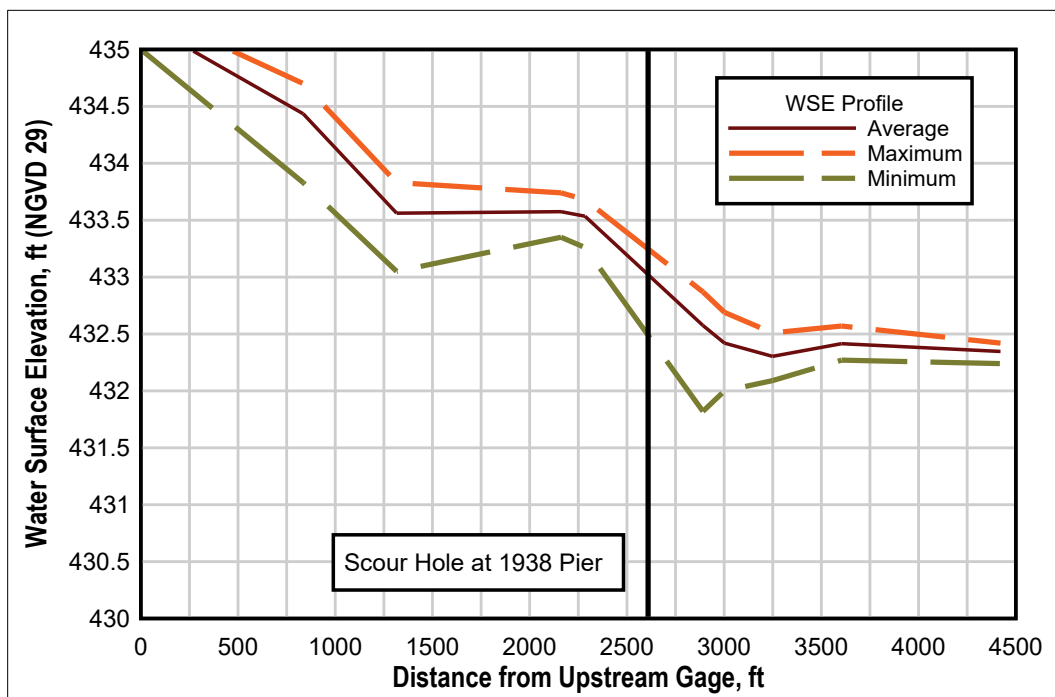


Figure A-11. Test 9 original proposed conditions 30,000 cfs.

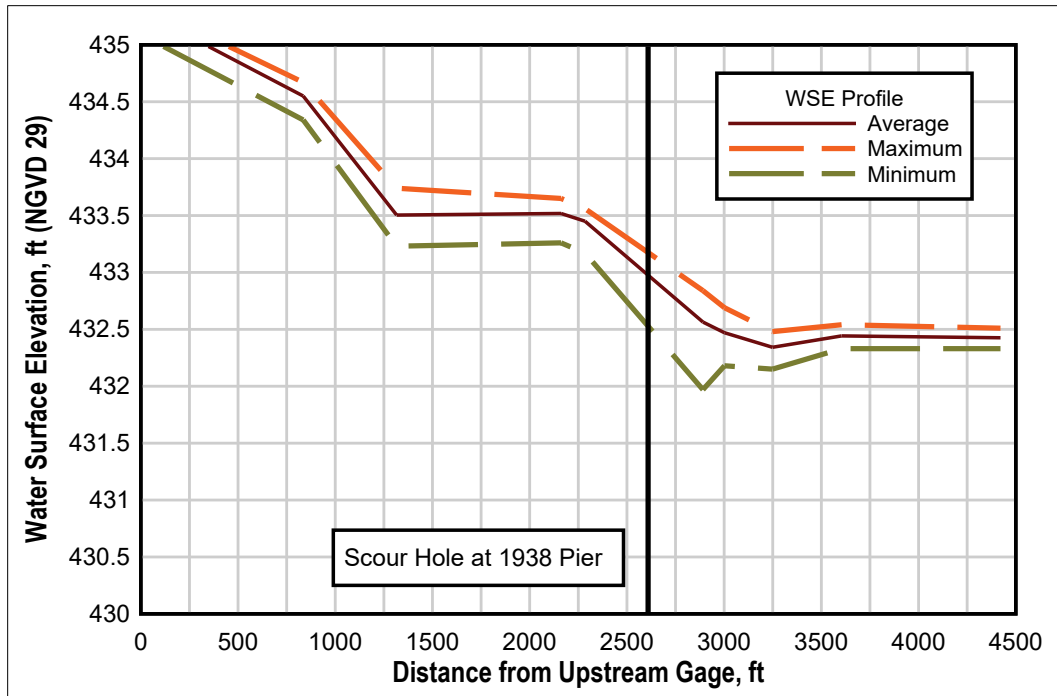


Figure A-12. Test 10 original proposed conditions 15,000 cfs.

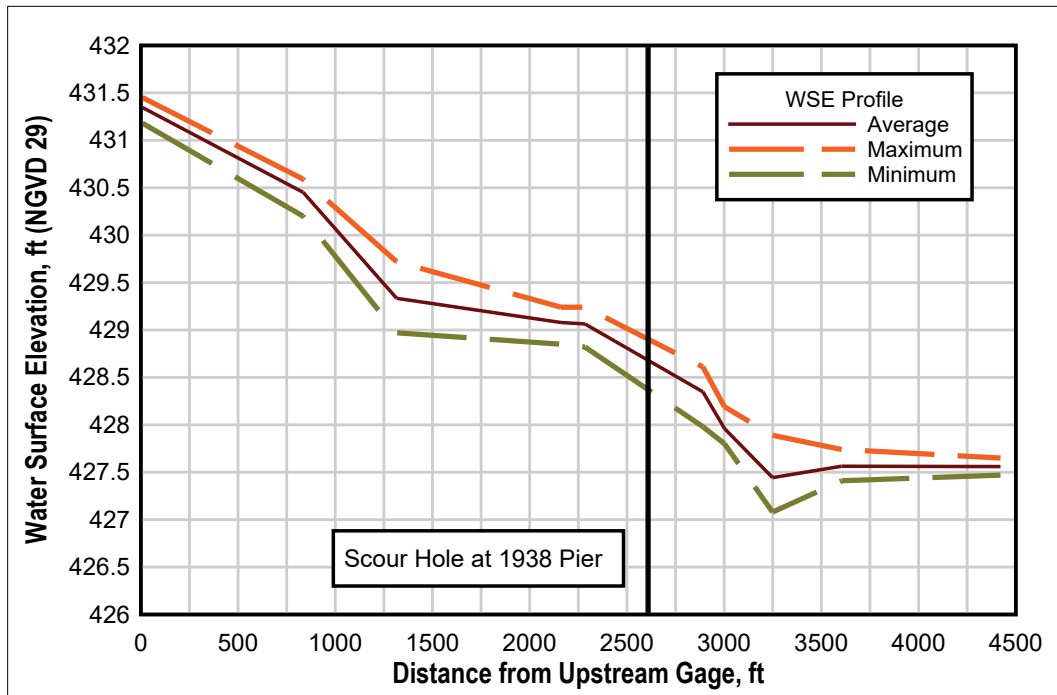




Figure A-13. Test 11 original proposed conditions simulating 6 ft of channel degradation  
30,000 cfs.

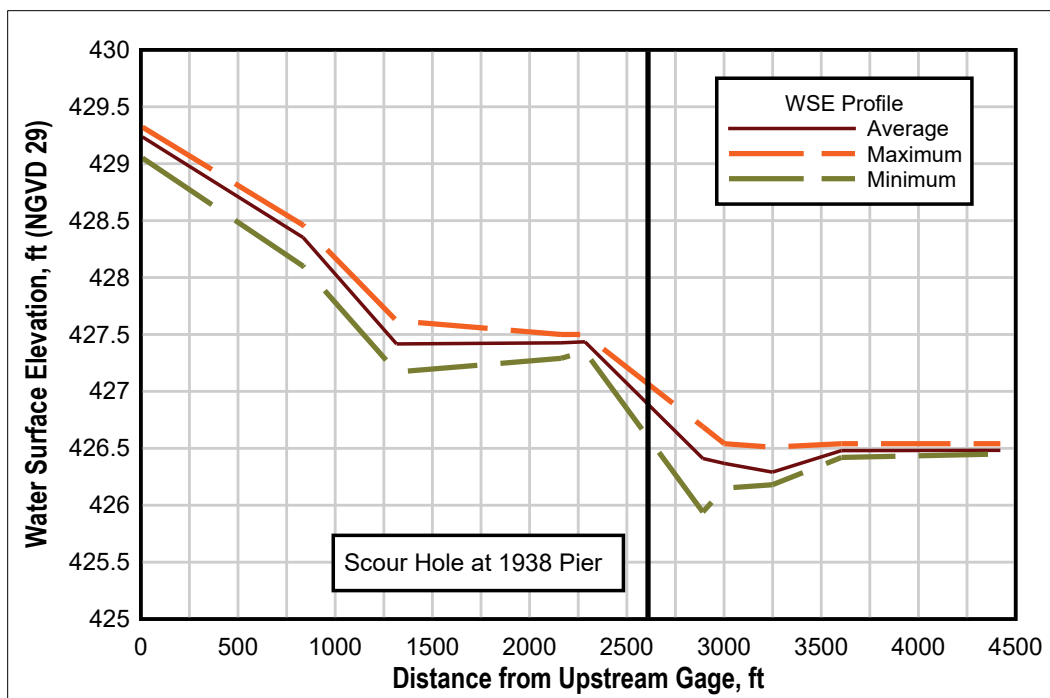


Figure A-14. Test 12 original proposed conditions simulating 6 ft of channel degradation and  
new channel bathymetry 30,000 cfs.

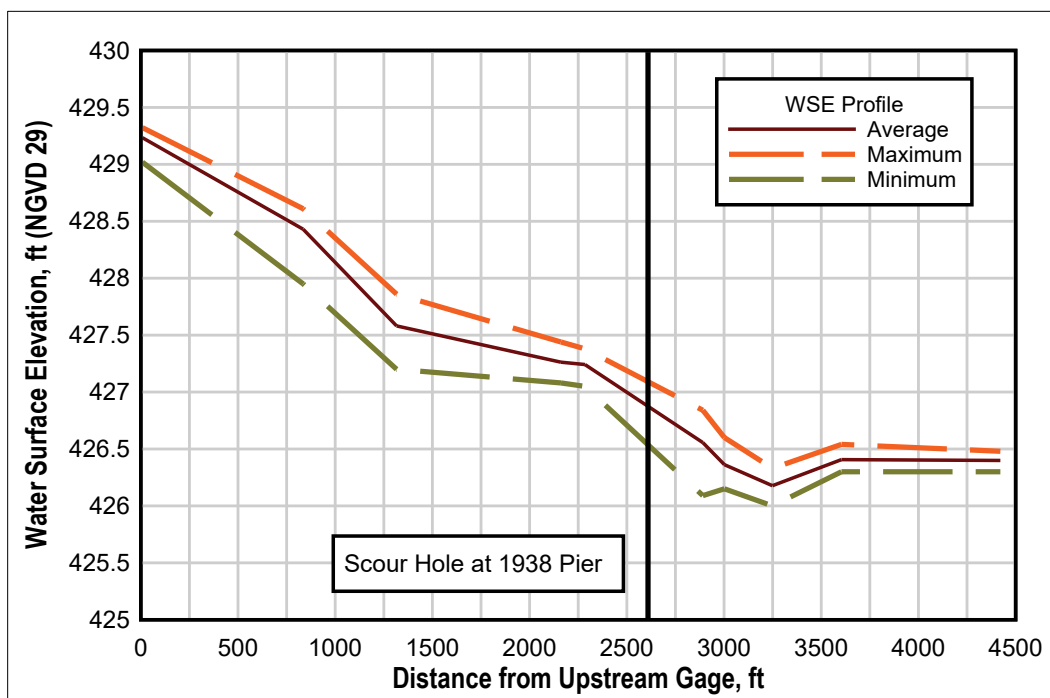


Figure A-15. Test 13 new proposed conditions 30,000 cfs.

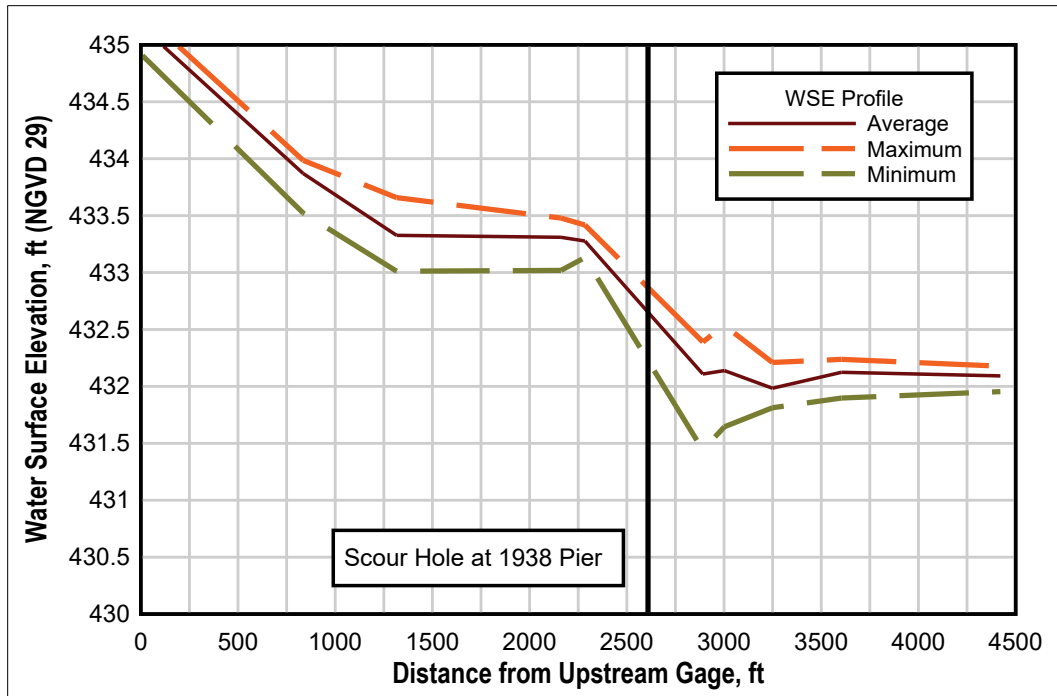


Figure A-16. Test 14 new proposed conditions 30,000 cfs.

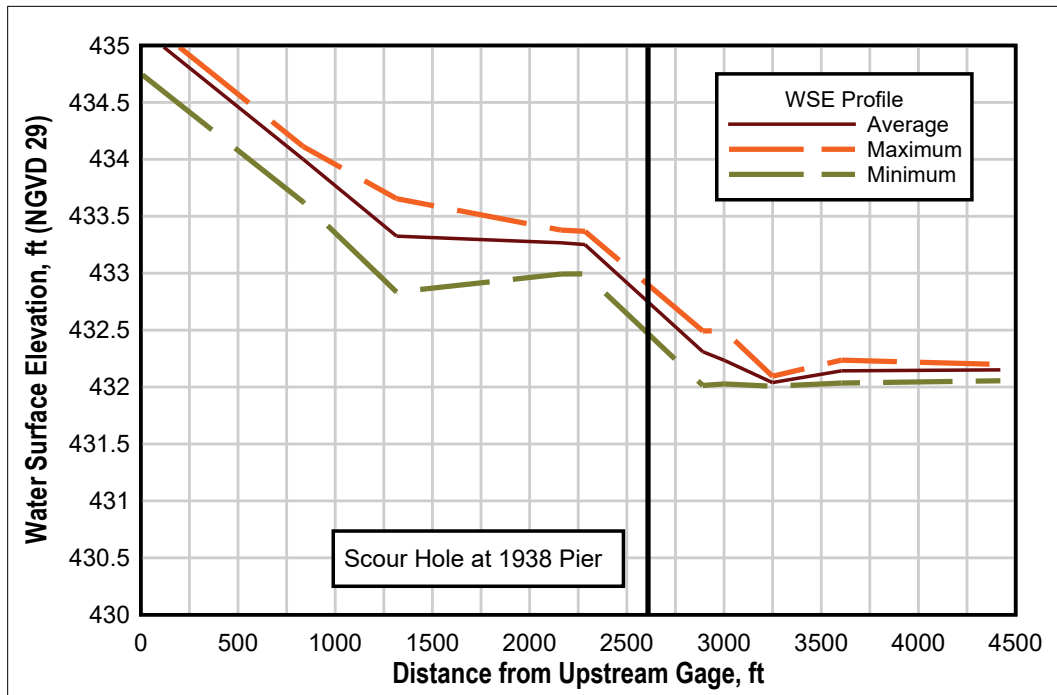


Figure A-17. Test 15 new proposed conditions 30,000 cfs.

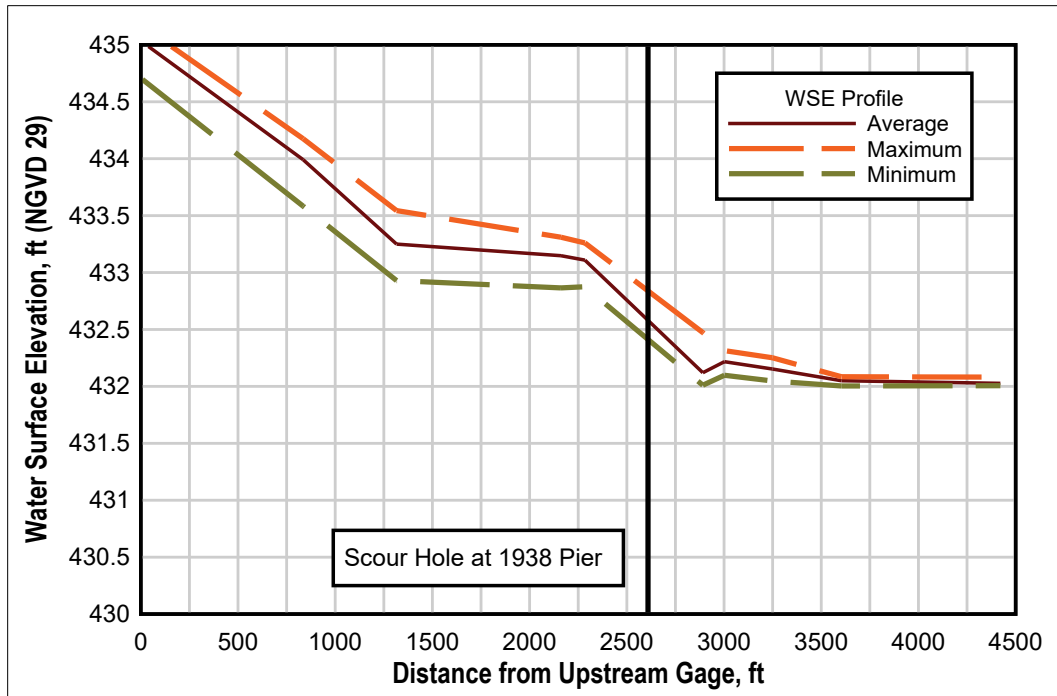
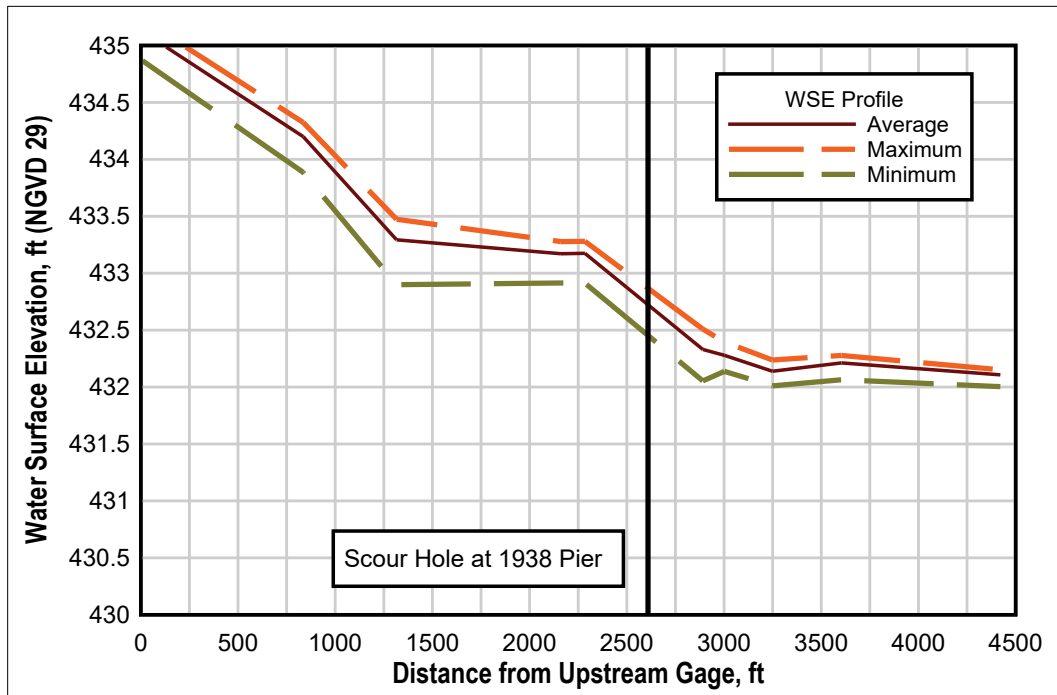


Figure A-18. Test 16 new proposed conditions 30,000 cfs.



## Appendix B: Approach Velocity Data

Figure B-1. Approach velocity for Test 2 existing conditions 30,000 cfs for the various tailgate settings.

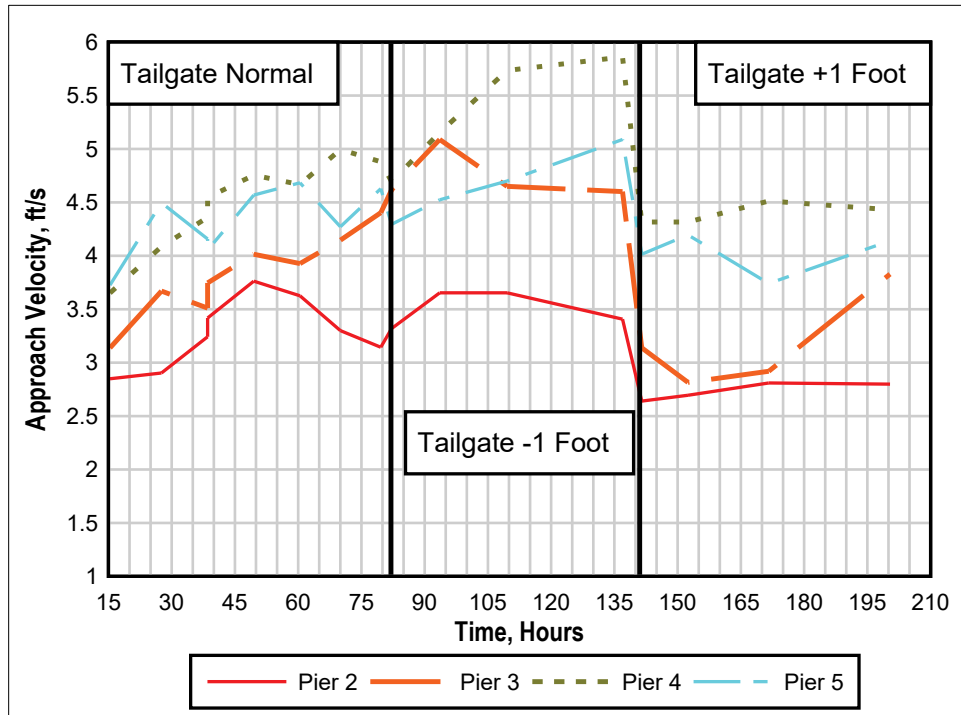


Figure B-2. Approach velocity for Test 3 existing conditions 15,000 cfs.

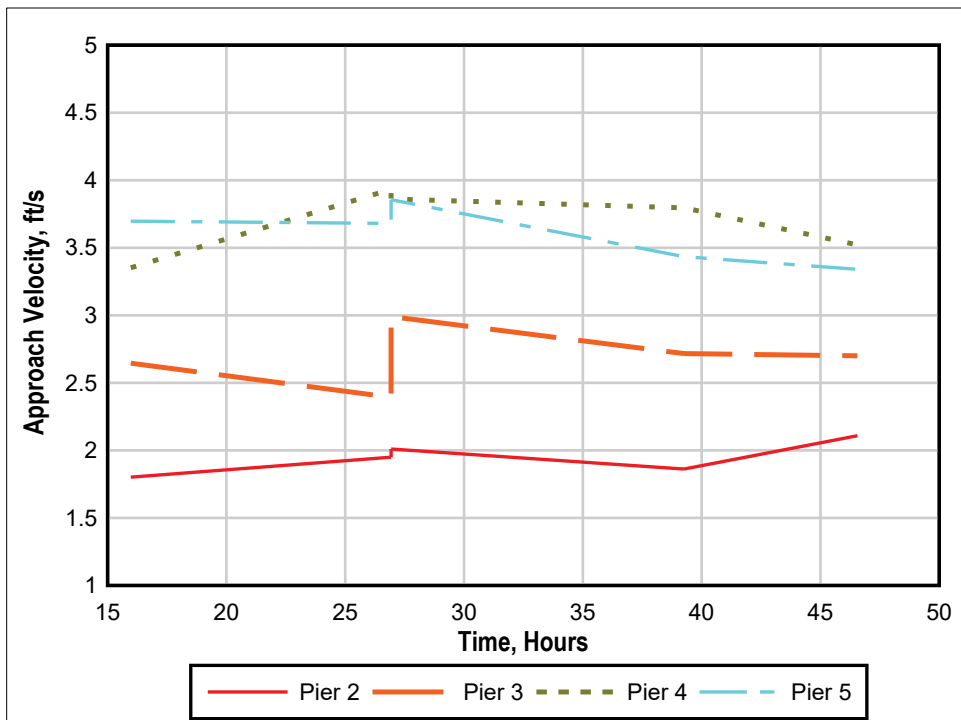


Figure B-3. Approach velocity for Test 4 existing conditions 15,000 cfs.

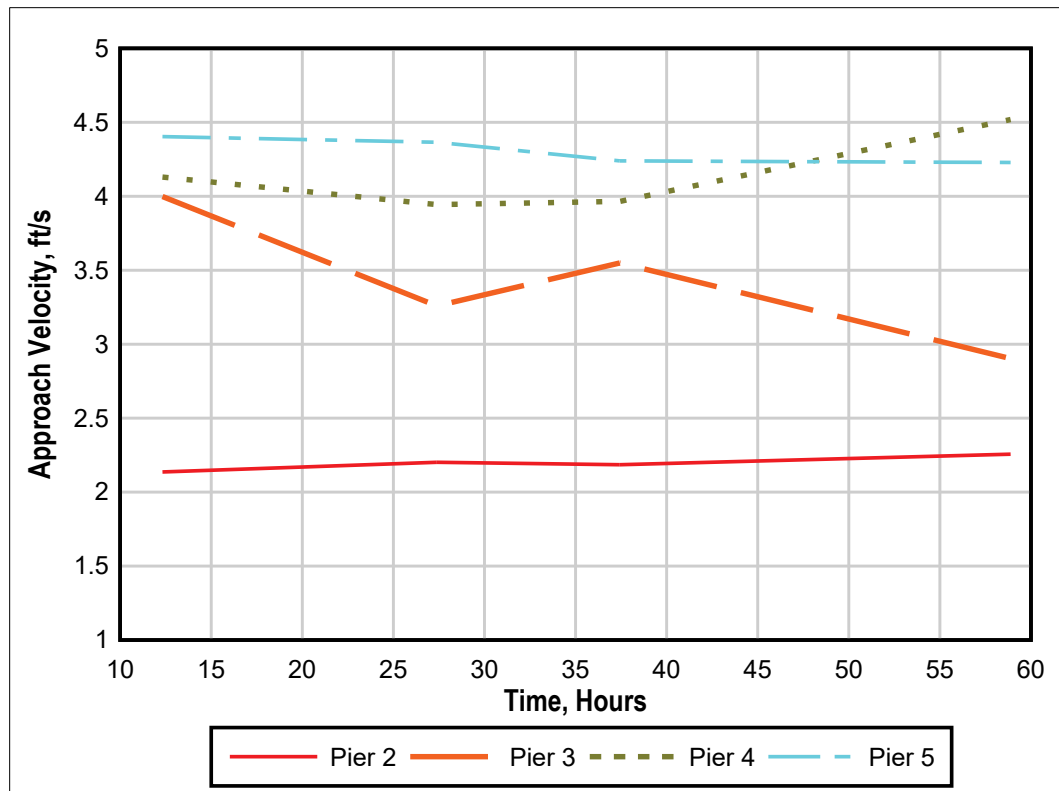


Figure B-4. Approach velocity for Test 5 existing conditions 30,000 cfs.

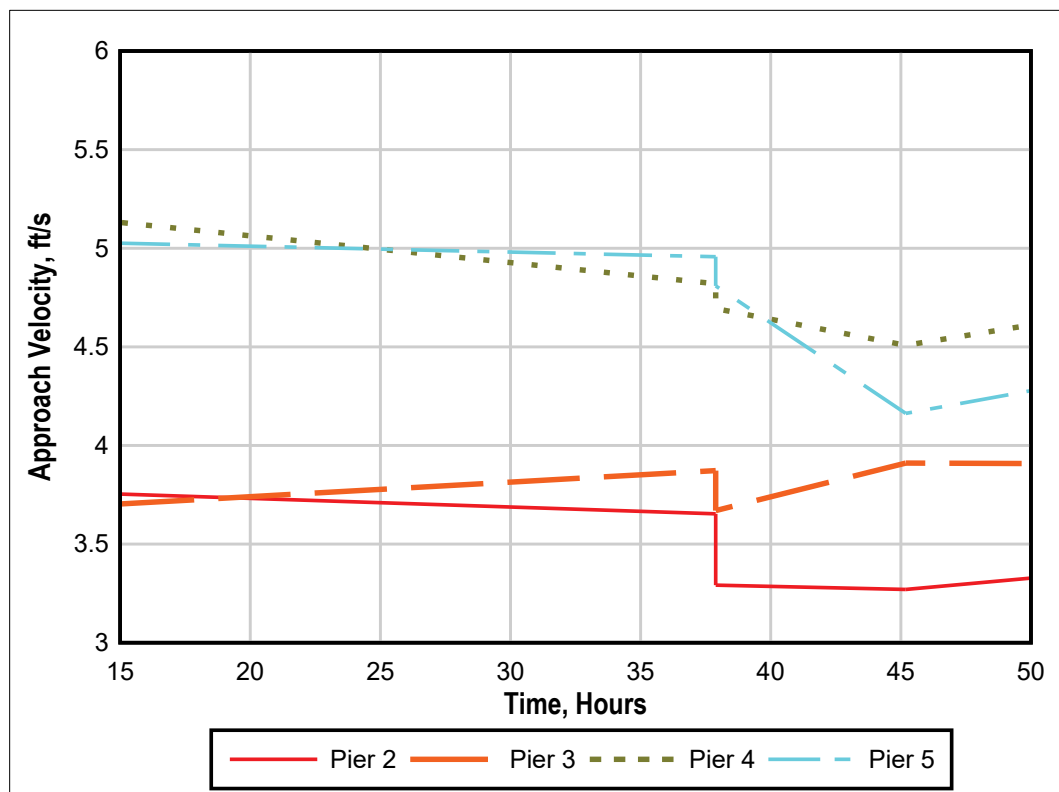




Figure B-5. Approach velocity for Test 6 existing conditions 30,000 cfs.

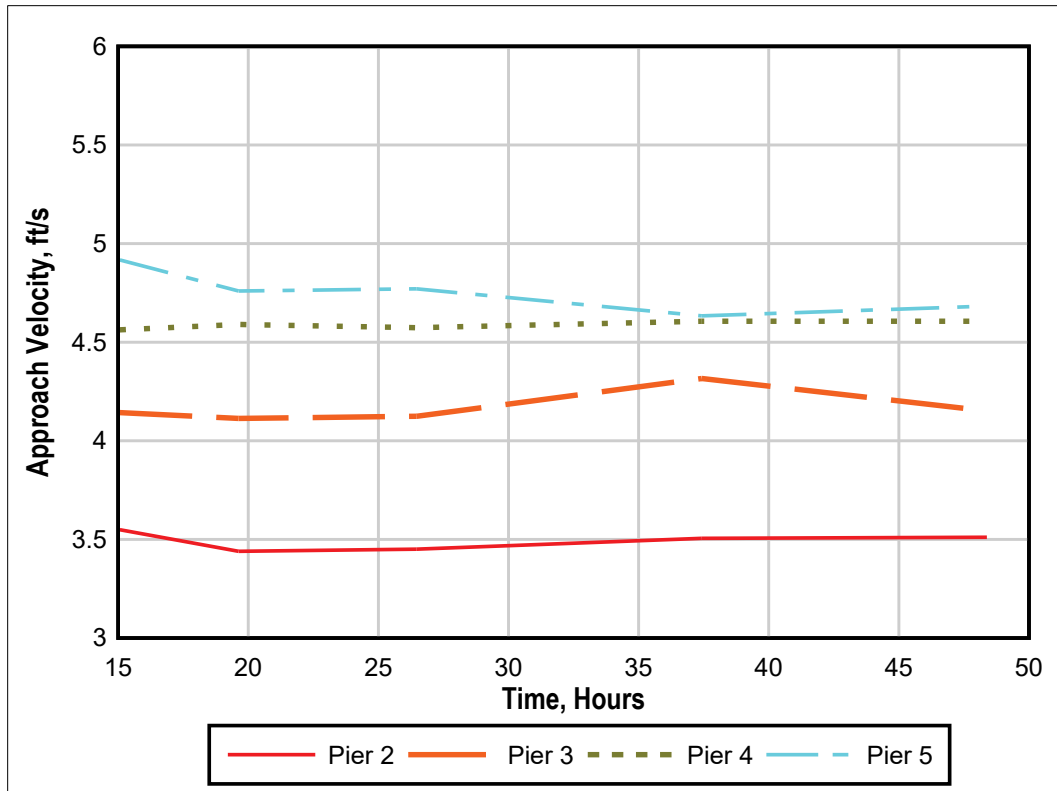


Figure B-6. Approach velocity for Test 7 proposed conditions 15,000 cfs.

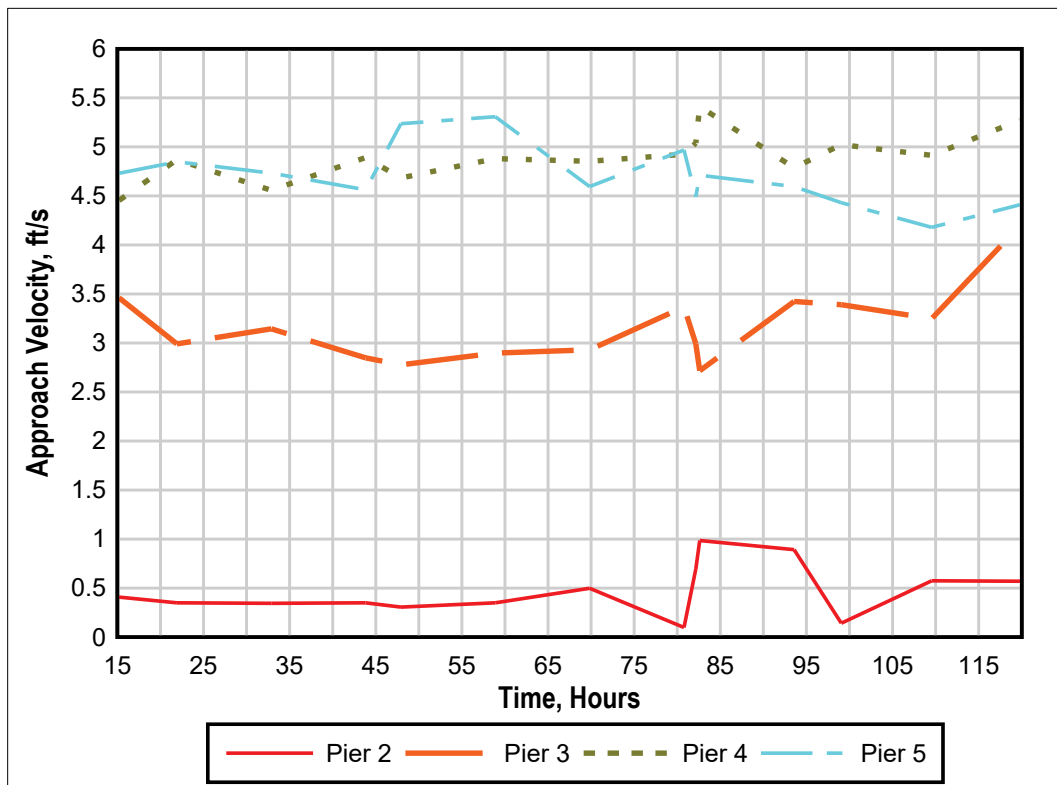


Figure B-7. Approach velocity for Test 8 proposed conditions 30,000 cfs.

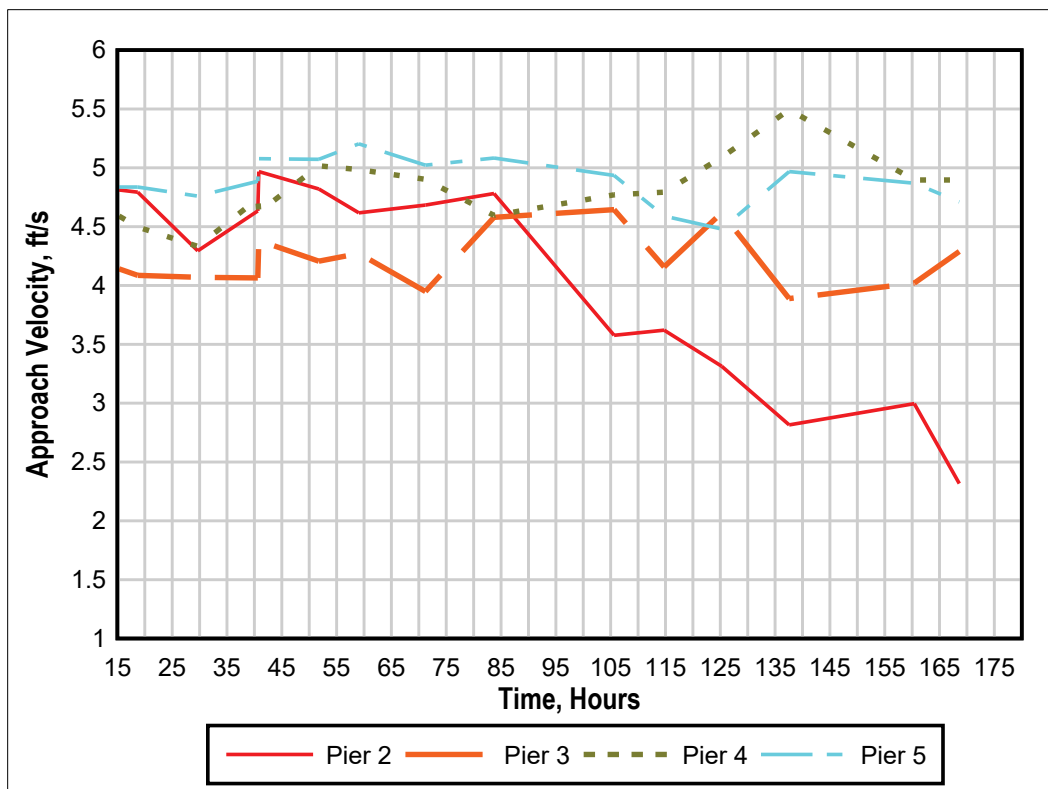


Figure B-8. Approach velocity for Test 9 proposed conditions 30,000 cfs.

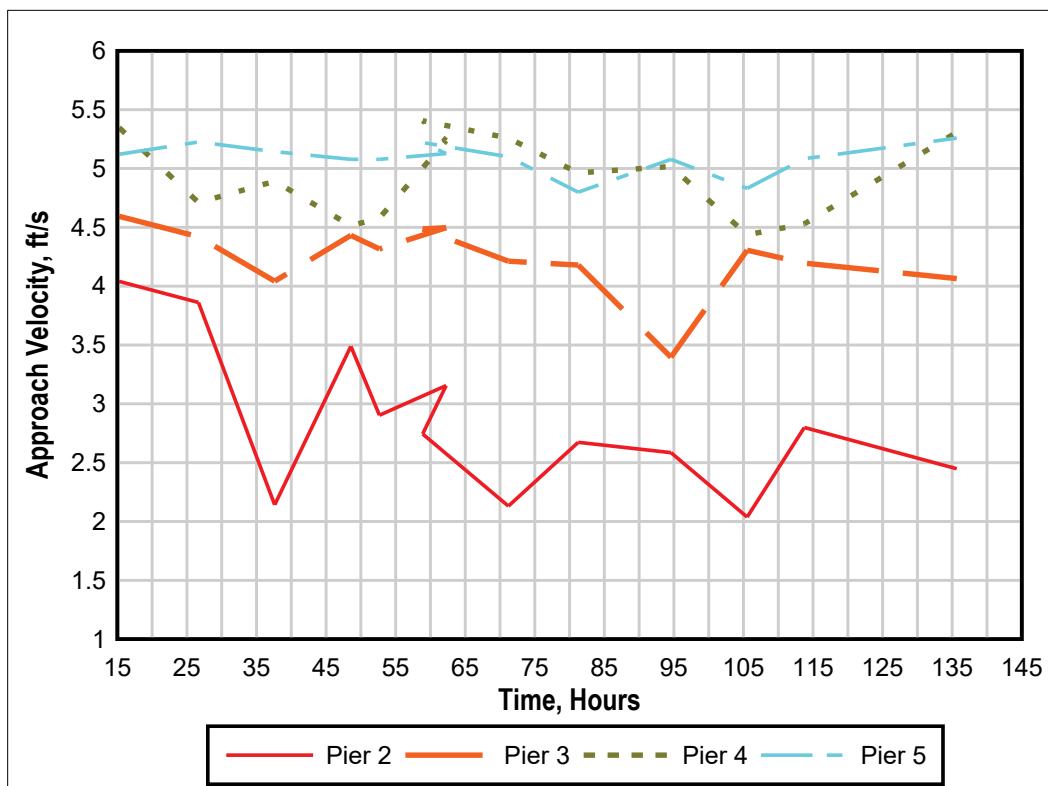


Figure B-9. Approach velocity for Test 11 proposed conditions simulating 6 ft of channel degradation 30,000 cfs.

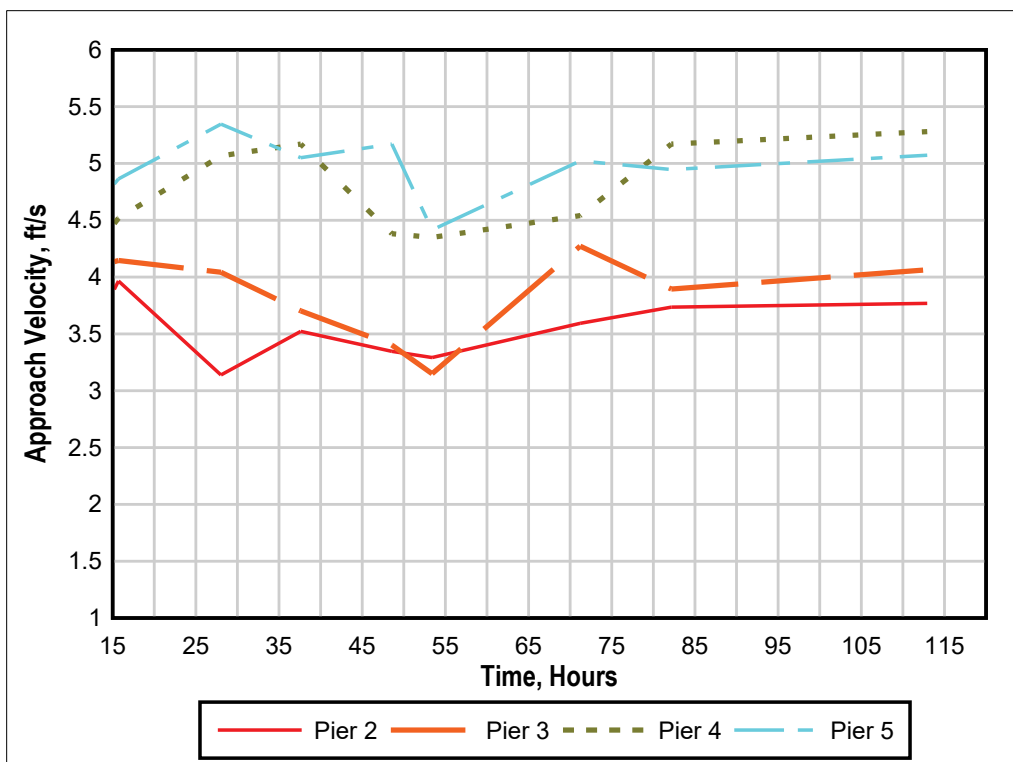


Figure B-10. Approach velocity for Test 12 proposed conditions simulating 6 ft of channel degradation and new bathymetry 30,000 cfs.

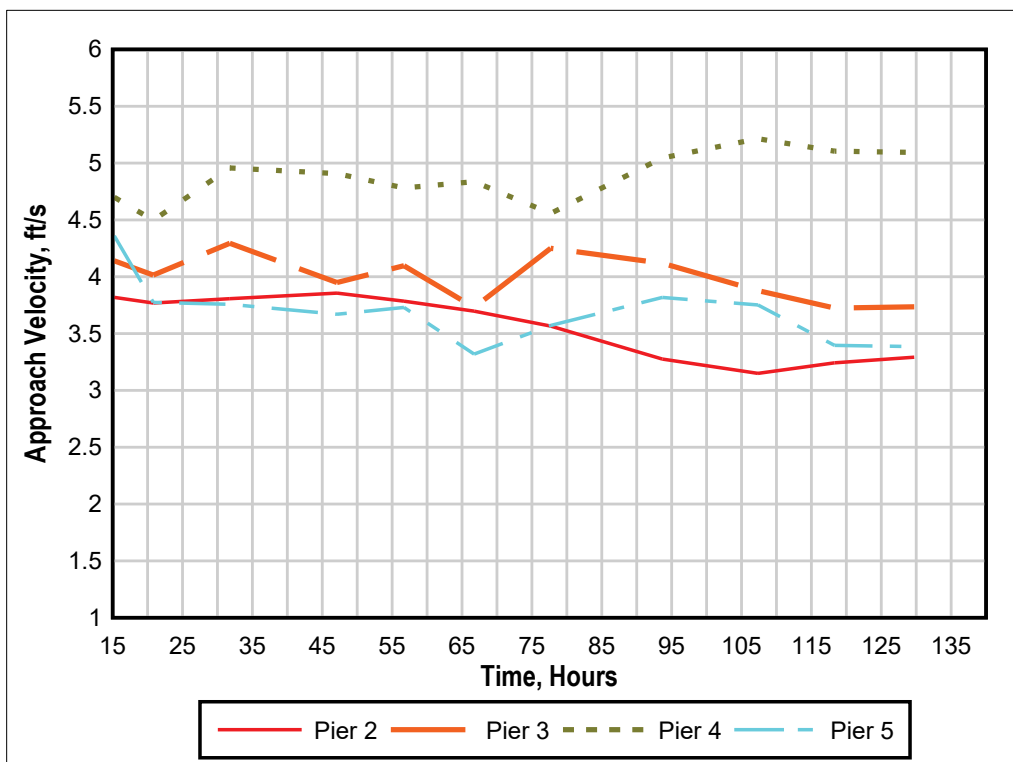


Figure B-11. Approach velocity for Test 13 new proposed conditions.

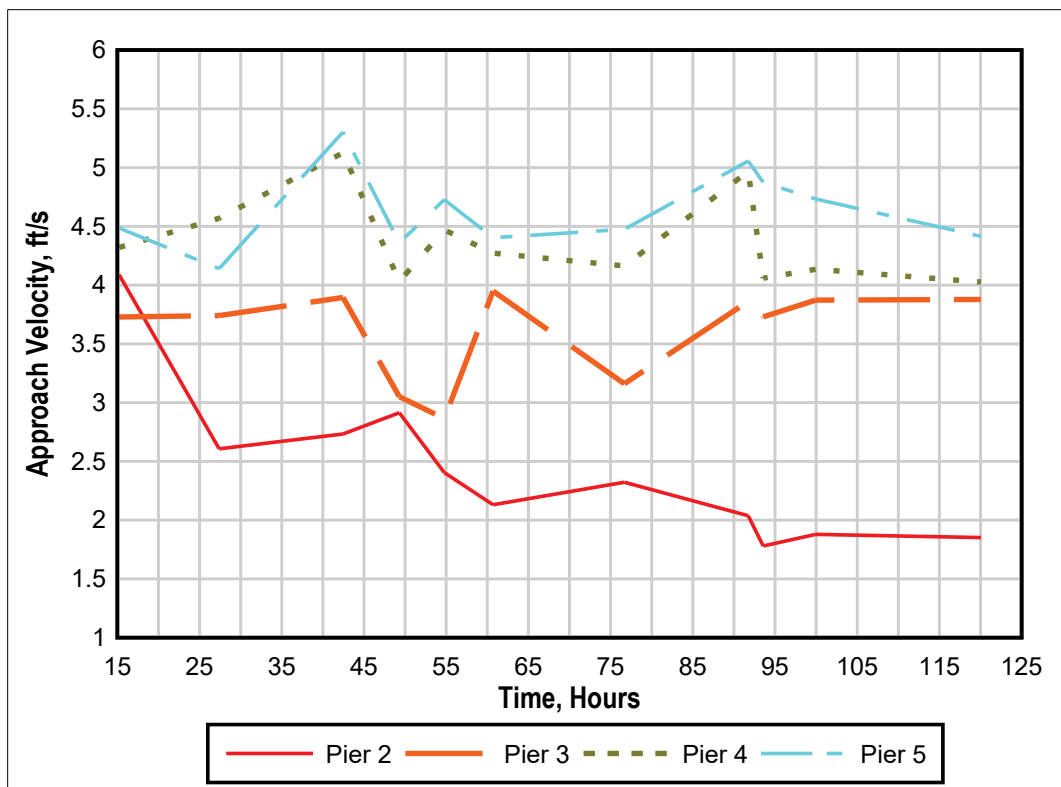


Figure B-12. Approach velocity for Test 14 new proposed conditions.

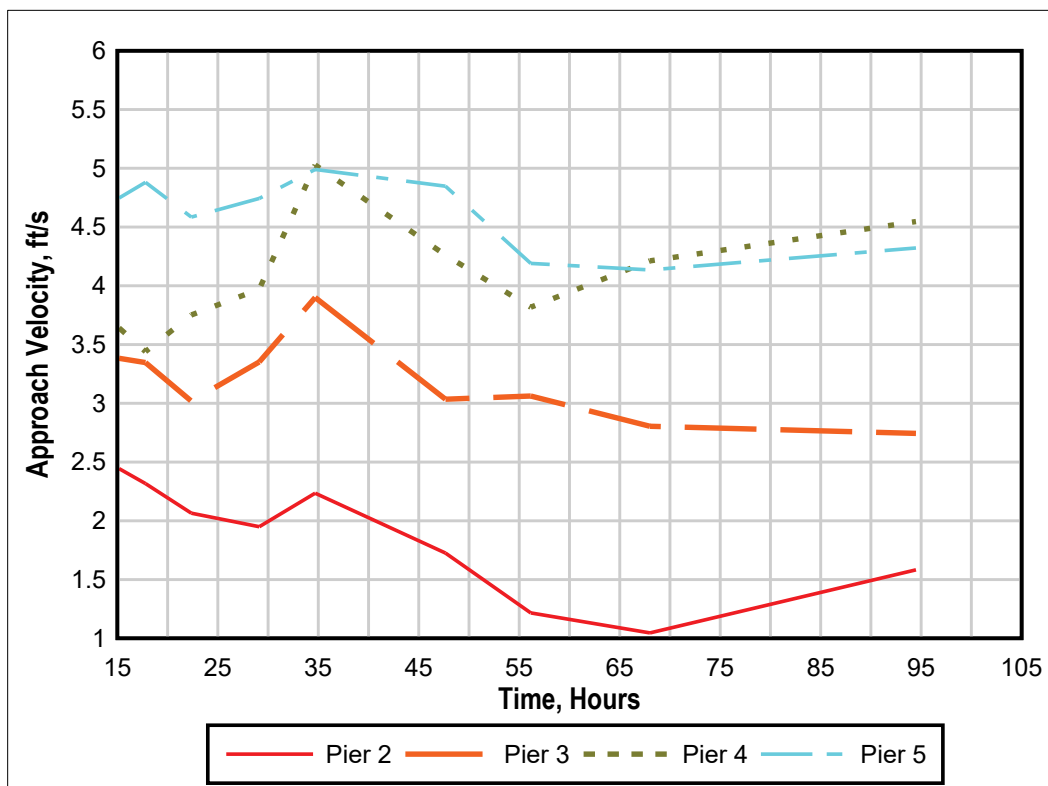


Figure B-13. Approach velocity for Test 15 new proposed conditions.

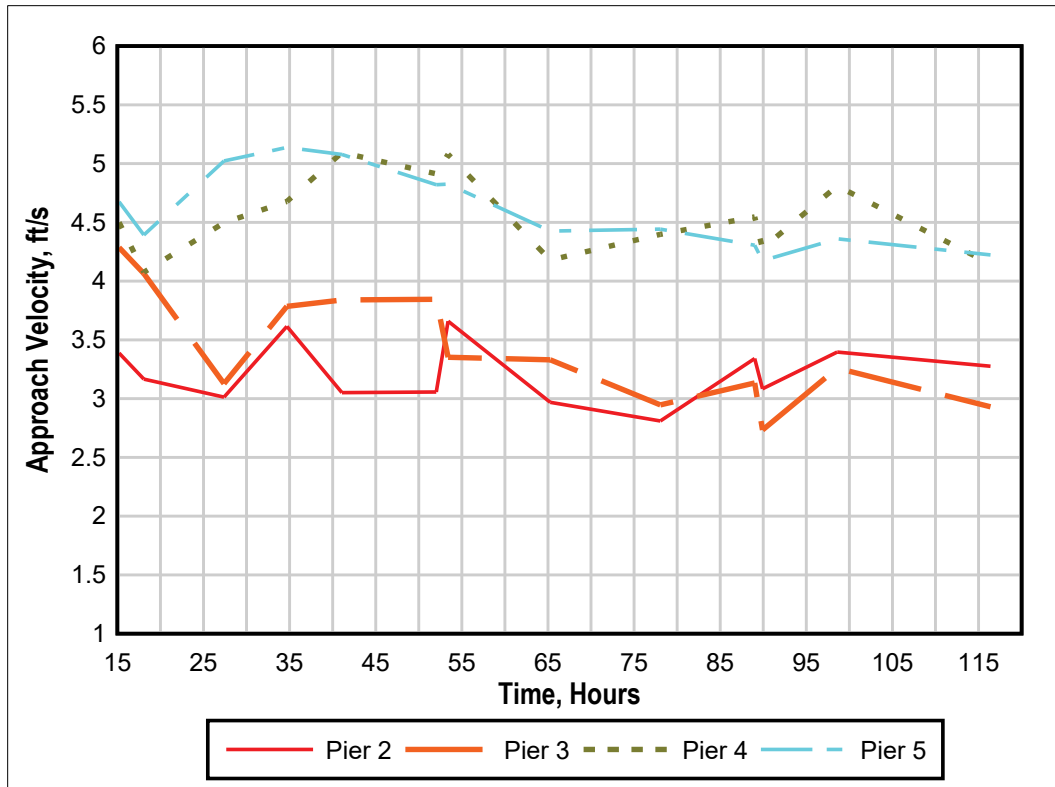
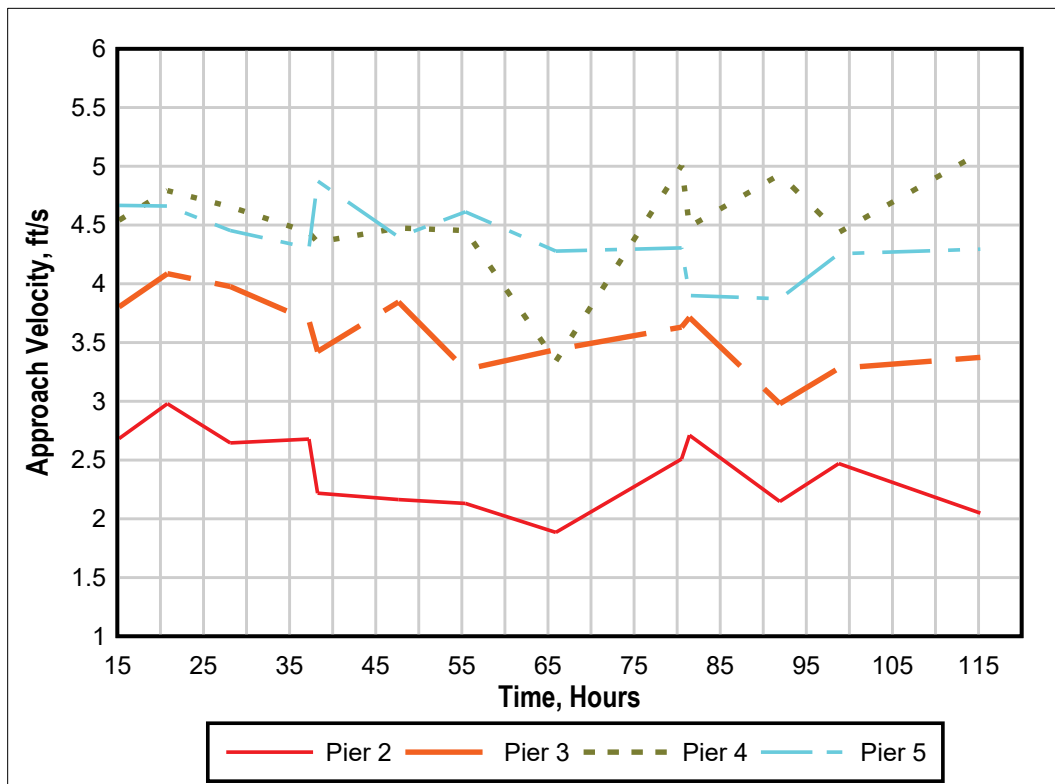


Figure B-14. Approach velocity for Test 16 new proposed conditions.





## Appendix C: Lidar Data

Figure C-1. Test 2 (30,000 cfs existing conditions) post-test lidar scan.

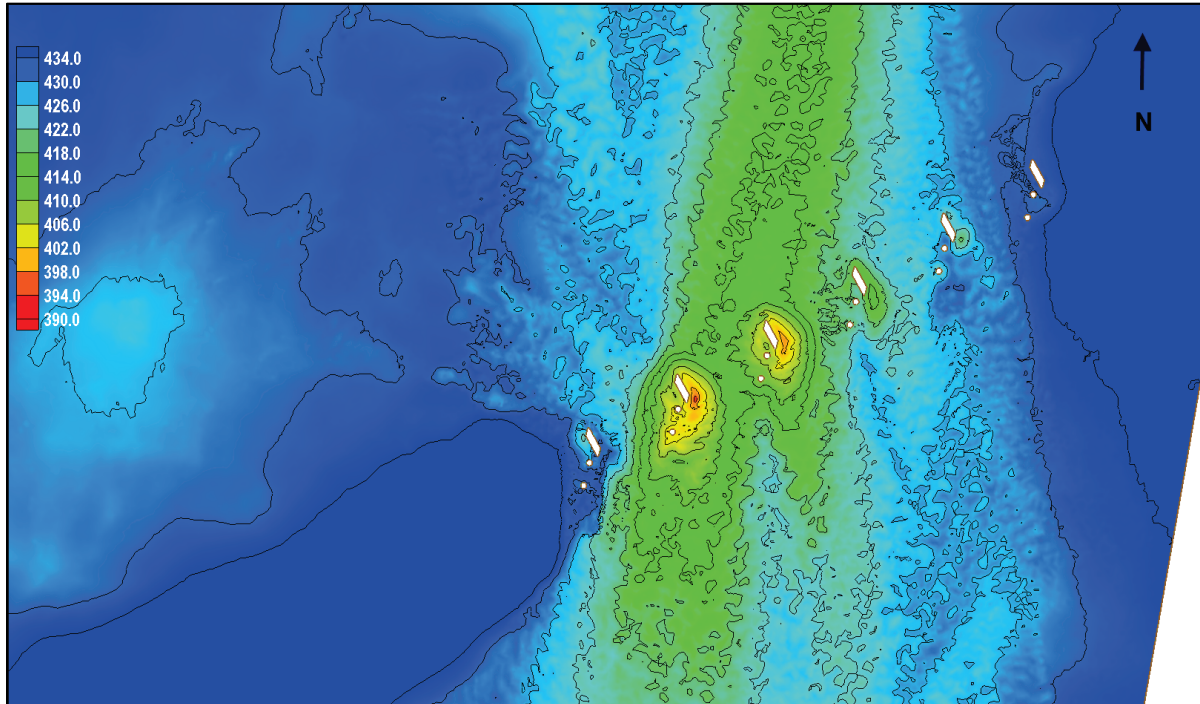


Figure C-2. Test 4 (15,000 cfs existing conditions) post-test lidar scan.

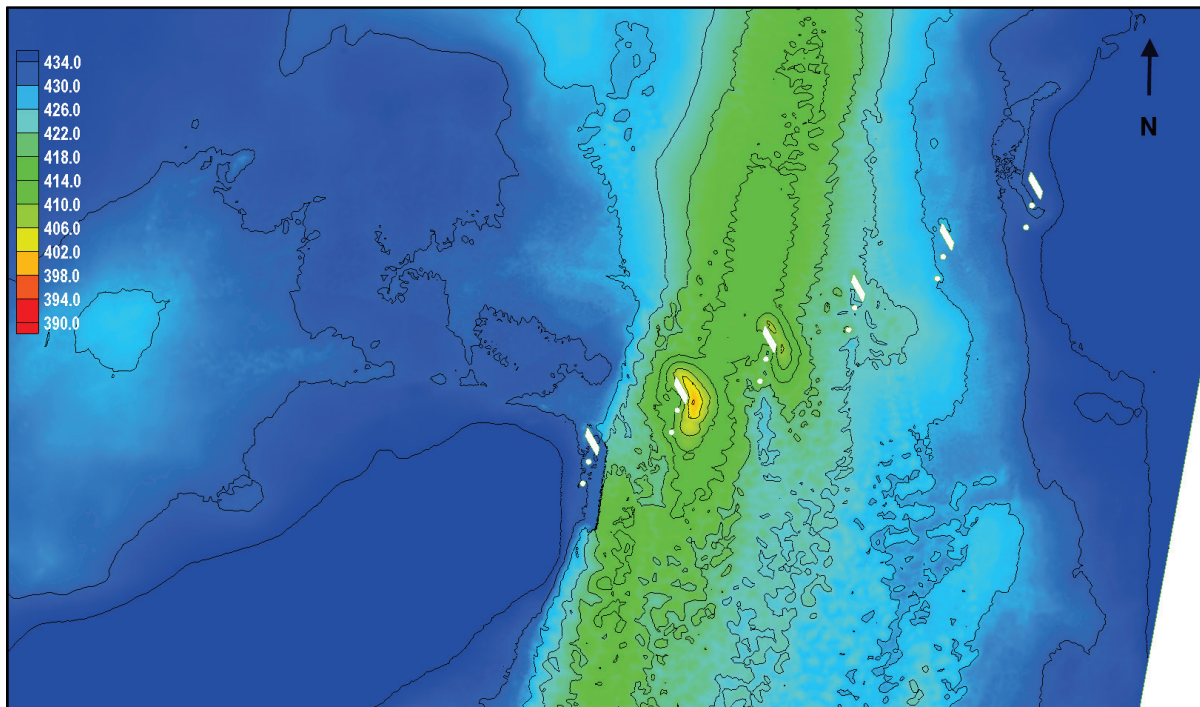


Figure C-3. Test 9 (30,000 cfs proposed conditions) post-test lidar scan.

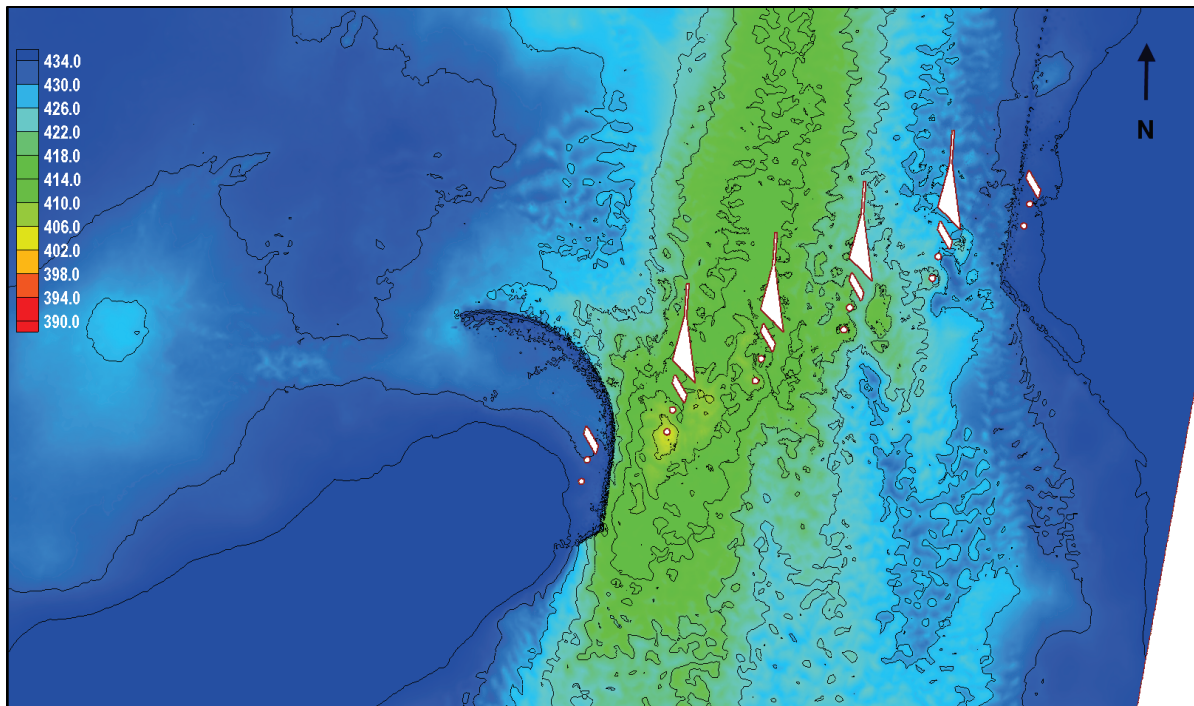


Figure C-4. Average (all 30,000 cfs existing conditions) post-test lidar scan.

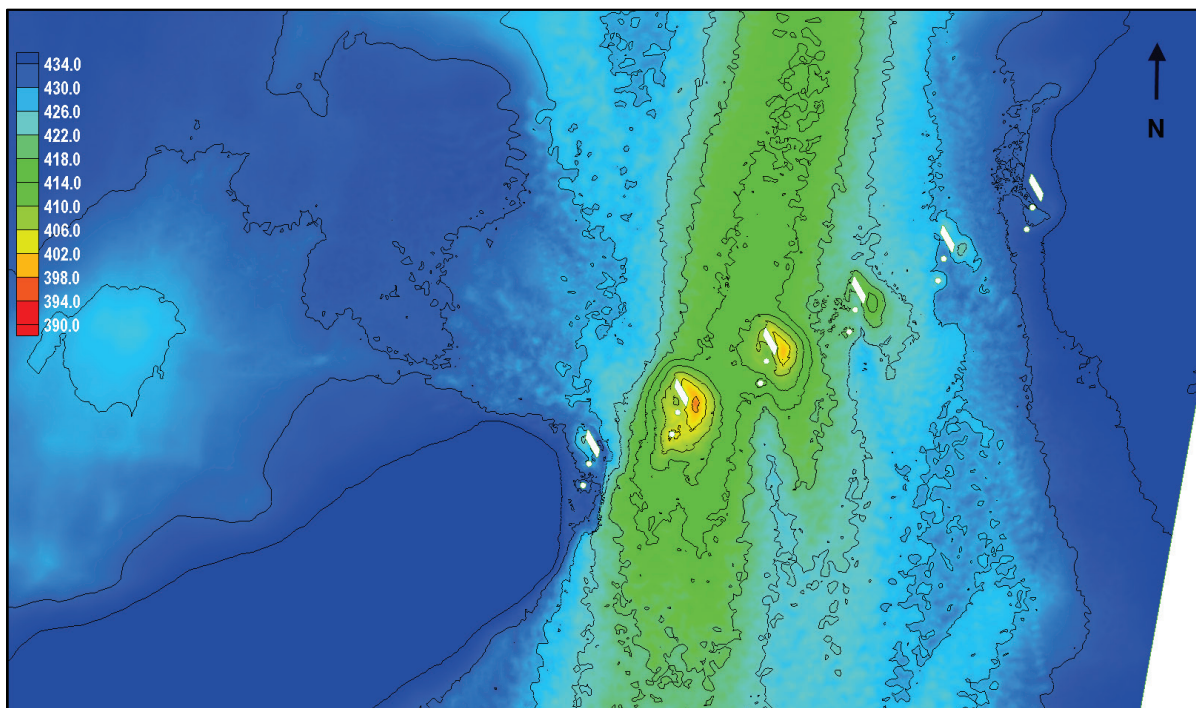




Figure C-5. Average (all 15,000 cfs existing conditions) post-test lidar scan.

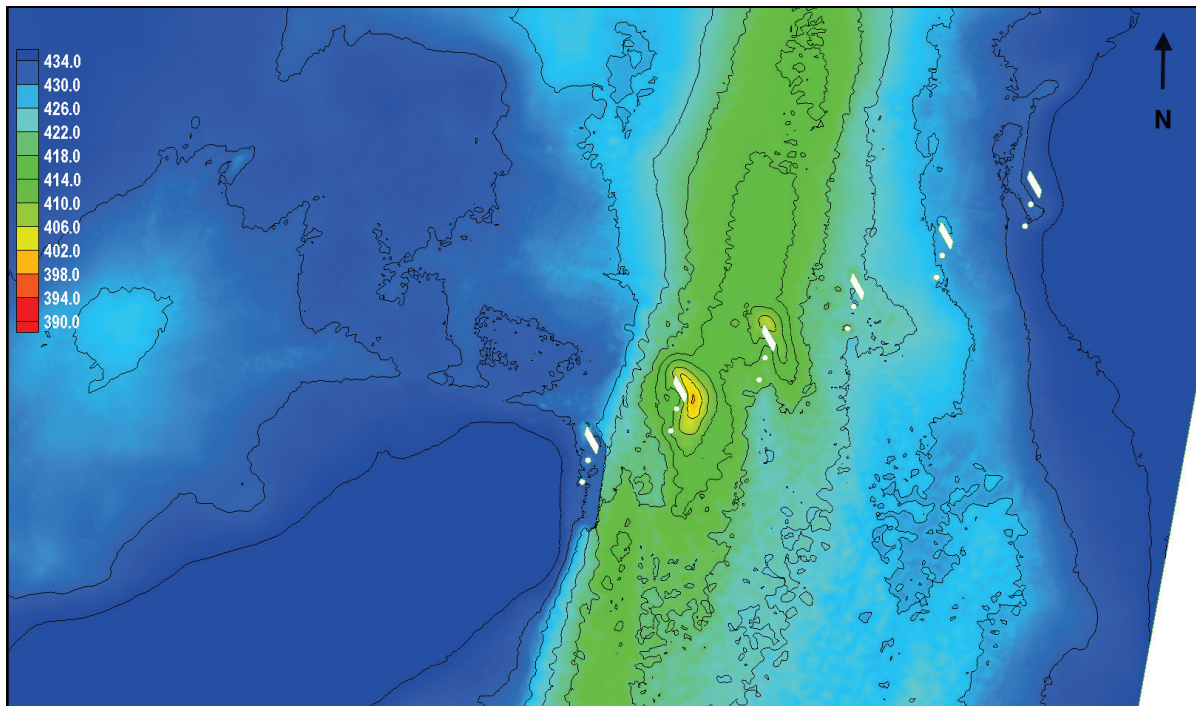


Figure C-6. Average (all 30,000 cfs proposed conditions) post-test lidar scan.

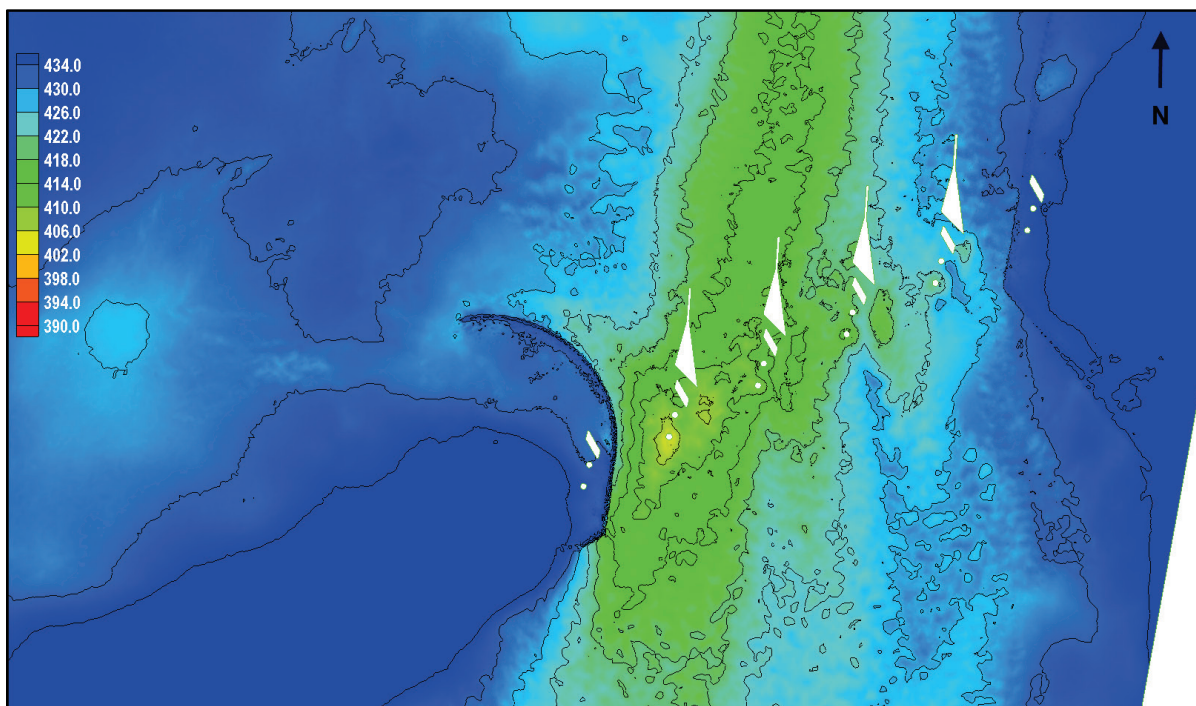


Figure C-7. Average (all 15,000 cfs proposed conditions) post-test lidar scan.

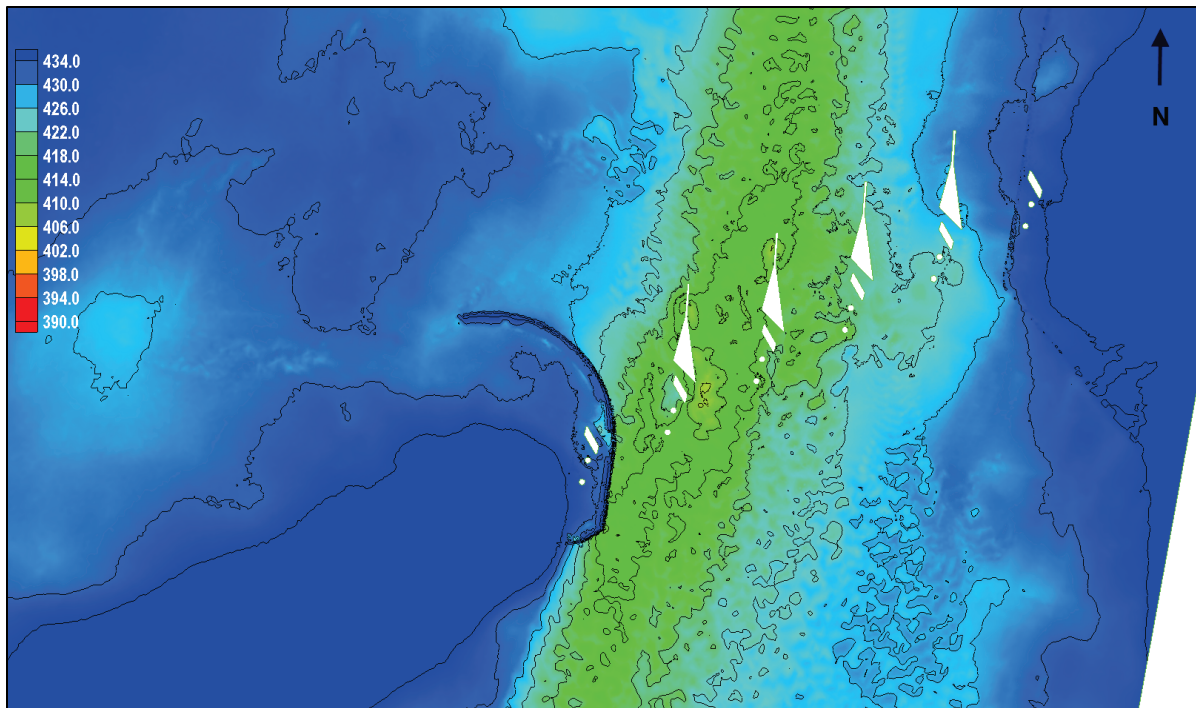


Figure C-8. Test 2 (30,000 cfs existing conditions) pre- minus post-test lidar survey.

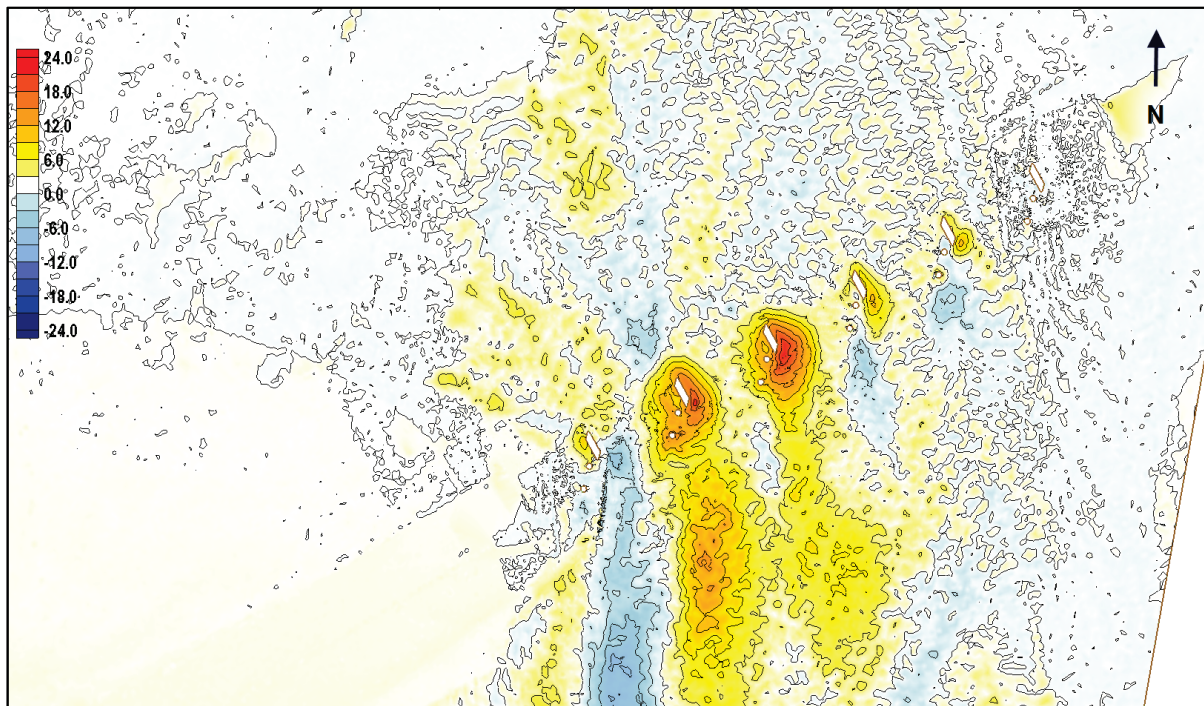




Figure C-9. Test 4 (15,000 cfs existing conditions) pre- minus post-test lidar survey.

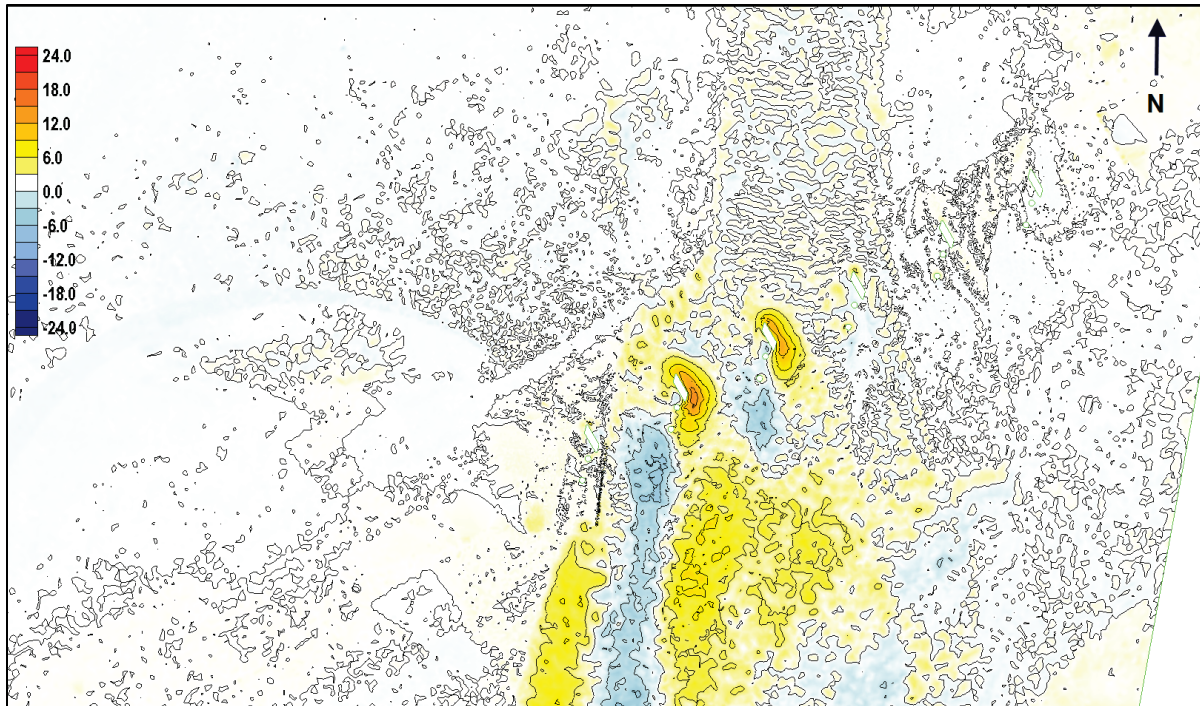
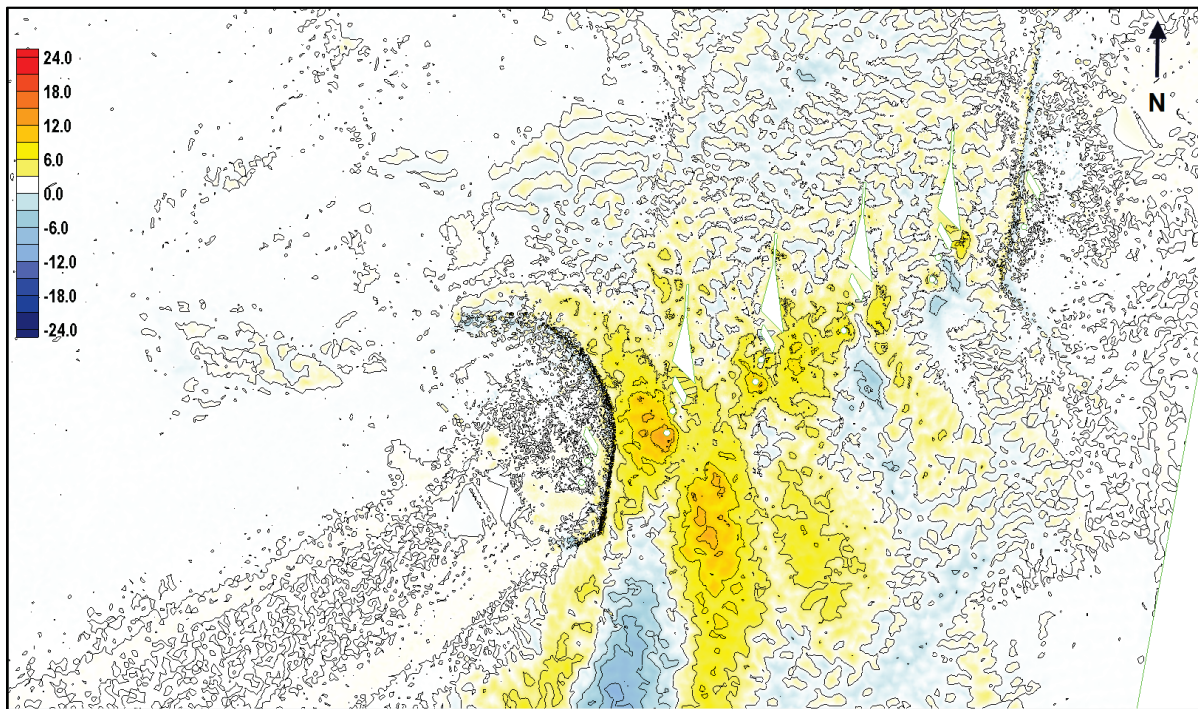


Figure C-10. Test 9 (30,000 cfs proposed conditions) pre- minus post-test lidar survey.





## **Appendix D: ERDC/CHL LR-15-2**

[Note: The authors of the following document have given permission for its inclusion in this technical report.]



DEPARTMENT OF THE ARMY  
ENGINEER RESEARCH AND DEVELOPMENT CENTER, CORPS OF ENGINEERS  
COASTAL AND HYDRAULICS LABORATORY  
WATERWAYS EXPERIMENT STATION, 3909 HALLS FERRY ROAD  
VICKSBURG, MISSISSIPPI 39180-6199

CEERD-HZ

25 March 2015

MEMORANDUM FOR Commander, U.S. Army Engineer District, Los Angeles District,  
915 Wilshire Blvd, Suite 1101 Los Angeles, CA 90017.

SUBJECT: Two-Dimensional Model Study of Santa Ana River Railroad Bridge Pier  
Extensions Letter Report, ERDC/CHL LR-15-2

1. The U.S. Army Engineer District, Los Angeles, requested that the U.S. Army Engineer Research and Development Center (ERDC), Coastal and Hydraulics Laboratory (CHL) investigate the validation of their HEC-RAS model at a railroad bridge located on the Santa Ana River through application of a two-dimensional model. The attached letter report ERDC/CHL LR-15-2 describes the findings of the study.

2. If you have any questions, please contact Mr. Jeremy A. Sharp at (601) 634-4212, or Dr. James Lewis at (601) 634-3895.

Encl

A handwritten signature in black ink, appearing to read "Jose E. Sanchez", is written over the typed name and title.

JOSÉ E. SÁNCHEZ, PE, SES  
Director



ERDC/CHL Letter Report  
January 2014

## Two-Dimensional Model Study of Santa Ana River Railroad Bridge Pier Extensions

*by Jeremy A. Sharp and Ronald E. Heath*

**PURPOSE:** This Coastal & Hydraulics Laboratory Letter Report contains a description of the process to formulate, construct, and apply a two-dimensional model of the Santa Ana River at the Burlington Northern Santa Fe Corporation (BNSF) railroad crossing near Corona, California. Data from a two-dimensional Adaptive Hydraulics model (AdH) were used to evaluate an existing HEC-RAS model and gain greater insight into the behavior of flow conditions at the railroad crossing both in its current and proposed configuration.

**INTRODUCTION:** There are three sets of adjacent piers supporting the BNSF railroad bridge downstream of Prado Dam near Corona, California that are set at a skewed angle across the Santa Ana River. The US Army Corps of Engineer Los Angeles District, (Los Angeles District) is concerned about local pier scour around the bridge due to potential increases in releases from the Prado Dam. The Los Angeles District would like to reduce potential local scour at the bridge piers by streamlining the flow approaching the bridge piers. To achieve this, pier extensions have been proposed by the Los Angeles District.

A one-dimensional model was constructed by the Los Angeles District to calculate the velocities through the bridge pier openings. However, there is no available validation dataset to evaluate the model's performance. Cross-section placement in one-dimensional model networks for complex hydraulic geometries, such as a skewed bridge crossing, can be difficult and a potential source of uncertainty. The Los Angeles District requested a two-dimensional (2D) depth-averaged, finite element hydraulic model investigation to compare with the results of the one-dimensional model. While flow conditions around the railroad bridge piers is a three-dimensional process, the two dimensional model is believed sufficient to estimate river stages and depth averaged velocities.

**PROCESS:** A 2D depth-averaged, finite element AdH model was constructed and applied to compare with the results of the existing HEC-RAS standard step method one-dimensional model. The AdH model domain was constructed over the same area as the HEC-RAS model, but resolution was focused on the bridge crossing to more accurately implement the bridge piers and pier extensions. Steady state model runs were applied for the existing and with project conditions (proposed conditions). The steady state flow rates applied include 5,000 cubic feet per second (cfs), 10,000 cfs, 15,000 cfs, 20,000 cfs, 25,000 cfs, 30,000 cfs, and 35,000 cfs. Data from both models were processed and analyzed for comparison. The datasets were compared visually and statistically. Professional judgment along with error metrics, including velocity differences and correlation coefficients, were used to compare the results from the one-dimensional and two-dimensional models. Flow velocity distributions for the various steady state flow

ERDC/CHL Letter Report  
January 2014

rates near the abutments were analyzed. The AdH model results assist in the determination of the overall functionality of the proposed conditions and the adequacy of the one-dimensional model.

**MODELING AND ANALYSIS APPROACH:** The AdH model provides an effective tool to determine the impact of pier extensions on the distribution of flow through the bridge and local variations in river stage and velocity. Two AdH models, existing condition and proposed condition, were built to simulate the effect of the proposed pier extensions. The existing condition model provides the base model for comparison. It simulates the current conditions that are in the field. The proposed condition model (Fig. 1) was constructed from the existing condition model, with the addition of upstream pier extensions. Flow guide walls and pier extensions for both models were defined as emergent for all flow conditions. Both domains were defined using an aerial image, topographic, and bathymetric data. Both models simulate hydrodynamics with the same steady state boundary conditions. With no field or historic data in the vicinity of the model domain, no model validation was performed. Therefore, the effort is a computational exercise intended to illuminate any significant differences in the 1D and 2D model results. While not ideal, the approach provided a timely and cost efficient means of analysis.

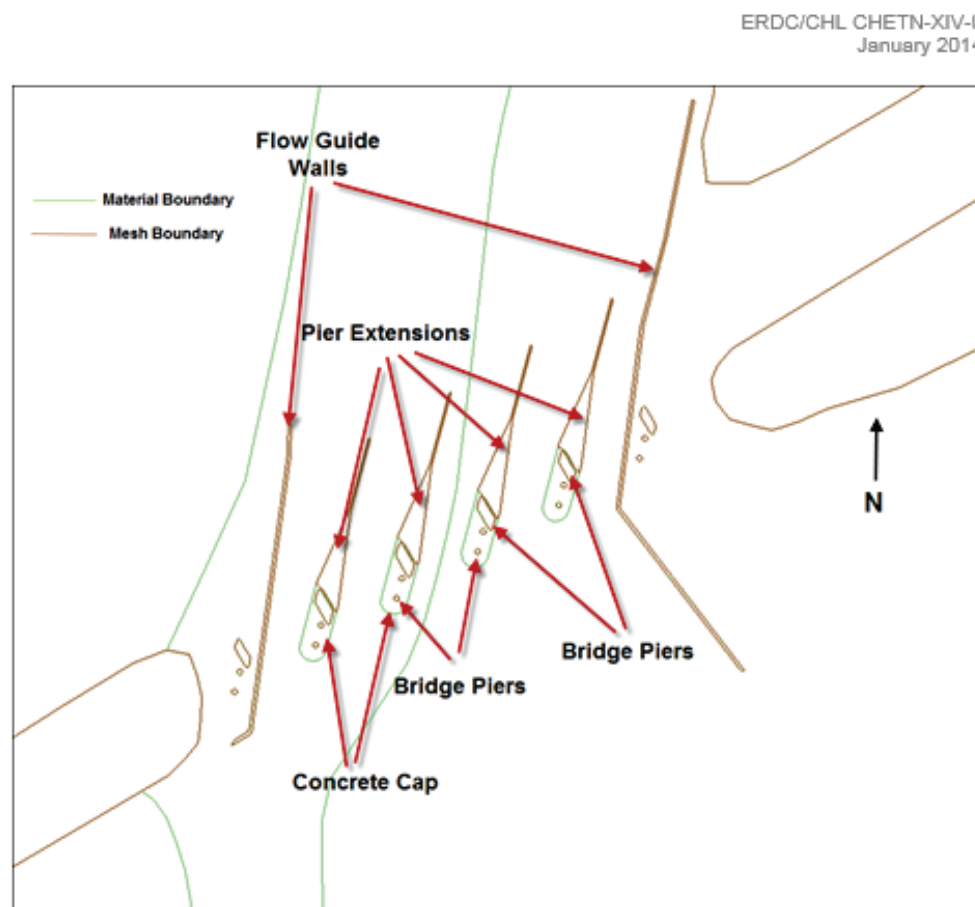


Figure 1. Proposed condition (pier extensions added to existing condition), Santa Ana River BNSF railroad crossing near Corona, California.

Results from both AdH and HEC-RAS provide insights into the behavior of the system both in its current and proposed configuration. For both configurations, velocity profile data were extracted along five arc lines between the upstream piers (Fig. 2). Velocity profiles were plotted and analyzed to evaluate velocity changes. The average velocity for the existing condition was subtracted from the average velocity of the proposed condition.

For both the AdH and HEC-RAS models, Manning's roughness values were applied to define bed friction. In the main channel each model used a Manning's value of 0.027. Overbanks values for areas that have brush and short vegetation cover, so Manning's values of 0.045 in AdH and 0.05 in HEC-RAS were applied. Overbanks with little to no vegetation were parameterized with a Manning's value of 0.035 in both models. For wooded overbanks AdH did not use a Manning's value but used an unsubmerged



ERDC/CHL Letter Report  
January 2014

vegetative roughness algorithm (Walton and Christensen 1980). The HEC-RAS model applied a Manning's value of 0.07.

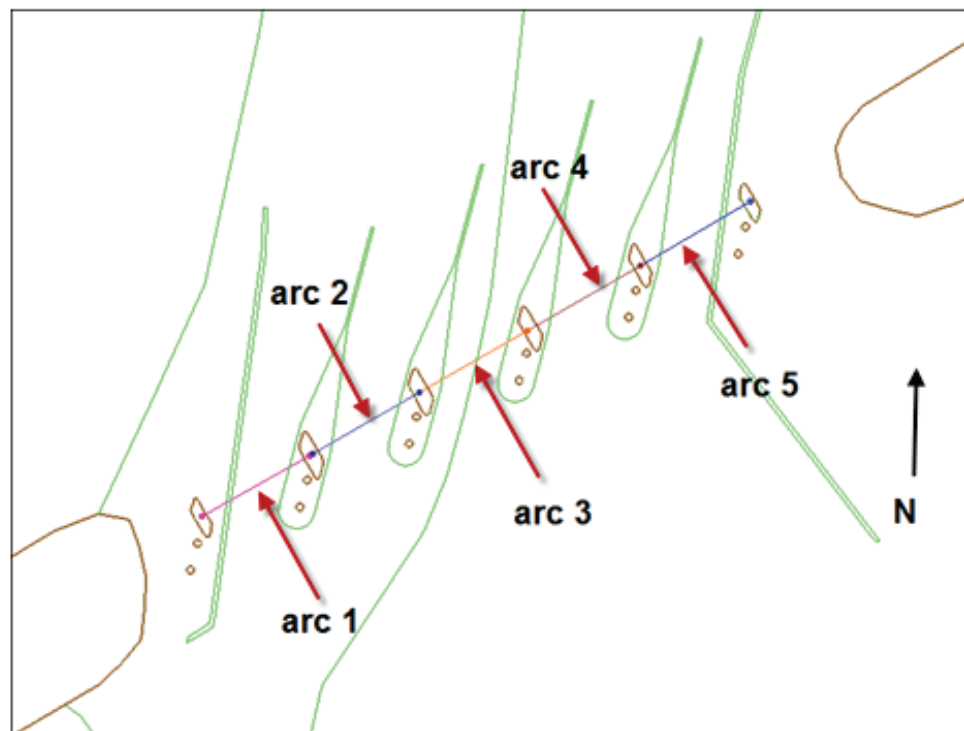


Figure 2. Arc location used for the analysis of velocity comparisons, Santa Ana River BNSF railroad crossing near Corona, California.

**RESULTS:** The average difference for all five arcs between the existing and proposed conditions was -0.47 feet per second (fps) as estimated by AdH, indicating that the proposed condition on average decreased velocities. This decrease is due to a portion of the arc being in the vortex wake produced by the upstream pier extension and the flow blockage from the flow guide walls. Similarly, the maximum velocity change averaged over all arcs was +1.23 fps, indicating that the proposed condition on average will result in a higher maximum velocity. Average velocity and maximum velocity changes by arc and flow condition are shown in table 1.

When comparing the AdH and HEC-RAS existing condition models (AdH minus HEC-RAS), the average velocity difference between the two models was -1.33 fps, indicating that the HEC-RAS model showed higher velocities in the existing condition than the AdH model (tables 2 and 3).

ERDC/CHL CHETN-XIV-9  
January 2014

Additionally, the water surface elevations and slopes were compared between the HEC-RAS and AdH model (see Figure 3). The water surface slopes were calculated over a channel section that extends 5,000 ft upstream of the bridge and 5,000 ft downstream of the bridge. The resulting slopes are shown in Figure 4. The average difference between the slopes for all flows (AdH minus HEC-RAS) is -0.00021. The correlation coefficient between the two arrays is 0.97.

The detail water surface profiles illustrated in Figures 5-9 show the drawdown in water surface and velocity as flow passes through the middle opening. The orientation in the pier results in a larger difference in computed stage and velocity between existing and proposed conditions along the left side of the opening.

Table 1. Average and maximum velocity comparison between the proposed and existing condition AdH models, Santa Ana River Burlington Northern Santa Fe Corp railroad crossing near Corona, California.

AdH average velocity difference (proposed - existing) feet/second							
	5,000 cfs	10,000 cfs	15,000 cfs	20,000 cfs	25,000 cfs	30,000 cfs	35,000 cfs
Arc 1	-0.38	-0.50	-0.71	-0.71	-0.69	-0.82	-0.72
Arc 2	0.20	0.15	0.34	0.57	0.80	0.97	1.18
Arc 3	0.17	0.12	0.31	1.63	0.78	1.05	1.34
Arc 4	-0.20	-0.20	-0.36	-0.30	-0.28	0.36	0.95
Arc 5	-2.07	-3.81	-4.54	-4.53	-3.02	-2.41	-1.15
AdH maximum velocity change (proposed - existing) feet/second							
	5,000 cfs	10,000 cfs	15,000 cfs	20,000 cfs	25,000 cfs	30,000 cfs	35,000 cfs
Arc 1	-0.74	-0.35	0.12	0.63	1.05	1.42	1.76
Arc 2	1.48	1.71	2.07	2.55	3.09	3.55	4.10
Arc 3	0.95	1.99	2.67	3.37	4.06	4.68	5.34
Arc 4	-0.56	-0.43	0.62	1.54	2.52	3.92	5.12
Arc 5	-5.66	-6.62	-6.42	-3.18	-2.10	2.56	6.31

ERDC/CHL Letter Report  
January 2014

Table 2. Existing condition velocities for the AdH (average) and HEC-RAS models, Santa Ana River Burlington Northern Santa Fe Corp railroad crossing near Corona, California.

AdH average velocity, feet/second							
	5,000 cfs	10,000 cfs	15,000 cfs	20,000 cfs	25,000 cfs	30,000 cfs	35,000 cfs
Arc 1	2.07	3.81	4.59	5.21	5.8	6.37	6.97
Arc 2	3.69	4.07	4.52	5.06	5.62	6.13	6.61
Arc 3	2.35	3.21	4.01	4.66	5.27	5.77	6.21
Arc 4	0.22	0.72	2.28	3.73	4.80	5.52	6.07
Arc 5	2.07	3.81	4.59	5.21	5.80	6.37	6.97
HEC-RAS velocity, feet/second							
	5,000 cfs	10,000 cfs	15,000 cfs	20,000 cfs	25,000 cfs	30,000 cfs	35,000 cfs
Arc 1	3.72	5.31	6.57	7.49	8.33	9.09	9.63
Arc 2	2.74	3.48	4.07	4.54	4.99	5.40	5.71
Arc 3	2.74	3.48	4.07	4.54	4.99	5.40	5.71
Arc 4	3.03	4.31	5.40	6.28	7.08	7.78	8.33
Arc 5	3.87	5.45	6.74	7.77	8.71	9.58	10.24

Table 3. Existing condition AdH velocity minus HEC-RAS velocity, Santa Ana River Burlington Northern Santa Fe Corp railroad crossing near Corona, California.

AdH average velocity minus HEC-RAS velocity, feet/second							
	5,000 cfs	10,000 cfs	15,000 cfs	20,000 cfs	25,000 cfs	30,000 cfs	35,000 cfs
Arc 1	-1.65	-1.50	-1.98	-2.28	-2.53	-2.72	-2.66
Arc 2	0.95	0.59	0.45	0.52	0.63	0.73	0.90
Arc 3	-0.39	-0.27	-0.06	0.12	0.28	0.37	0.50
Arc 4	-2.81	-3.59	-3.12	-2.55	-2.28	-2.26	-2.26
Arc 5	-1.80	-1.64	-2.15	-2.56	-2.91	-3.21	-3.27

ERDC/CHL CHETN-XIV-9  
January 2014

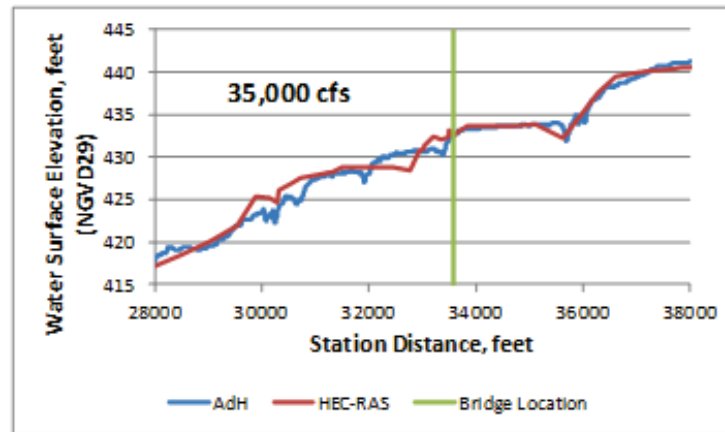


Figure 3. Water surface profiles for a flow of 35,000 cubic feet per second showing the AdH and HEC-RAS existing condition model at the Santa Ana River BNSF railroad crossing near Corona, California.

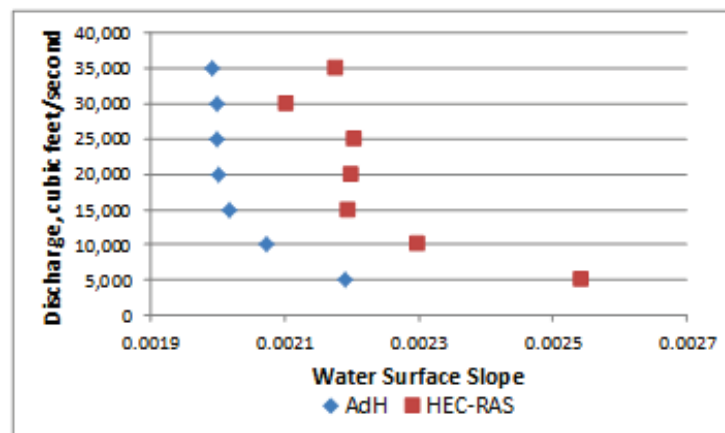


Figure 4. Water surface slopes comparison showing the AdH and HEC-RAS existing condition model over a 10,000 ft reach at the Santa Ana River BNSF railroad crossing near Corona, California.

ERDC/CHL Letter Report  
January 2014

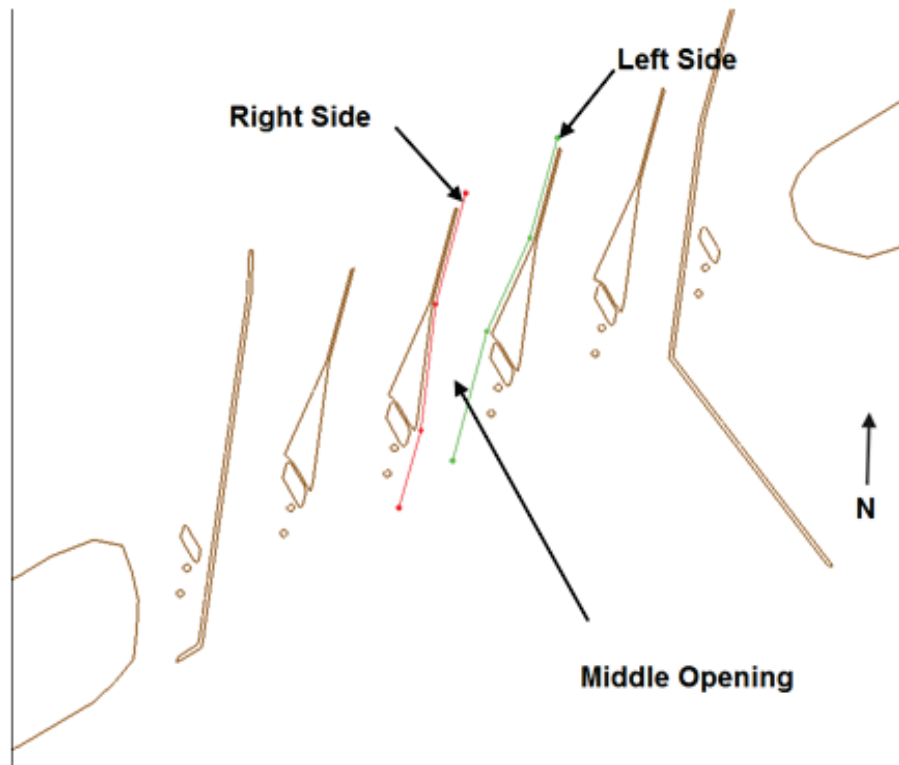


Figure 5. Location of profiles along the bridge piers and pier extension.



ERDC/CHL CHETN-XIV-9  
January 2014

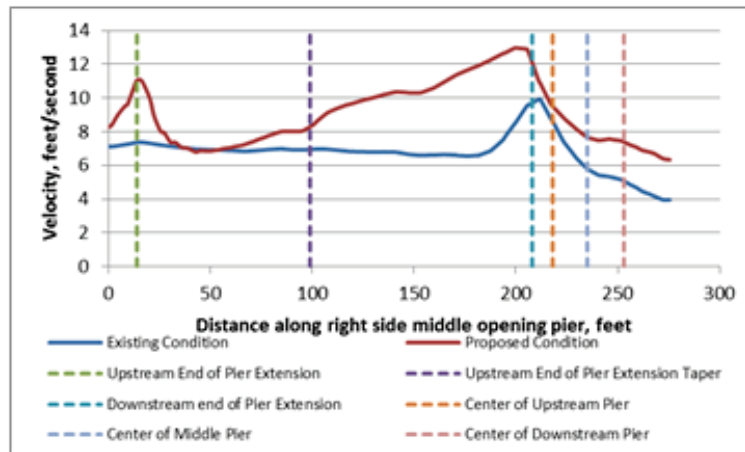


Figure 6. Velocity profile on right side of the middle opening pier for existing and proposed AdH models, feet/second.

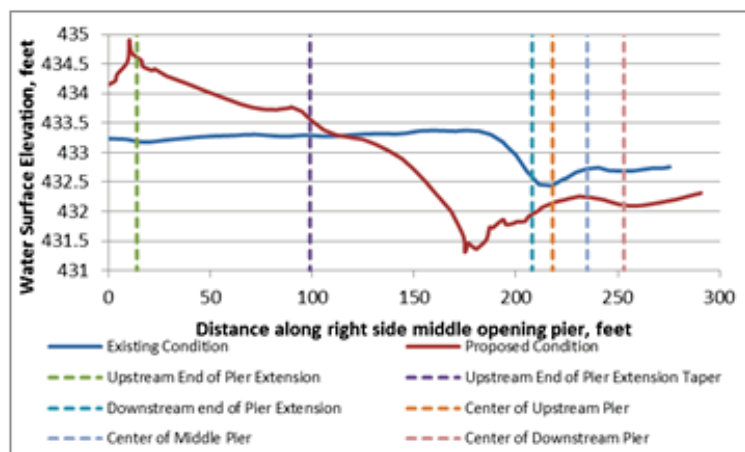


Figure 7. Water surface elevation profile on right side of the middle opening pier for existing and proposed AdH models, feet/second.

ERDC/CHL Letter Report  
January 2014

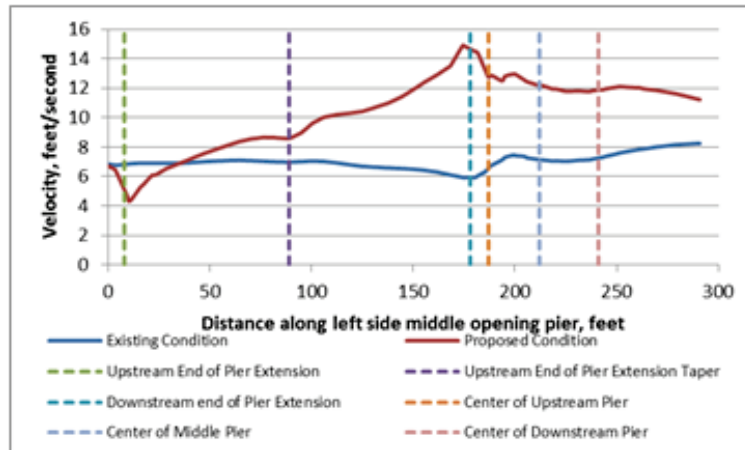


Figure 8. Velocity profile on left side of the middle opening pier for existing and proposed AdH models, feet/second.

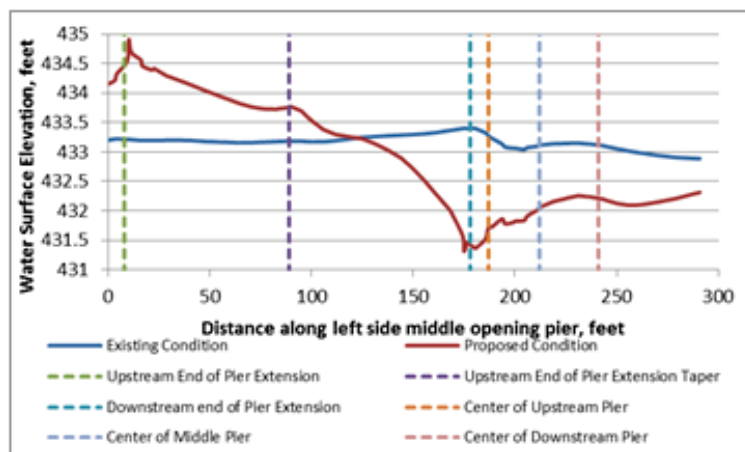


Figure 9. Water surface elevation profile on left side of the middle opening pier for existing and proposed AdH models, feet/second.

ERDC/CHL CHETN-XIV-9  
January 2014

**DISCUSSION:** The AdH model illustrates the two-dimensional nature of the flow field through the bridge pass. As compared to existing conditions, the proposed conditions models showed a decrease in the average velocities while the maximum velocity at each arc was typically higher with the exception of arc 1 and 5. This is reasonable because the pier extensions are skewed to the cross-section and extend into the flow such that they systematically capture the flow. Once captured, the flow is channeled through the inner passes reducing the flow to the two outside-most passes. Therefore, the capture, streamlining, and acceleration cause the increase in the maximum velocity. The increase in maximum velocity through the passes would contribute to greater contraction scour. Conversely, the average velocity decreases due to the shadow that is cast from the pier extensions (Fig. 10). The shadow from the pier extensions is generated from a turbulent slip layer next to the piers where the unidirectional flow is broken up, which decreases the velocity. The velocities shadows are formed from the shedding eddies of the pier extensions. Additionally, the arc cross-sectional area is reduced by the presence of the pier extensions.

In general, for the existing condition model, the HEC-RAS velocities were higher than those in the AdH model for arc 1, 4, and 5, while they were lower for the two inside arcs (arcs 2 and 3). However, the maximum velocity was higher in the AdH model.

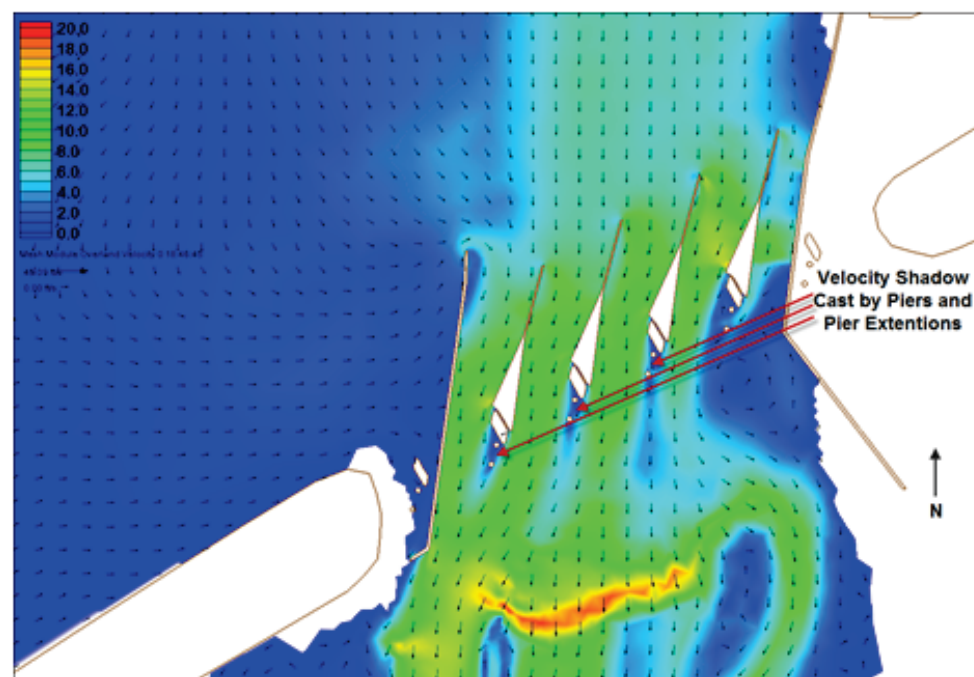


Figure 10. Velocity, in feet per second vectors for the proposed condition at 25,000 cubic feet per second, Santa Ana River BNSF railroad crossing near Corona, California.

ERDC/CHL Letter Report  
January 2014

**CONCLUSION AND RECOMENDATION:** The AdH and HEC-RAS models have been shown to be within reasonable level of agreement. From the analysis it is assumed that the models are behaving appropriately. Roughness coefficients in both models are based on profession judgment. Thus it is recommended that sensitivity testing be conducted for both models to determine the uncertainty in the computed stage and velocity.

The AdH model indicates that the proposed pier extension orientation is increasing the flow through the 2<sup>nd</sup> and 3<sup>rd</sup> opening. Asymmetry of the proposed alignment is causing turbulence at the pier nose extension inducing flow separation prematurely. A re-alignment of the initial pier extension design is recommended to optimize the flow distribution through the pier openings and generate a more uniform flow field through the openings.

The AdH model is showing an increase in maximum velocity through the bridge pier openings. Part of the increase is from the pier extension alignment and part is contraction induced by the guide walls. If possible it is recommended that the guide walls be set back to reduce the contraction.

More investigations will be required to fully evaluate the proposed plan. Local scour around a bridge pier is outside the capability of the 2-D AdH model. A physical model should be used to determine the true dynamics of the pier extensions in a mobile bed. A single set of piers could be tested to efficiently and cost effectively evaluate the local scour generated by the piers and proposed pier extensions.

**REFERENCES:** Walton R., and Christensen, B.A. (1980). "Friction factors in storm surges over inland areas" *Journal of Waterway, Port, Coastal, and Ocean Engineering*, ASCE, 106(2), 261-271.

**ADDITIONAL INFORMATION:** This letter report was prepared by Jeremy A. Sharp, Research Hydraulic Engineer at the Coastal & Hydraulics Laboratory, US Army Engineer Research and Development Center. Questions about this letter report can be addressed to Mr. Sharp at 601-634-4212 or [Jeremy.A.Sharp@usace.army.mil](mailto:Jeremy.A.Sharp@usace.army.mil).

## **Appendix E: ERDC/CHL LR-15-1**

[Note: The authors of the following document have given permission for its inclusion in this technical report.]





**DEPARTMENT OF THE ARMY**  
ENGINEER RESEARCH AND DEVELOPMENT CENTER, CORPS OF ENGINEERS  
COASTAL AND HYDRAULICS LABORATORY  
WATERWAYS EXPERIMENT STATION, 3909 HALLS FERRY ROAD  
VICKSBURG, MISSISSIPPI 39180-6199

CEERD-HZA

26 March 2015

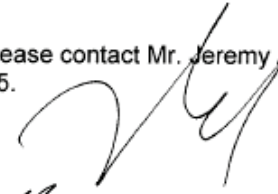
MEMORANDUM FOR Commander, U.S. Army Engineer District, Los Angeles District,  
915 Wilshire Blvd, Suite 1101, Los Angeles, CA 90017.

SUBJECT: Scour Model Study of Proposed Pier Extensions Letter Report, ERDC/CHL  
LR-15-1

1. The attached letter report, ERDC/CHL LR-15-1, describes the findings of the U.S. Army Engineer Research and Development Center (ERDC), Coastal and Hydraulics Laboratory's investigation of the local scour at the BNSF railroad bridge located on the Santa Ana River. Our method of modeling and our conclusion and recommendation are included.

2. If you have any questions, please contact Mr. Jeremy A. Sharp at (601) 634-4212, or Dr. James Lewis (601) 634-3895.

Encl

  
JOSÉ E. SÁNCHEZ, PE, SES  
Director



ERDC/CHL LR-15-1  
March 2015

## Scour Model Study of Proposed Pier Extensions

*by Jeremy A. Sharp, Ronald E. Heath, Howard E. Park, and  
David P. May*

**PURPOSE:** This Coastal & Hydraulics Laboratory Letter Report contains a description of the process to construct, apply, and evaluate a physical model of a single set of piers of the Burlington Northern Santa Fe Corporation (BNSF) railroad crossing on the Santa Ana River near Corona, California. Data from the physical model provides a qualitative evaluation of the scour behavior at the estimated worst case scenario flow conditions for the current bridge configuration and a proposed alternative. The alternative includes using a concrete cap and pier extensions.

**INTRODUCTION:** The BNSF railroad bridge includes three rail lines crossing the Santa Ana River. The bridge is supported in six locations across the river, each of which consists of a set of three piers. The bridge is at a skewed angle across the Santa Ana River. The U.S. Army Corps of Engineers, Los Angeles District (Los Angeles District), is investigating the effect of proposed changes in the maximum discharge from Prado Dam on downstream channel degradation and pier scour at the BNSF railroad bridge. The Los Angeles District aims to identify an effective and cost-efficient approach that will protect the BNSF railroad bridge from scour caused by increased discharge from Prado Dam. To achieve this, the Los Angeles District has proposed flow guide walls protecting the outer abutments and a concrete cap. Additionally, pier extensions are proposed for the four inner sets of piers supporting the BNSF railroad bridge (Figure 1).

A one-dimensional (1D) numerical model was constructed by the Los Angeles District to calculate the velocities at the bridge. However, there was no available dataset to evaluate the performance of the 1D model. The U.S. Army Corps of Engineers, Engineer Research and Development Center, Coastal and Hydraulics Laboratory (CHL) constructed a two-dimensional (2D) depth-averaged, finite element hydraulic model to compare with the one-dimensional model. The 1D and 2D models were shown to be within a reasonable level of agreement in terms of maximum velocity. Additional details of the 1D and 2D numerical model comparison are found in Sharp and Heath 2014.

Around the piers and for a range of flows, the 2D numerical model showed an increase in the maximum velocity between the existing and proposed conditions. The increase in maximum velocity ranged from 1 – 6 feet per second (fps) (Sharp and Heath 2014). While the increase in velocities might suggest increased scour depths, the 2D numerical model is not capable of simulating scour around the bridge piers. Therefore, a physical model of a single set of piers (one of the six), was used to estimate the difference in local scour at the BNSF railroad bridge piers with and without the proposed concrete cap and pier extensions.

ERDC/CHL LR-15-1  
March 2015

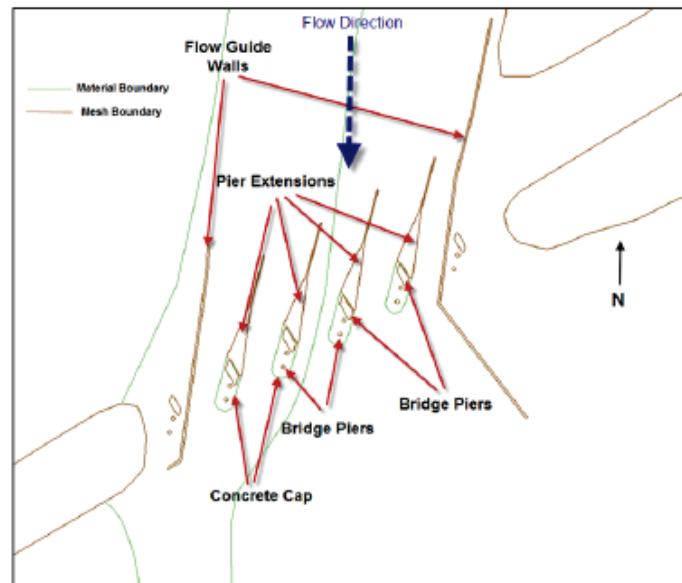


Figure 1. Burlington Northern Santa Fe Corporation railroad bridge crossing on the Santa Ana River near Corona, California.

**PROCESS AND SETUP:** Three conditions were simulated: existing, using a concrete cap with pier extensions skewed from the direction of flow, and using a concrete cap with pier extensions aligned in the direction of flow. Each set of piers includes three individual piers, two that are round and one that is parallelogram-shaped. The intent of the pier extensions is to move scour upstream of the BNSF railroad bridge piers and to streamline flow under the bridge. The intent of the concrete cap is to protect the pier foundation for all three piers. A 1:67 Froude-scaled physical model of a single set of piers was constructed in a tilting bed flume at the Coastal and Hydraulics Laboratory in Vicksburg, Mississippi. The model scale was selected based on the width (3 feet) and depth (1 foot) of the flume. The flume dimensions together with the model scale of 1:67 provide the correct prototype span distance between adjacent piers and allowed for a maximum of 30 feet of prototype scour.

Only a single set of piers was tested in the physical model. For the existing and proposed conditions, pier set four, the fourth set of piers over from the left descending bank, was selected for simulation. This pier set was chosen because the 2D model identified it as exposed to the greatest discharge. The maximum estimated discharge at the site is 35,000 cubic feet per second. At this flow, 22,200 cubic feet per second pass pier set four. Additionally, a second potential worst case situation for the proposed conditions is 15,000 cubic feet per second at the bridge. At this flow, 10,600 cubic feet per second pass pier set four. These two flow conditions (greatest discharge and discharge corresponding to the water surface at the elevation of the top of the pier

ERDC/CHL LR-15-1  
March 2015

extension) represented the presumed worst case scenarios, in terms of scour potential for each of the existing and proposed conditions based on information from the 2D model. The flow was scaled using the Froude criteria. In the absence of field data, the Froude number from the 2D numerical model was used (0.32 – 0.36). The Froude number was in the correct range for both flow conditions where the 22,200 and 10,600 were 0.32 and 0.35, respectively.

The 2D model showed that the proposed pier extensions were designed to be at a 16 degree skew from the direction of flow. The physical model was set at this same skew (Figure 2). The physical model bed upstream of and downstream from the piers is a flat bed with uniformly graded sand with a median particle size diameter of 0.4 millimeters. The elevation of the bed at the location of the piers in the physical model represents an elevation of 417.5 feet in prototype.

For two physical model tests (10,600 cfs and 22,000 cfs), the pier extensions were aligned in the direction of flow (Figure 3) rather than skewed at a 16 degree angle, and lengthened to provide coverage for the piers. The left wall of the pier extension was lengthened by 41 feet and the right descending wall of the pier extension was lengthened by 104 feet.

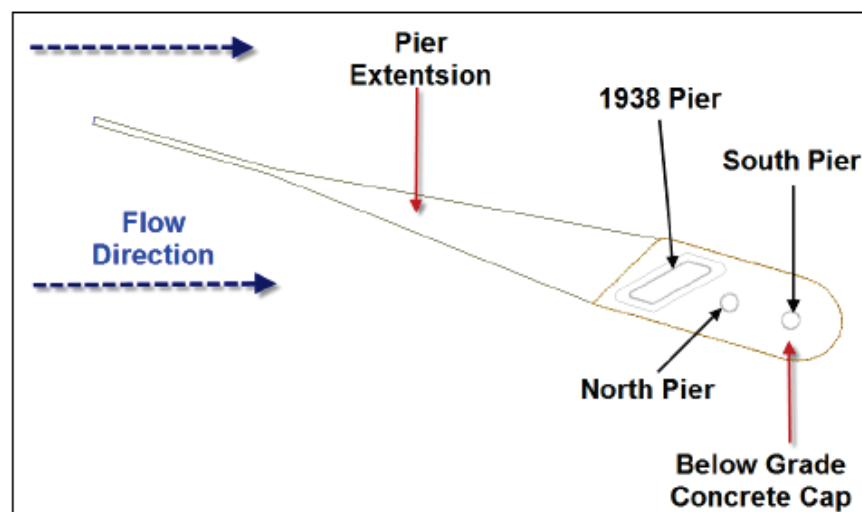


Figure 2. Proposed bridge pier set protection design, with 16 degree skew, for the Burlington Northern Santa Fe railroad bridge pier set evaluated in the physical model.

ERDC/CHL LR-15-1  
March 2015

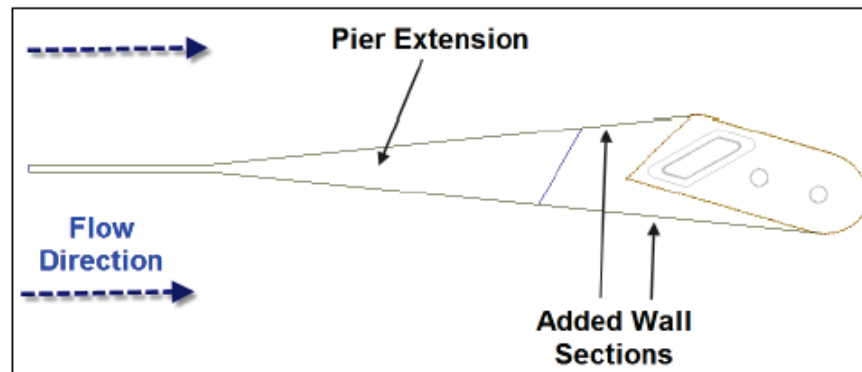


Figure 3. Proposed bridge pier set protection design, with 0 degree skew, for the Burlington Northern Santa Fe railroad bridge pier set evaluated in the physical model.

**DATA AND RESULTS:** Water surface profiles were determined at the start and finish of each test based on measurements at 13 stations. Flow was set with a gate valve and was measured with a differential manometer across a Venturi meter and checked with a velocity meter in the flume. Bathymetry was collected at the completion of each test. The flume was dewatered and photogrammetry was used to generate point clouds of bed bathymetry. The photogrammetry was geo-referenced with established benchmarks from a LiDAR scan. The bathymetry point clouds were scaled and adjusted to the prototype dimension and maximum scour depth was estimated.

A total of 21 tests were run, 6 for model set-up and adjustments, 9 at 35,000 cfs, and 6 at 15,000 cfs. The adjustments enabled clear water scour conditions to be met and boundary conditions to be tuned. Maximum scour depth for tests 7–21 are shown in Table 1. Though depth value estimates are provided, the values represent a qualitative difference and are intended for comparison purposes only. The typical scour and shoaling patterns are shown in Figure 4 for the existing bridge pier configuration and in Figure 5 for the proposed design with the concrete cap and pier extensions skewed at a 16 degree angle. Tests 20 and 21 were not repeated. The other test set ups were repeated between 2 and 5 times.



ERDC/CHL LR-15-1  
March 2015

Table 1. Test results for physical model production runs of a single set of piers supporting the Burlington Northern Santa Fe railroad bridge over the Santa Ana River near Corona, California.

Test	Plan			Water surface elevation, in feet	Flow, in cubic feet per second	Scour Elevation, Initial Bed of 417.5 feet			Max scour depth, in feet
	Existing	16 degree skew	0 degree skew			Right side of 1938 pier, in feet	Left side of 1938 pier, in feet	Pier extension, in feet	
7	X			436	35,000	407	402	Not applicable	15.5
8	X			436	35,000	407	402	Not applicable	15.5
9	X			436	35,000	407	403	Not applicable	14.5
10	X			436	35,000	406	402	Not applicable	15.5
11	X			436	35,000	407	403	Not applicable	14.5
12		X		436	35,000	Not available			
13		X		436	35,000	409	408	412	9.5
14		X		436	35,000	412	411	412	6.5
15		X		428	15,000	405	No scour	405	12.5
16		X		428	15,000	407	No scour	407	10.5
17		X		428	15,000	406	No scour	407	11.5
18	X			428	15,000	409	408	Not applicable	9.5
19	X			428	15,000	411	410	Not applicable	7.5
20			X	428	15,000	405	408	Not applicable	12.5
21			X	436	35,000	413	410	Not applicable	7.5

ERDC/CHL LR-15-1  
March 2015

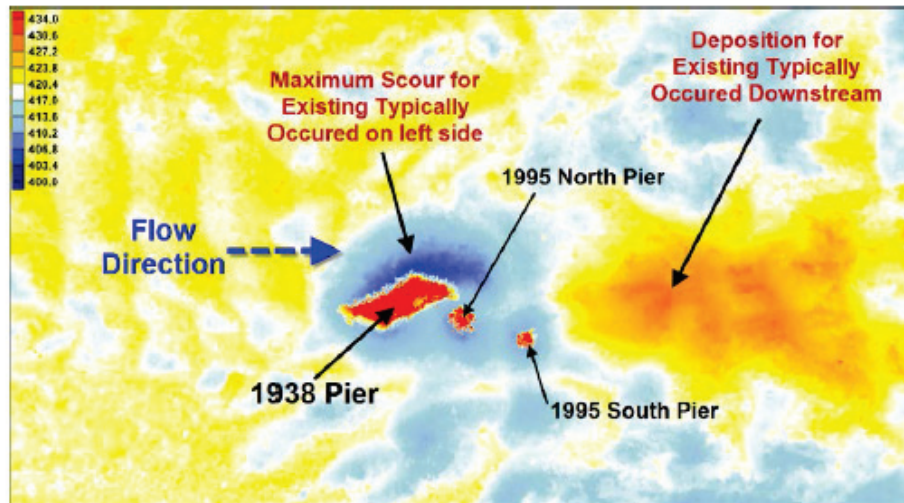


Figure 4. Physical model test 7 bathymetry, in feet, for the existing bridge pier configuration at 35,000 cubic feet per second.

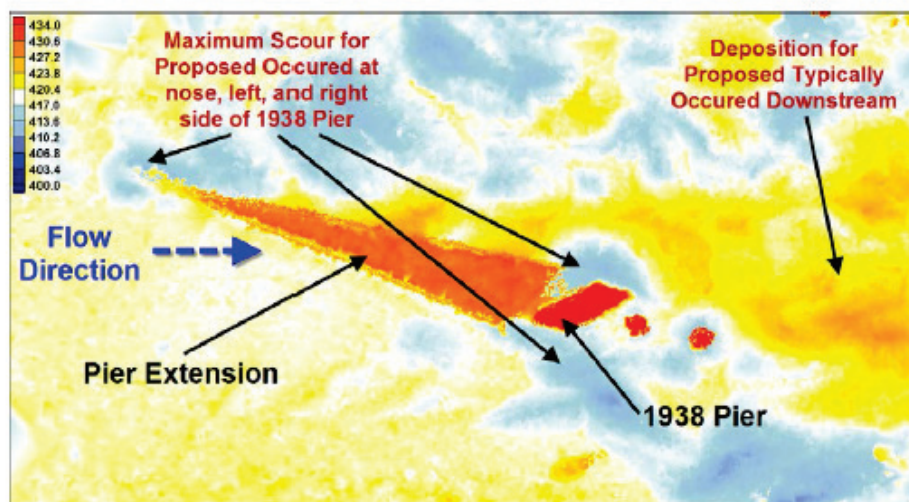


Figure 5. Physical model test 13 bathymetry, in feet, for the proposed concrete cap and skewed pier extensions at 35,000 cubic feet per second.

ERDC/CHL LR-15-1  
March 2015

**DISCUSSION:** Clear-water scour conditions were generated and repeated for multiple tests in the physical model. Tests reached quasi-equilibrium within the test run time, with one hour equivalent to eight hours in prototype. At the end of each simulation, the observed scour rates were essentially zero, indicating that a quasi-equilibrium condition had been attained. Sediment transport into the test section was negligible; however, small perturbations upstream (from dye or velocity measurements) caused ripples to form. The estimated maximum scour depth is believed to be reasonable for qualitative comparisons between the evaluated configurations.

For the 35,000 prototype flow condition (Figure 6a), the flume model shows a decrease in the estimated maximum local scour depth at pier set four between the existing configuration and the proposed concrete cap and pier extension for both the 0 degree and 16 degree skewed orientations. The greatest scour in all tests occurred with the existing pier configuration during the 35,000 cfs tests. At 15,000 cfs (Figure 6b), the local scour associated with the proposed concrete cap and pier extensions increased in comparison to the scour for the existing configuration at the same discharge, but the maximum scour depth at 15,000 cfs for all conditions was less than the maximum scour depth for the existing configuration at 35,000 cfs. The skew of the pier nose extension generated a condition where the 15,000 cfs flow was the worst case for the proposed pier extension. This was due to forcing flow down the right descending side and generating flow separation off the pier extension nose on the left descending side. The concrete cap and pier extensions, under the presumed two worst-case scenarios, result in less scour than the existing configuration. However, it is important to note that the maximum scour depth in the prototype is influenced by non-uniform bed gradation and other factors that were not evaluated in this model.

This analysis represents a qualitative evaluation of local scour at pier set four of the BNSF railroad bridge across the Santa Ana River near Corona, California. Interaction from adjacent piers and pier extensions are not considered here and may play a meaningful role in affecting the maximum local scour depth. The dynamic nature of local scour requires site-specific considerations. Understanding the interaction and alignment of the proposed pier extensions is critical for scour reduction.

ERDC/CHL LR-15-1  
March 2015

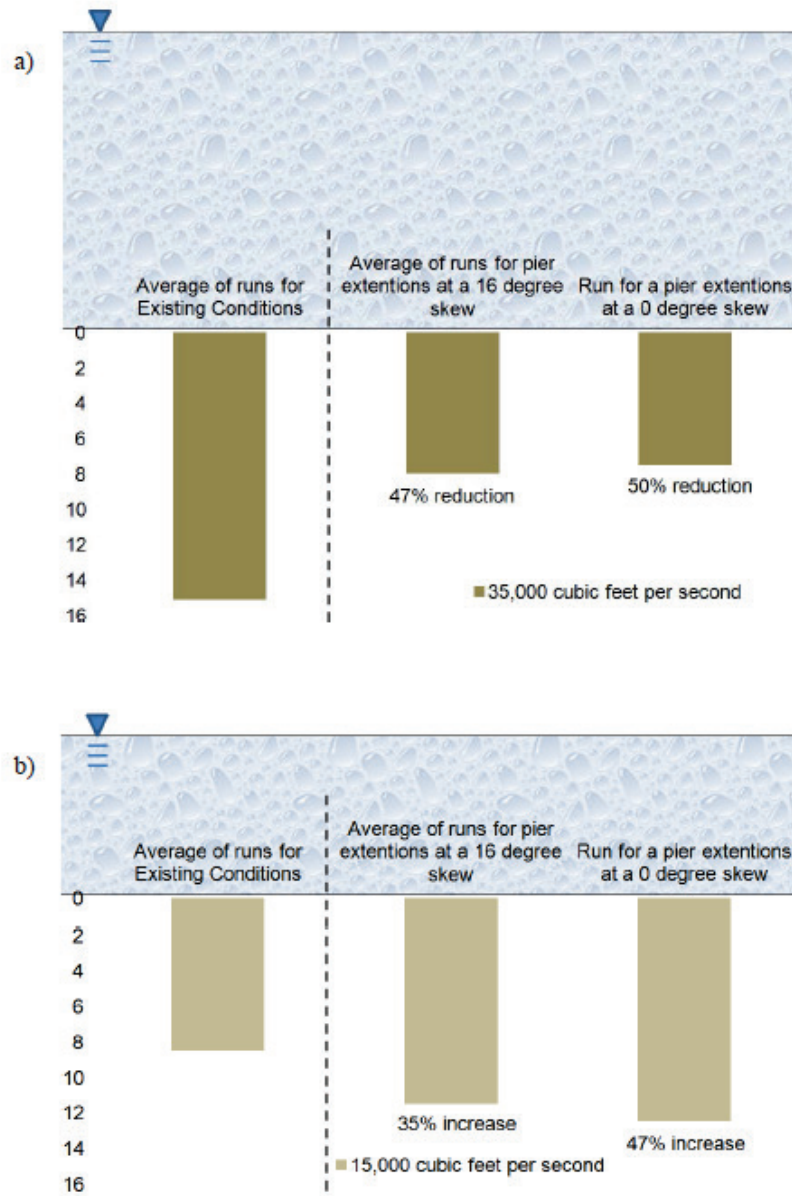


Figure 6. Estimated maximum scour depth for model conditions showing percent change from the average runs of the existing conditions at a) 35,000 cubic feet per second, and b) 15,000 cubic feet per second.

ERDC/CHL LR-15-1  
March 2015

**CONCLUSION AND RECOMENDATION:** The concrete cap and pier extensions result in less maximum scour than the existing configuration. A full physical model representing all piers, pier extensions and flood guide walls should be used to determine the interactive dynamics of the piers and pier extensions between each other in a mobile bed.

**REFERENCES:** Sharp, J.A., and Heath, R.E. (2015). Two-Dimensional Model Study of Santa Ana River Railroad Bridge Pier Extensions. US Army Engineer and Research Development Center, Coastal and Hydraulics Laboratory, ERDC/CHL-LR-15-2.

**ADDITIONAL INFORMATION:** This letter report was prepared by Jeremy A. Sharp, Research Hydraulic Engineer at the US Army Corps of Engineers, Engineer Research and Development Center, Coastal & Hydraulics Laboratory. Questions about this letter report can be addressed to Mr. Sharp at 601-634-4212 or [Jeremy.A.Sharp@usace.army.mil](mailto:Jeremy.A.Sharp@usace.army.mil).



REPORT DOCUMENTATION PAGE				Form Approved OMB No. 0704-0188	
<p>The public reporting burden for this collection of information is estimated to average 1 hour per response, including the time for reviewing instructions, searching existing data sources, gathering and maintaining the data needed, and completing and reviewing the collection of information. Send comments regarding this burden estimate or any other aspect of this collection of information, including suggestions for reducing the burden, to Department of Defense, Washington Headquarters Services, Directorate for Information Operations and Reports (0704-0188), 1215 Jefferson Davis Highway, Suite 1204, Arlington, VA 22202-4302. Respondents should be aware that notwithstanding any other provision of law, no person shall be subject to any penalty for failing to comply with a collection of information if it does not display a currently valid OMB control number.</p> <p><b>PLEASE DO NOT RETURN YOUR FORM TO THE ABOVE ADDRESS.</b></p>					
1. REPORT DATE November 2017		2. REPORT TYPE Final Report		3. DATES COVERED (From - To)	
4. TITLE AND SUBTITLE General Model Study of Scour at Proposed Pier Extensions – Santa Ana River at BNSF Bridge, Corona, California				5a. CONTRACT NUMBER	
				5b. GRANT NUMBER	
				5c. PROGRAM ELEMENT NUMBER	
6. AUTHOR(S) Jeremy A. Sharp, Tate O. McAlpin, Gary L. Bell, Howard E. Park, Ronald E. Heath				5d. PROJECT NUMBER 104779	
				5e. TASK NUMBER	
				5f. WORK UNIT NUMBER	
7. PERFORMING ORGANIZATION NAME(S) AND ADDRESS(ES) U.S. Army Engineer Research and Development Center Coastal and Hydraulics Laboratory 3909 Halls Ferry Road Vicksburg, MS 39180-6199				8. PERFORMING ORGANIZATION REPORT NUMBER ERDC/CHL TR-17-17	
9. SPONSORING/MONITORING AGENCY NAME(S) AND ADDRESS(ES) U.S. Army Corps of Engineers, Los Angeles District 915 Wilshire Blvd, Suite 1101 Los Angeles, CA 90017				10. SPONSOR/MONITOR'S ACRONYM(S) SPL	
				11. SPONSOR/MONITOR'S REPORT NUMBER(S)	
12. DISTRIBUTION/AVAILABILITY STATEMENT Approved for public release; distribution is unlimited.					
13. SUPPLEMENTARY NOTES					
14. ABSTRACT A proposed pier nose extension intended to reduce the local pier scour at the Burlington Northern Santa Fe Railway crossing on the Santa Ana River near Corona, CA, was tested in a general physical model. The applied model was a 1:30 Froude-scaled model of the bridge piers, other related structures, and the adjacent channel. Data from the model provided a qualitative and quantitative evaluation of the local scour behavior at the estimated worst-case scenarios for both the existing and proposed conditions. The existing conditions represent the current prototype configuration exposed to potentially larger future dam releases from the upstream Prado Dam. The proposed condition includes pier nose extensions, concrete caps (pile enclosures), and flow guide walls, all intended to reduce scour at the bridge. The primary location for the minimum scour elevation (maximum scour depth) occurred around pier set 5. The proposed conditions showed as high as 60% improvement in reducing the scour depth with the proposed conditions configuration.					
15. SUBJECT TERMS Bridges, Hydraulic structures, Piers, Santa Ana River (Calif.), Scour at bridges, Scour (Hydraulic engineering), Sediment transport					
16. SECURITY CLASSIFICATION OF:			17. LIMITATION OF ABSTRACT	18. NUMBER OF PAGES	19a. NAME OF RESPONSIBLE PERSON
a. REPORT	b. ABSTRACT	c. THIS PAGE			Jeremy A. Sharp
Unclassified	Unclassified	Unclassified	SAR	125	19b. TELEPHONE NUMBER (Include area code) 601-634-4212